



NUCLEAR ENERGY INSTITUTE

**Adrian P. Heymer**  
SENIOR DIRECTOR, NEW PLANT DEPLOYMENT  
NUCLEAR GENERATION DIVISION

October 13, 2006

Mr. Eugene Imbro  
Chief Mechanical and Civil Engineering Branch  
Office of Nuclear Reactor Regulation  
U.S. Nuclear Regulatory Commission  
Washington, DC 20555-0001

**PROJECT NUMBER: 689**

**SUBJECT:** Transmittal of the industry's partial responses to the NRC Staff's fifty-two Requests for Additional Information (RAIs) on the S2.1 task report, *Effect of Seismic Wave Incoherence on Foundation and Building Response*

Dear Mr. Imbro:

This letter is the formal transmittal of the industry's partial responses to the NRC Staff's fifty-two RAIs on the S2.1 task report, *Effect of Seismic Wave Incoherence on Foundation and Building Response*. During recent meetings with the NRC staff, we agreed to forward these responses in advance of the final report to expedite the schedule for incorporating the use of incoherency within the regulatory framework for new plants in either updates to the Standard Review Plan or incorporation into Regulatory Guides.

The attached RAI responses consist of one of the following formats:

- The RAI response is complete and given in the attached Appendix A,
- The RAI response is partially contained within the attached Appendix A and partially contained within the one of the Chapters of the main report or another Appendix to the report, or
- The RAI response is completely contained within one of the Chapters of the main report or another Appendix of the report and a reference is made to that location.

Mr. Eugene Imbro

October 13, 2006

Page 2

The draft versions of the following chapters of the report are enclosed because many of the responses fall within one of the last two categories due to the complex nature of the RAI. The enclosures are:

- Appendix A of the final S 2.1 report, responses to the 53 RAIs, June 1, 2006 (Enclosure 1);
- Appendix B – Validation of Incoherency Effects Through Recorded Events, (Enclosure 2);
- Appendix D – Uncertainty Effects on Incoherency Response, (Enclosure 3);
- Chapter 3 – Technical Approach, (Enclosure 4);
- Chapter 4 – Rigid Massless Foundation Response, (Enclosure 5); and
- Chapter 5 – SSI and Structure Response (the Direct Approach portion is included; the simplified portion of this Chapter is still being refined and will be included in the final report), (Enclosure 6)

The final S2.1 report will be forwarded to you in the near future.

If you have any questions, please contact me directly or Rick Hill (831-420-7607; rahill@erineng.com) the industry project director for this task.

Sincerely,



Adrian P. Heymer

c: Mr. Thomas A. Bergman, NRC  
Dr. Anthony H. Hsia, NRC  
Dr. Andrew J. Murphy, NRC

## Enclosure 1

# APPENDIX A

## COMMENTS AND RESPONSES TO NRC REQUESTS FOR ADDITIONAL INFORMATION (RAIs)

---

The NRC submitted 53 RAIs related to the S2.1 Task on June 1, 2006. These RAIs were titled “Section 4.0 –Comments on EPRI Report 1012966 *Effect of Seismic Wave Incoherence on Foundation and Building Response (S2.1)*”. The industry responses and resolutions for these 53 RAIs are documented below.

### NRC Comment/Question:

4.1 The report seems to be written well and different topics of discussion are well laid out.

### Industry Response/Resolution:

4.1 Thank you.

---

### NRC Comment/Question:

4.2 An important gap in this study is the lack of any treatment of kinematic interaction of embedded foundations or any questioning of the validity of the use of the proposed Abrahamson coherency function for those foundations.

### Industry Response/Resolution:

4.2 Embedment – the question of validity of Abrahamson coherency function at depth is addressed within the EPRI Report 1014101 (Spatial Coherency Models for Soil Structure Interaction). Dr. Abrahamson has included additional material within this report relative to the data available to support the validity of using the coherency function with depth.

Embedment effects on SSI response of NPP structures are due to kinematic response and inertial response. Kinematic response effects are due to spatial variation of ground motion and the integrating effects of the embedded foundation and partially embedded walls. Two aspects of spatial variation of ground motion are to be considered: the variation of free-field ground motion with depth in the soil or rock from the surface to foundation for a partially embedded structure; and the incoherency effects. The first has a significant effect on the foundation input motion generally reducing the translational

motion of the foundation and increasing the rotational motion. This effect exists independent of incoherency. The assumption and judgment is that the effects of incoherency are separable from this aspect of spatial variation of ground motion with depth. Appendix E on effects of embedment and incoherence will address this assumption and judgments in this area. A further assumption is that the coherency functions are applicable at depth as well as on the surface of the soil or rock. Given these assumptions, kinematic interaction effects can be treated separately and combined at the later stage or treated simultaneously in a methodology, such as SASSI. If treated separately, one needs to be careful not to double count the effect of incoherence and vertical spatial variation of motion. It should be noted that Abrahamson coherency function is developed for horizontal separation distance only. Any ground motion incoherency effects due to elevation (or depth) differences of ground nodal points is ignored. In SASSI, the Abrahamson coherency model is applied at all horizontal planes within the embedded part of the foundation based on the horizontal distance of the nodal points. Appendix E is being developed and will address the subject of embedment in more detail.

---

**NRC Comment/Question:**

- 4.3 The standard practice of performing SSI analysis using coherent ground motion was based on observation and interpretation of data from down hole arrays that show a large percentage of the power of ground motion comes from vertically propagating waves. It appears that the recommended method of SSI analysis in this report is simply to reduce the amplitudes of ground motion at frequencies generally above 10 Hz, and then apply the reduced motion uniformly (coherently) across the entire foundation.

**Industry Response/Resolution:**

- 4.3 Chapter 6 itemizes the two methods of treating incoherency of ground motion:
- 1) Take the coherency function directly and input to the SSI analysis using a program that incorporates both the SSI and incoherence effects (what we have labeled as the direct approach).
  - 2) Modify the input motion and evaluate the new input as coherent motion (what we have labeled as the simplified approach).

Both of these methods are considered to be acceptable approaches for the treatment of incoherency effects and further elaboration will also be provided within the EPRI I1.1 integration report.

---

**NRC Comment/Question:**

- 4.4 This report needs to clearly layout the approach and implementation scheme for using the SSE (design ground motion) derived from a performance-based approach in conducting engineering analyses. Detailed steps of the implementation in carrying out the SSI analysis using the incoherent motion approach, including guidance on soil parameter modeling are needed.

**Industry Response/Resolution:**

- 4.4 This requested overall approach and implementation scheme will be defined within the EPRI Integration task I1.1 and documented within that report. The overall implementation approach is a broader scope than that of this incoherence task and will include the risk calculations and SSE determination within task G1.1, G1.2 and G1.3, as well as the implementation of the results from S2.1. Chapter 6 describes two alternatives to incorporating the effects of incoherency of ground motion and its association with the SSI analysis.

---

**NRC Comment/Question:**

- 4.5 Complicated equations are described that use rectangular and square matrices, which are appropriately multiplied by column matrices to obtain resulting equations. These are described in text, however a step-by-step process of converting the matrices using conceptual layout in matrix form will enhance the reader's understanding.

**Industry Response/Resolution:**

- 4.5 We reviewed the text in Chapter 3 and introduced some further clarifications to assist with the enhancement of the reader's understanding.

---

**NRC Comment/Question:**

- 4.6 The ASCE Journal of Geotechnical and GeoEnvironmental Engineering issue of April 2003, Volume 129, Number 4 published an article, "Kinematic Soil-Structure Interaction from Strong Motion Recordings" by Seunghyun Kim and Jonathan Stewart. This article points out that the incoherence parameter is dependent on the site shear wave velocity. This paper also points out that the use of incoherent motion introduces torsional motion.

**Industry Response/Resolution:**

- 4.6 Appendix B of this report discusses the Kim and Stewart paper and its applicability to the present study. The Kim and Stewart paper and its ramifications were also discussed at the May 11-12 meetings at the NRC. Incoherency does introduce both torsion and rocking. Chapters 4, 5, and 6 have been

expanded in this area and discuss the impact of induced rotations on foundation and structure response.

In Chapter 3, it is demonstrated that the incoherency transfer function for random spatial variations is independent of any soil properties. Of course, incoherence effects on response spectra are dependent on soil properties.

---

**NRC Comment/Question:**

- 4.7 Page iv: As discussed here, seismic wave incoherence occurs because of the horizontal spatial variation of both horizontal and vertical ground motions. The variation in the horizontal input motions will result in torsional input at the foundation while the variation in the vertical motions will cause rocking of the base mat. Please discuss in detail the basis for not considering the torsion and rocking effects and state whether these effects will be considered in the individual plant ESP and/or COL applications.

**Industry Response/Resolution:**

- 4.7 Torsion and rocking have been considered within this study. See the response to question 4.6 and the new material within Chapters 4, 5 and 6 of this report.

---

**NRC Comment/Question:**

- 4.8 Page iv: This section states that the seismic response is evaluated for rigid, massless foundations and for example structural models on foundation mats that behave rigidly. Please discuss how the results would be impacted by taking into account the flexibility and mass of the foundation and state whether these effects will be considered in the individual plant ESP and/or COL application. (See also page 1-2 for the same subject).

**Industry Response/Resolution:**

- 4.8 a. Flexibility - the basis for the industry teams' recommendation that the S2.1 methodology is applicable to NPP structures (containments, internal structure/NSSS, and heavy shear wall structures) is based on published data, including ASCE (2000), *Seismic Analysis of Safety-Related Nuclear Structures and Commentary*, American Society Civil Engineers, Report. ASCE 4-98 and engineering judgment. The SSI analysis procedures implemented in CLASSI and SASSI validated the approach to treating the phenomena. CLASSI is limited to foundations effectively behaving "rigidly", i.e., the combined effective stiffness of the inter-connecting structure and the foundation behaves rigidly for overall soil-structure response analysis. This assumption is applicable to NPP structures mentioned above. The SASSI implementation of the incoherence effects is not limited to foundations behaving "rigidly" and foundation flexibility can be considered in the SASSI solution.
- b. Mass – the substructure approach to SSI as implemented in CLASSI was discussed at the May 12 meeting. The foundation input motion is derived by multiplying the free-field

ground motion times the scattering matrices and accounts for kinematic interaction – the next step is solving the SSI problem including mass of foundation and dynamic characteristics of the structure.

---

**NRC Comment/Question:**

- 4.9 Page iv: This section states that the incoherency transfer functions depend on the foundation area and are independent of site soil conditions but that the resulting spectral reductions strongly depend on site soil conditions. This seems to be inconsistent. Please explain. (This statement also appears on page ix.)

**Industry Response/Resolution:**

- 4.9 The transfer functions are not dependent on the site conditions (See response to RAI 4.47). The effects on free-field response spectra are highly dependent on these free-field ground response spectra: those with significant high-frequency content (rock site profile) will experience significant reductions in frequency content above 10 Hz; those with minimal amplified frequency content above 10 Hz (soil site profile) will experience minimal impact on the free-field response spectra. The report text (Chapters 4 and 5) has been modified to make the description of this more complete in order to alleviate any misconception of an inconsistency.

---

**NRC Comment/Question:**

- 4.10 Page v: This section describes some of the research activities and uncertainties that have been identified. These include: additional analyses for different and more complex foundation shapes; verification based on foundation responses in real earthquakes; sensitivity study; and validation through peer review. Please discuss the status of these tasks and provide assurance that these tasks will not impact the incoherency functions presented in this report.

**Industry Response/Resolution:**

- 4.10 In response to the 4 different areas from the RAI above:
- a. Additional studies.
    - (i) Different and more complex foundation shapes
      - a circular foundation was analyzed and the results reported in Chapter 4.
    - (ii) Verification based on foundation responses in real earthquakes. Appendix B discusses the validation of the SSI incoherence phenomena with recorded data.
    - (iii) Sensitivity study – sensitivity studies on foundation shapes and coherency uncertainty are being conducted. Foundation shape was addressed in (i). Sensitivity study concerning the effect of uncertainty in the coherence function is

discussed in Appendix D. Neither of these sensitivity studies produced results that impacted the methods/results in this study.

- b. Peer Review for the coherency function has been completed (see Abrahamson 2006 report), with no effect or changes to the coherency function results.

---

**NRC Comment/Question:**

- 4.11 Page viii: This page states that in this study, the assumption was made that mat foundations of typical nuclear power plant (NPP) structures behave rigidly. This assumption may not be valid in all cases. Please discuss the effect of mat flexibility on the results reported in this study and whether the mat flexibility will be considered in the individual plant ESP and/or COL application.

**Industry Response/Resolution:**

- 4.11 The issue of flexibility of foundations is discussed in section 4.8a above.

---

**NRC Comment/Question:**

- 4.12 Page 1-1: This page states that this study considers both the “local wave scattering” and “wave passage effects” but that the final results are based on “local wave scattering” only. Please provide the basis of excluding “wave passage effects” and state whether the “wave passage effects” will be considered in the individual plant ESP and/or COL applications. See also Page 5-1.

**Industry Response/Resolution:**

- 4.12 Wave passage vs. local wave scattering (randomness) is discussed and results presented in Chapter 4. Excluding wave passage effects is conservative and, thus, individual plants would not be required to address either within ESP or COL applications.

---

**NRC Comment/Question:**

- 4.13 Page 2-2: It is not clear which equation is plotted in Figures 2-1 and 2-2, and which equation is to be used for “no wave passage effect”. Please explain.

**Industry Response/Resolution:**

- 4.13 The curves plotted in Figures 2-1 and 2-2 are derived from Equation 2-1 for local wave scattering only. No wave passage effects are included. The report (Chapter 2) was updated to ensure this is clear.
-

**NRC Comment/Question:**

- 4.14 Page 2-3: This section states that the ground motion data analyzed to develop the coherency functions have frequency content of 20 Hz and less, but that the trends can be extrapolated to higher frequencies. It is not obvious why and how these trends can be extrapolated. Please explain.

**Industry Response/Resolution:**

- 4.14 These bullets are merely a summarization of the conclusions from EPRI report 1012968 “Spatial Coherency Models for Soil-Structure Interaction”. The bases for this extrapolation are described within that report (Abrahamson, 2005a). Extrapolation of coherency function values for frequencies greater than 20 Hz as constant and equal to the 20 Hz value or extrapolated to smaller values has no material effect on the results. That is, the coherency values at 20 Hz are already so small that the incoherency transfer functions would be minimally affected by reducing them further. Similarly for foundation and structure response.

---

**NRC Comment/Question:**

- 4.15 Page 2-3: This section rightfully states that the mean input ground motion is the goal for the design of NPP structures, and as a result, the goal is to use mean coherency. However, this section further states that the coherency functions stated in the report are median coherency functions. Please provide justification for using the median instead of the mean coherency functions.

**Industry Response/Resolution:**

- 4.15 The mean and median are approximately the same with a difference of only a few percent. The median is slightly higher than the mean, as has been documented in the report by Dr. Norm Abrahamson in *Spatial Coherency Models for Soil-Structure Interaction*, EPRI 1012968. Thus, the justification for using the median is that it is slightly conservative to do so.

---

**NRC Comment/Question:**

- 4.16 Page 2-3: Tables 2-2 and 2-3 do not seem to be consistent with Figure 2-4. Please explain.

**Industry Response/Resolution:**

- 4.16 The soil curve in Figure 2.4 is the low strain shear wave velocity. Table 2-3 lists the properties associated with the assumed  $10^{-2}$  % strain level. The text has been changed to reflect this and to clarify any inconsistency.

---

---

**NRC Comment/Question:**

- 4.17 Page 2-5: This section states that the shear wave velocity of the bedrock is 4300 fps but Table 2-3 indicates a value of 4150 fps. Please explain the discrepancy and its potential impact.

**Industry Response/Resolution:**

- 4.17 The 4150 fps value is consistent with the assumed  $10^{-2}$  % earthquake strain level and this section has been modified to clarify any inconsistency.

---

**NRC Comment/Question:**

- 4.18 Page 2-5 and 2-6: This section quotes the EPRI 1993 Guidelines for Determining Design Basis Ground Motion. Please provide the full reference.

**Industry Response/Resolution:**

- 4.18 Agree. The full reference has been provided within the reference list.

---

**NRC Comment/Question:**

- 4.19 Page 2-6: This section states that the soil damping and shear modulus were determined based on an earthquake strain level of  $10^{-2}$ %. This is the same strain value as was stated for rock. Please explain why the strain value for the soil is not higher than that of the rock.

**Industry Response/Resolution:**

- 4.19 The  $10^{-2}$  % strain level was assumed for the entire profile (including bedrock) for the purpose of developing an example soil case. CLASSI and SASSI are based on equivalent linear response, thus, the soil properties of each layer are associated with a strain level. These values were assumed for illustrative purposes only to develop an example to show the effect of incoherence on a soil site. The text has been clarified that this is not a recommended design practice which, in general, would need to demonstrate that the properties are consistent with strain levels obtained from a SHAKE analysis or other analytical technique.
-

**NRC Comment/Question:**

- 4.20 The structural model to evaluate kinematic interaction is presented in Figure 2-8. The stick model has mass, stiffness and damping representing a fixed-base condition. The use of this model for studying the kinematic interaction should be further explained. Presumably the inertial interaction part is to be evaluated in a separate step. In this context, the use of superstructure with masses hinders the demonstration of kinematic effects. Please explain.

**Industry Response/Resolution:**

- 4.20 See response 4.8b above. Figure 2-8 is a schematic of the structure/foundation used as an example. The solution to the problem is performed in steps; the first step is to solve the kinematic interaction problem, the final step is to solve the inertial interaction problem including the impedances, the foundation mass and structure dynamic properties subjected to the foundation input motion derived as the scattering functions times the ground motion. The scattering functions times the ground motion is the kinematic interaction effects.

---

---

**NRC Comment/Question:**

- 4.21 It is stated in the general section that the goal is to obtain an engineering-modified input ground motion accounting for incoherency effects. Presumably, the modified ground motion will be applied as a completely coherent time function in the SSI analysis. It appears that the effect of proposed incoherency effect is only to reduce time histories along three orthogonal directions without any rotational input. This seems to render the very idea of incoherency incongruent. Please explain the value of this approach.

**Industry Response/Resolution:**

- 4.21 The effect of incoherence of ground motion on foundation/structure response is detailed in Chapters 4, 5, and 6. These effects include alterations in translational input motions and induced rotations. At the rigid, massless foundation level, the results are presented in Chapter 4. The effect on structure response is presented in Chapter 5. A simplified, but conservative approach for considering incoherence in which free-field ground motion is modified is presented in Chapter 5. This approach includes both the effects of translation and rotation.
- 
-

**NRC Comment/Question:**

- 4.22 Based on Figure 4-1, the effect of incoherency transfer functions for the vertical and horizontal directions are about a factor of 2 apart. Can this be validated from actual recordings, or is this to be expected in the CEUS region? This effect also shows up later in the report.

**Industry Response/Resolution:**

- 4.22 Generally, the coherency functions (Figures. 2-1 and 2-2) are less for horizontal motions than vertical. Hence, the ITFs for horizontal should be less than for the vertical. The basis for these vertical and horizontal coherency functions were developed from all applicable ground motion recordings available from dense instrument arrays as described in Abrahamson (2005). As a result, this behavior is expected in the CEUS region.

---

**NRC Comment/Question:**

- 4.23 Page 5-4: This section states that to study the effect of foundation shape, square vs. rectangular foundations were considered, while different foundation sizes of square foundations were investigated to study the effect of foundation area. Please explain whether you have studied circular foundations, especially in light of the fact that a significant number of NPP foundations are circular. Please explain whether this effect will be considered in the individual plant ESP and/or COL application.

**Industry Response/Resolution:**

- 4.23 A circular foundation shape was considered and the results are presented in Chapter 4.

---

**NRC Comment/Question:**

- 4.24 At the end of this chapter it is concluded that the incoherency transfer function (ITF) is independent of the input motion. This would be one of the most important points that would allow the use of the ITF without any dependence on the seismologically (performance-based) obtained ground motion spectrum. The validation of this point needs to be demonstrated by observed behavior.

**Industry Response/Resolution:**

- 4.24 EPRI 1012968 concludes that the coherency functions are independent of many ground motion attributes. The development of the ITF as described in Chapter 3 demonstrates the independence from the input motion.
-

**NRC Comment/Question:**

- 4.25 Figures 5-17 and 5-18 show the reduction effect at PGA, but the reduced vertical PGA (0.15g) is less than the horizontal (0.2g). Can this be validated by observed data?

**Industry Response/Resolution:**

- 4.25 Looking at the response, the free-field motion has amplified spectral accelerations of over 0.6g for the horizontal direction and over 0.4g for the vertical. This portion of the spectra likely drives the response of the structure/foundation – hence, the lower PGA is not surprising.

---

**NRC Comment/Question:**

- 4.26 Page 6-10: This section discusses whether correction factors need to be applied to take into account rotational effects of torsion and rocking. Please elaborate on the statement *“The exact solution includes rocking induced by consideration of incoherence but the incoherence transfer function (ITF) scaled solution only includes translational input motion.”*

**Industry Response/Resolution:**

- 4.26 The descriptions of the effects of induced rotations have been significantly expanded to address multiple similar RAI questions on rotations. Chapters 4, 5, and 6 contain expanded descriptions that should address the treatment of both rocking and torsion.

---

**NRC Comment/Question:**

- 4.27 This section also states that translational foundation response after SSI when subjected to rotations only were less than 0.01g, and the in-structure response was similarly low. Were these results for a soil or rock site? A soil site may be subject to more rocking. The staff would like to see the details of these results.

**Industry Response/Resolution:**

- 4.27 The expanded descriptions of the effects of induced rotations are discussed in Chapters 4, 5, and 6. Note the effect of incoherency on in-structure response is dependent on the free-field ground motion. Incoherence has the greatest effect on free-field ground motion with high frequencies, i.e., frequency content greater than 10 Hz, representative of rock sites. The effect on in-structure response is less mainly due to the differences in the free-field ground motion characteristics.
-

**NRC Comment/Question:**

- 4.28 Furthermore, this section states that for the rock condition, no additional consideration of rotations due to ground motion incoherence appears to be warranted. Please explain if additional consideration of rotations due to ground motion incoherence would be warranted for a soil site.

**Industry Response/Resolution:**

- 4.28 See above discussions on the treatment of rotations. The revised Chapters 4, 5, and 6 contain additional details on this subject.
- 

**NRC Comment/Question:**

- 4.29 Page 6-17: This section states that all the analyses in this report are conducted for surface foundations even though many NPP structures have embedded foundations. This section further states that it is anticipated that the effects of embedment and the effects of incoherence are independent of each other but that analyses to demonstrate this relationship have not been performed. Please provide the basis of this assumption and state whether embedment effects will be considered in the individual plant ESP and/or COL application.

**Industry Response/Resolution:**

- 4.29 Embedment effects. See response to 4.2.  
A sensitivity study demonstrating the effects of incoherency on surface founded and embedded structures will be added as Appendix E of this report in the near future. This work will demonstrate the relation between incoherence and embedment. Considerations for individual plant ESP and/or COL application content are not part of this project. These considerations will be addressed within the EPRI Integration report (Task I1.1) as appropriate.
- 

**NRC Comment/Question:**

- 4.30 Page 6-17: This section states that in-structure spectra for one horizontal direction and for a surface founded and embedded model are shown in Figures 6-26 and 6-27, respectively. It is not clear what these Figures illustrate. Please elaborate.

**Industry Response/Resolution:**

- 4.30 These results were removed because the case analyzed did not have significant embedment effects, i.e., the embedment depth compared to the plan dimensions was small.
-

**NRC Comment/Question:**

4.31 PGAs for horizontal and vertical direction are almost a factor of 2 apart, see series of figures marked 6 -1 through 6-6.

**Industry Response/Resolution:**

4.31 Agree. See response to 4.22. Not sure what the question is here, but we assume it is similar or the same as RAI 4.22.

---

**NRC Comment/Question:**

4.32 Figures 6-14 through 6-25 use the label SSI-CTF, but CTF does not seem to have a definition.

**Industry Response/Resolution:**

4.32 Agree – Figures 6-14 through 6-25 in the original report use “CTF”. This should be “ITF”. This typo was corrected in this revised report.

---

**NRC Comment/Question:**

4.33 Page 7-2: This section states that it was judged to be slightly conservative to not include wave passage effects. Please explain if the wave passage effect might have a bigger impact on rocking and torsion.

**Industry Response/Resolution:**

4.33 Wave passage might have larger effect on torsion and rocking, but only accompanied with a corresponding reduction in effective translational input. It is judged to be slightly conservative to ignore wave passage because, at the well-recognized apparent wave velocities (values approximating 4 km/sec or greater), the effect of wave passage on SSI response of these types of foundations/structures is calculated to be minimal. Results have been added to the report for the cases of apparent wave velocities of 2 km/sec and 4 km/sec in Chapter 4. The results show that it is conservative to ignore the effects of wave passage.

---

**NRC Comment/Question:**

4.34 The conclusions are well laid out; however the issue of embedded foundations is not discussed and majority of reactor designs use structures that are embedded to depths between 20 to 60 ft.

**Industry Response/Resolution:**

4.34 Thank you. Please see response to 4.2 above for embedment.

---

**NRC Comment/Question:**

4.35 p. ix first bullet and p. 8-6 second bullet: It is stated that: *“The basic effect of incoherence on seismic response of structures has been demonstrated and validated through recorded ground motions and analyses of their effects with alternative methods and programs.”* The report presents analyses utilizing a simulated time history based on the response spectra of Fig. 2-5 or using random vibration theory with power spectra derived from the response spectra of Figs. 2-5 and 2-6. Was there a separate analysis performed with recorded ground motions?

**Industry Response/Resolution:**

4.35 This conclusion bullet has been modified in response to this RAI in order to alleviate any confusion on the review performed relative to recorded ground motions. Appendix B addresses the review of recorded ground motions to assess the potential to validate the methods recommended within this study on seismic wave incoherence.

---

**NRC Comment/Question:**

4.36 There are two typos in Table 2-1, p. 2-1: for the horizontal ground motion  $f_c$  the first term in the expression should be  $-1.886+...$  instead of  $1.886+...$ , and for the vertical ground motion  $f_c$  the last term of the expression should be  $...+1))^2)$  instead of  $...+1))2)$ .

**Industry Response/Resolution:**

4.36 Agree, these two typos were corrected. Thank you.

---

**NRC Comment/Question:**

- 4.37 The variation of the soil shear wave velocity with depth in Fig. 2-4 (p. 2-5) does not fully correspond to the values provided in Table 2-3 (p. 2-6). Additionally, it is stated on bottom of p. 2-5 that "...and then a half-space of bedrock at a shear wave velocity of 4300 fps". The entry for the half-space shear wave velocity in Table 2-3 is 4150 fps. Which is the soil profile used in the analysis?

**Industry Response/Resolution:**

- 4.37 See answers to previous RAIs 4.16 and 4.17. Appropriate clarifications have been made in the report.

---

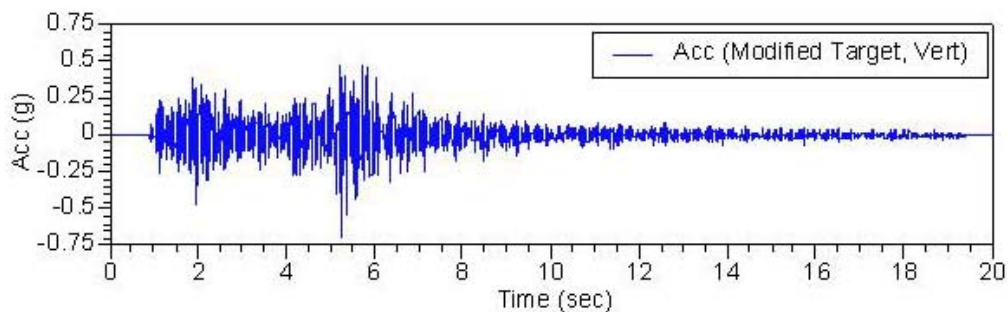
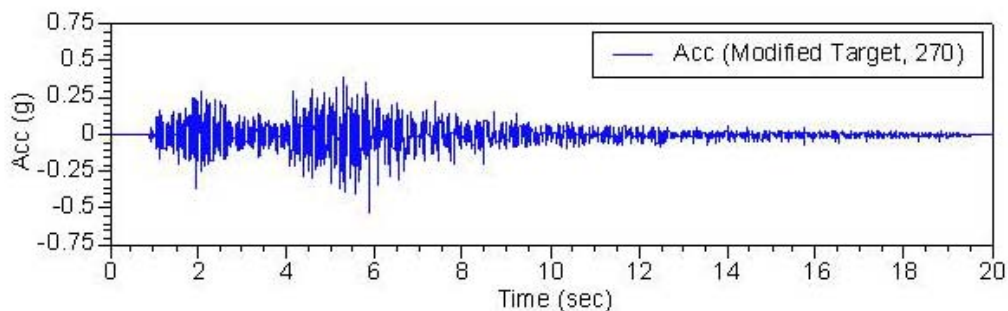
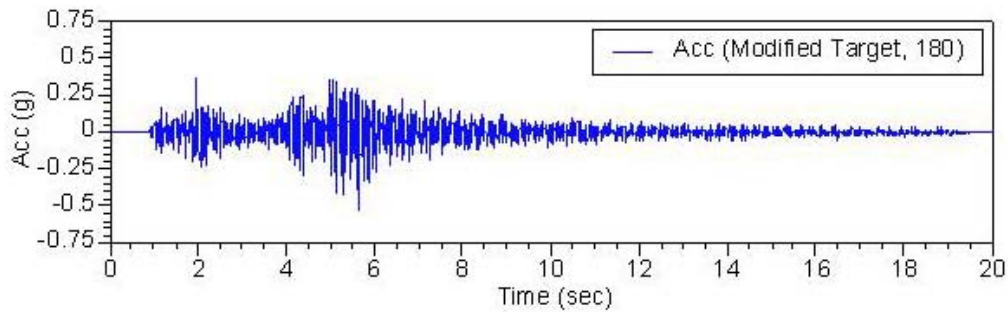
---

**NRC Comment/Question:**

- 4.38 It is stated on p. 2-8 last paragraph that: "For soil-structure interaction analyses and the evaluation of structure response including the effects of seismic wave incoherence, spectrum compatible time histories for the rock site were required. Three uncorrelated components were generated for two horizontal directions and the vertical direction." What was the time step for the generation of the time histories? What was the duration? What amplitude modulating function was utilized to transform the generated stationary time histories to non-stationary? It would be helpful if the time histories were presented.

**Industry Response/Resolution:**

- 4.38 These were generated by Dr. Abrahamson as being appropriate to the site conditions and the likely earthquake parameters. The reference time history that was selected for the development of the spectrum compatible time histories was recorded at the USGS station at the Keenwild Fire Station in Southern California (June 12, 2005 Anza Earthquake). The time duration was approximately 15 seconds. The time step was 0.005 seconds. The acceleration time histories are depicted below.



**NRC Comment/Question:**

4.39 It is stated on p. 2-9 that: “The SSI seismic analyses, by CLASSI and SASSI, were performed for the 150-ft square foundation footprint. For these analyses the foundation was assumed to be 15-ft thick. ...” Wasn’t the foundation massless in the CLASSI and SASSI benchmark problem comparisons (Section 4)? Were there additional comparisons made? Why was a 15-ft foundation thickness selected?

**Industry Response/Resolution:**

4.39 Original benchmark problems were for rigid massless foundation response. Recently, benchmark problems have been added comparing CLASSI, Bechtel SASSI, and ACS SASSI by ARES. These new benchmark problems included the 3 stick structural model and the 15-ft thick foundation. In addition, all analyses described in Chapter 5 of the

current report utilized the 3 stick structure model with the 15-ft thick foundation. All of the benchmark comparison problems are documented in Appendix C. We examined the basemats of several new plant designs and the foundation thicknesses vary between designs and over the plan dimensions. A 15-ft uniform thickness was assumed for the benchmark models for comparison purposes only, and is not meant to represent an AP1000 specific model.

---

---

**NRC Comment/Question:**

- 4.40 Figure 2-8: Shouldn't the foundation footprint dimensions be < 150' or 225' > instead of < 100' or 225' > in the X-direction and < 150' or 100' > instead of < 100' > in the Y-direction?

**Industry Response/Resolution:**

- 4.40 Dimensions on Figure 2-8 have been revised.

---

---

**NRC Comment/Question:**

- 4.41 There are some typos in Eq. 3-14 (p. 3-5): It should read  $[HT] = ([\alpha s] + [\varphi s] [D] [\Gamma s]) [HF]$  instead of  $[HT] = ([\alpha s] / [\varphi s] T [D] [\Gamma s]) [HF]$ .

**Industry Response/Resolution:**

- 4.41 Agree. Equation 3-14 has been changed to reflect the removal of the transpose. The Wen Tseng 1997 EPRI report contained a typo and the divide symbol was included in the equation. This also has been changed.

---

---

**NRC Comment/Question:**

- 4.42 It is stated in subsection "Procedure to Evaluate the Foundation and Structure Incoherent Response Spectra by CLASSI" that "The complete random vibration approach described above could have been employed herein" (p. 3-5), but that "Ground motion time histories are transformed into the frequency domain, SSI parameters (impedances and scattering matrices) are complex-valued, frequency-dependent, and the structure is modeled using fixed-base eigen systems. SSI analyses are performed—output are time histories of interest from which in-structure response spectra are computed. The resulting in-structure response spectra at structure and foundation locations of interest include the effects of soil-structure interaction and seismic wave incoherence" (p. 3-6). This process is not random vibration analysis – this is a deterministic time history analysis utilizing the frequency domain.

## **Industry Response/Resolution:**

4.42 The actual text follows for p. 3-5:

“The complete random vibration approach described above could have been employed herein. However, the formulation of CLASSI and its ease of use permitted implementation of a more direct approach to the SSI analysis of structure/foundation.”

The random vibration approach was used to generate the incoherency transfer functions (ITFs), which in CLASSI nomenclature are the scattering functions. These scattering functions are the key element to account for the effects of incoherence on the foundation input motion. This approach is described in detail in Chapter 3.

Once having determined the scattering functions, their application to the SSI analysis of a foundation/structure system could have been performed assuming random vibration theory only. This approach would have consisted of converting the free-field ground response spectra into PSDs, analyze the soil-structure system using the frequency-dependent impedance matrix and scattering functions, incorporating the dynamic characteristics of the foundation and structure system, and solving for the PSDs of in-structure response. Then, converting those in-structure response PSDs to in-structure response spectra as appropriate.

The alternative was to use CLASSI in a conventional manner, i.e., perform all of the above solution steps, again with scattering functions developed from RVT approaches as described in detail in Chapter 3, perform SSI analyses in the frequency domain, which entails converting the free-field ground motion time histories (derived to be compatible with the free-field ground response spectra) into its FFT, performing SSI analysis in the frequency domain, i.e., using the same steps as described above, calculating the Fourier Transform of in-structure response and Inverse Fourier transform those into the time domain. These in-structure time histories are processed to calculate in-structure response spectra for response comparisons.

In conclusion, the RVT approach is used to develop the ITFs, or scattering functions, which are used in the standard CLASSI SSI analysis procedure.

---

## **NRC Comment/Question:**

4.43 It is stated on p. 3-6 that “For this application, a 6 by 6 complex incoherency transfer function matrix [ITF] is evaluated by taking the square root of  $[S_{UoI}]$ , the 6 by 6 complex cross PSD matrix of rigid massless foundation motion to unit PSD input. The scattering matrix for vertically propagating waves is replaced by the columns of the incoherency transfer function matrix at each frequency of interest that correspond to the directions of input excitation”. Was the square root of the entire  $[S_{UoI}]$  matrix considered in the approach by replacing all columns of the scattering matrix by the columns of the ITF matrix, as indicated on p. 3-6, or were only the diagonal elements of the ITF matrix considered as indicated throughout the rest of the report?

## **Industry Response/Resolution:**

- 4.43 The diagonal elements of the CPSD matrix were used to define the scattering functions. For developing these scattering functions, each of the three directions was analyzed separately and the scattering functions extracted for the each of the three directions of free-field ground motion.

---

---

## **NRC Comment/Question:**

- 4.44 In Section 4 it is stated that the benchmark problem comparison utilized:

Two different algorithms; CLASSI–stochastic method and SASSI-eigen decomposition method

Two different analytical approaches; random vibration theory (RVT) by CLASSI and time history dynamic analyses by SASSI

Regarding the second bullet: Both CLASSI and SASSI utilize a time history analysis, with the only difference being that the CLASSI approach described in the report transforms the time history in the frequency domain, conducts the evaluation in the frequency domain and transforms the results back into the time domain as noted in I-8. Hence, the results regarding this aspect should be expected to be identical, assuming that CLASSI and SASSI have been validated before regarding fully coherent incident motions.

Regarding the first bullet: The approach used in CLASSI is described in the report, whereas that of SASSI is not. However, Report TR-102631 (1997) describes an eigen decomposition approach for the incorporation of the spatial incoherence of seismic ground motions in SASSI through the module “INCOH”, which also utilizes eigen decomposition. If the evaluations by SASSI are based on the approach described in Report TR-102631 (1997), the following is observed regarding the benchmark comparison: The CLASSI – stochastic method described in this report in Section 3 is identical to the stochastic approach described in the TR-102631 report (1997), also in their Section 3.

The only difference is that this report incorporates the coherency matrix  $[\gamma]$  fully in the analysis by using matrix analysis and taking the square root of the cross spectral density matrix of the rigid massless foundation motion  $[S_{UoI}]$  (Eq. 3-2 on p. 3-2), whereas the “INCOH” module of the TR-102631 report performs an eigenvalue decomposition of  $[\gamma]$  and retains its dominant modes. The module “INCOH” was validated in Section 5 of Report TR-102631 (1997) utilizing SASSI with previous studies conducted by Luco and Mita (1987) for a circular, rigid, massless foundation and Mita and Luco (1986) for the response of a flexible, cylindrical structure.

If the evaluations by SASSI are based on the “INCOH” module described in Report TR-102631 (1997), the benchmark comparison in this report simply suggests that the eigen decomposition of the coherency matrix  $[\gamma]$  by SASSI contained sufficient number of modes to capture the full effect of  $[\gamma]$  considered by CLASSI. Additionally, if this is the

case, retaining higher modes in the decomposition would render the SASSI results in Figs. 4-1, 4-2 and 4-3 smoother, as are those evaluated by CLASSI.

**Industry Response/Resolution:**

- 4.44 The approach to modeling incoherence of ground motion in CLASSI is derived in detail in Chapter 3 of the report. The approach follows EPRI (1997). Changes to the methodology are in the form of the coherency of ground motion and its application to the particular problems investigated. The approach of SASSI is similar to that described in EPRI (1997). Two versions of SASSI were used in the comparison studies. The two versions have been generated from the same basic approach, but have evolved separately over time. The approaches, including key differences, are summarized in Chapter 6.

The comparisons of the foundation and in-structure responses as reported in Appendix C are remarkably close. The differences in methodologies, computer programs (CLASSI, and two versions of SASSI), and analysts performing the analyses would be expected to lead to some greater differences than observed. The one similarity in methodology for the CLASSI and SASSI is the fact that they both solve the SSI problem in the frequency domain. These very good comparisons adequately validate the two approaches.

---

**NRC Comment/Question:**

- 4.45 What input motion was used in the benchmark comparison? It is stated on p. 4-1 that “Input earthquake excitation was the rock input motion for which the response spectra are shown in Figure 2-5”. However, the maximum horizontal acceleration in Fig. 2-5 is ~ 1.48g whereas the maximum horizontal acceleration in Fig. 4-2 is ~ 1.0g, and the maximum vertical acceleration in Fig. 2-5 is ~ 1.38g whereas the maximum vertical acceleration in Fig. 4-3 is ~ 0.9g.

**Industry Response/Resolution:**

- 4.45 The rock input motion used for studies reported in the body of the report are those of Figure 2-7. Some of the Benchmark Comparisons documented in Appendix C were based on ground motions with the same basic characteristics, but with different amplitudes.

---

**NRC Comment/Question:**

- 4.46 It is stated on p. 2-3 that a damping ratio of 0.02 is assumed, whereas on p. 4-1 for the benchmark problem the damping is considered as 1 percent. Also, the bedrock shear wave velocity for the bedrock is considered as 4300 fps on p. 2-5, 4150 fps in Table 2-3 and 6300 fps for the benchmark comparison. Which damping values and shear wave velocities were used? Or were there different response spectra and corresponding time histories developed for the benchmark problem? This may also be associated with I-11.

### **Industry Response/Resolution:**

- 4.46 Tables 2-2 and 2-3 itemize the rock and soil properties used in the studies presented in the body of the report. Appendix C itemizes rock material properties used in the Benchmark Analyses.

---

### **NRC Comment/Question:**

- 4.47 It is stated on p. 5-4 that the soil profile does not affect the ITFs, which are basically identical at all frequencies for soil and rock (Figs. 5-13 and 5-14). This should be expected if the matrix  $[S_{U_{01}}]$  in Eq. 3-2 were controlled by  $[\gamma]$  only, which is considered identical for rock and soil sites according to the coherency model. However,  $[S_{U_{01}}] = [F] [S_{U_{GI}}] [FC]^T$  (Eq. 3-2) also contains the scattering transfer function  $[F]$ , and the ITFs are the square root of the diagonal terms of  $[S_{U_{01}}]$ . How dependent is  $[F]$  (Eq. 3-3) on the site properties or is it only function of location and frequency? If  $[F]$  depends on the site properties, this should be reflected in the ITFs, which, consequently, should differ for soil and rock sites.

### **Industry Response/Resolution:**

- 4.47 The independence of the scattering transfer function  $[F]$  from soil properties is a direct result of the CLASSI formulation which considers the response of a rigid surface inclusion on a layered half-space (i.e., a rigid massless foundation) as the driving input motion for the SSI solution. Let the modification of the field-field surface motion due to the presence of the rigid surface inclusion be represented by six component vector  $\{U_0^*\}$ . The average free-field surface motion of each of  $n$  sub-regions that represents the interface of the rigid foundation area with the half-space surface is represented by the  $3n$  component vector  $\{U_n\}$ . We seek the motion of a reference point of the rigid inclusion  $\{U_0^*\}$  in terms of the set of sub region motions  $\{U_n\}$  and define the  $6 \times 3n$  scattering transfer function  $[F]$  as  $\{U_0^*\} = [F] \{U_n\}$ . Given the  $3n \times 3n$  array  $[G]$  of Green's functions integrated over each sub-region, and the  $3n \times 6$  rigid body transformation array  $[\alpha_b]$ , defined by  $\{U_n\} = [\alpha_b] \{U_0^*\}$ , we may compute the impedance of the driving forces  $\{P_0\}$  applied to the rigid inclusion as the  $6 \times 6$  array,  $[K] = [\alpha_b]^T [G]^{-1} [\alpha_b]$ , where  $\{P_0\} = [K] \{U_0^*\}$ . We note that  $\{P_0\} = [\alpha_b]^T [G]^{-1} [\alpha_b] \{U_0^*\} = [\alpha_b]^T [G]^{-1} \{U_n\}$ . The array  $[G]^{-1} [\alpha_b]$  may be identified as the  $3n \times 6$  traction array  $[T]$  for which  $[T]^T = [\alpha_b]^T [G]^{-1}$  and thus  $\{P_0\} = [T]^T \{U_n\}$ . Since,  $\{P_0\} = [K] \{U_0^*\} = [T]^T \{U_n\}$ , we may write  $\{U_0^*\} = [K]^{-1} [T]^T \{U_n\} = [C] [T]^T \{U_n\}$  where  $[C] = [K]^{-1}$  is the  $6 \times 6$  compliance array of the rigid inclusion reference point. Referring to the definition of the scattering transfer function we may identify  $[F] = [C] [T]^T$ .

Since  $\{U_n\} = [\alpha_b] \{U_0^*\}$ , we may also form,  $[\alpha_b]^T \{U_n\} = [\alpha_b]^T [\alpha_b] \{U_0^*\}$ . Now,  $\{U_0^*\} = ([\alpha_b]^T [\alpha_b])^{-1} [\alpha_b]^T \{U_n\}$  which may be identified as the least squares solution for the average motion of the rigid surface inclusion given the over-determined free-field motion of the  $n$  sub-regions  $\{U_n\}$ . Again, referring to the definition of the scattering

transfer function, we may identify  $[F] = ([\alpha_b]^T[\alpha_b])^{-1}[\alpha_b]^T$  from which it may be verified that the scattering transfer function is independent of any soil properties, being determined only by the rigid body kinematics of the rigid foundation motion. The use of the identity  $[F] = [C][T]^T$  is actually equivalent to the least squares solution and is a convenient means of computation for the scattering transfer function given the CLASSI computation of  $[K]$  and  $[T]$  for solution of the SSI problem.

Now, given the  $3n \times 3n$  cross spectral density response matrix of the rigid massless foundation accounting for incoherence as  $[SUG] = [S01/2][\gamma][S01/2]$ , then the  $6 \times 6$  cross PSD of the rigid massless foundation is found from  $[SU0^*] = [F] [SUG][FC]^T$ , where  $[FC]$  is the complex conjugate of  $[F]$ . Thus, the response of the rigid massless foundation is controlled by  $[\gamma]$  only.

---

**NRC Comment/Question:**

4.48 In the subsection “Spectral Corrections” on p. 5-10, where random vibration analysis is utilized, what was the equivalent duration of the seismic motions used in the conversion between power spectra and response spectra?

**Industry Response/Resolution:**

4.48 Six seconds was used for the seismic motions, which was judged to be typical/representative of EUS rock motions.

---

**NRC Comment/Question:**

4.49 It is stated in the subsection “Spectral Corrections” on p. 5-10, as well as earlier on p. 5-4, that the response spectra for the square 150 ft x 150 ft and the rectangular 100 ft x 225 ft are identical. Is there an explanation for this? It is also mentioned that the ITFs are identical for the two foundation shapes. Are all terms of the  $[S_{UoI}]$  matrix in Eq. 3-2 identical (or close) for both foundation shapes?

**Industry Response/Resolution:**

4.49 The studies performed in this scope of work have demonstrated that the most important parameter affecting translational responses is the area of the foundation. Induced rotations are dependent on the foundation shape. These observations are discussed in detail in Chapter 4.

---

**NRC Comment/Question:**

4.50 On p. 5-11 it is stated that “It may be seen that spectral reductions are significantly greater than the ASCE 4 values for the rock site but are actually somewhat similar for the soil site.” There seem, however, to be very significant differences between the ASCE 4 and the soil spectral corrections especially for the 150-ft square foundation in both

horizontal and vertical directions, and the 300-ft square foundation in the vertical direction. Also, is there a reason behind the increase in the values of the horizontal spectral corrections at the 50.0 Hz frequency for all foundations supported on soil?

**Industry Response/Resolution:**

4.50 Chapter 4 revises these observations.

---

**NRC Comment/Question:**

4.51 A previous analysis by Luco and Wong (1986) evaluated the response of a rectangular, rigid, massless foundation subjected to spatially random ground motions. Because their analysis and results are closely related to those presented in this report, their work is briefly described herein for clarity in this question.

**Industry Response/Resolution:**

4.51 Thank you for the effort undertaken to summarize that work here. This NRC comment labeled 4.51 is not a question and thus, doesn't require a response. The question is within RAI 4.52.

---

**NRC Comment/Question:**

4.52 Figure I-1 presents the layout and coordinate system of the Luco and Wong analyses. It is considered that the rectangular ( ) massless, rigid foundation is bonded to a visco-elastic half-space with Poisson's ratio of 1/3 and material damping ratio of 0.01.

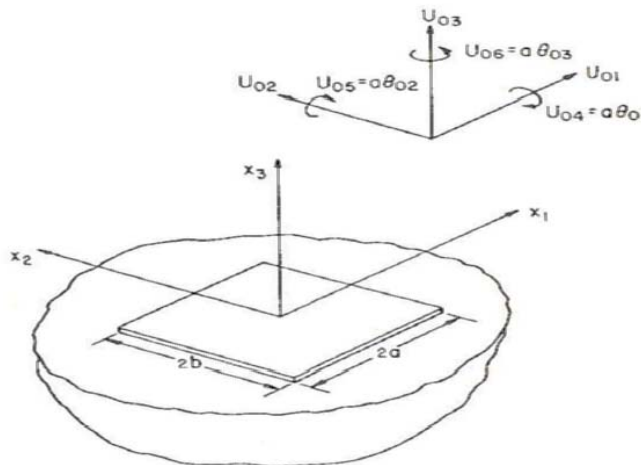


Figure I-1. Layout of foundation and coordinate system (from Luco and Wong, 1986).

The coherency expression of Luco and Wong (1986) is of the form:

$$\gamma_{LW}(f, \xi) = \exp[-(v2\pi f \xi / \beta)^2] \quad (I-1)$$

where  $v$  is a coherency drop parameter associated with random inhomogeneities and variations in elastic properties along the path of body waves,  $\beta$  is an estimate of the elastic wave velocity,  $f$  is frequency in Hz and  $\xi$  is separation distance in m. Figure I-2 presents a comparison of the Abrahamson coherency model used in this report for horizontal and vertical motions (Eqs. 2-1 and 2-2 in the report) with the Luco and Wong coherency (Eq. I-1 herein) for  $\beta = 1921.5$  m/sec (=6300 fps), i.e., the one used in the benchmark problem,  $v = 0, 0.1, 0.2, 0.3, 0.4,$  and  $0.5$  as used by Luco and Wong, and at separation distances of 10 m and 45.75 m (= 150 ft), the latter being the length of each side of the foundation in the benchmark problem. The approach described in Luco and Wong assumes that the coherency decay is the same in the two horizontal and the vertical directions. The value  $v = 0$  represents fully coherent motions. The model of Luco and Wong decays more slowly with frequency at the shorter separation distances than the Abrahamson coherency model. At the longer separation distance, the value of  $v = 0.5$  falls in-between the horizontal and vertical Abrahamson models. At longer separation distances, the Luco and Wong model falls off more sharply with frequency than the Abrahamson models.

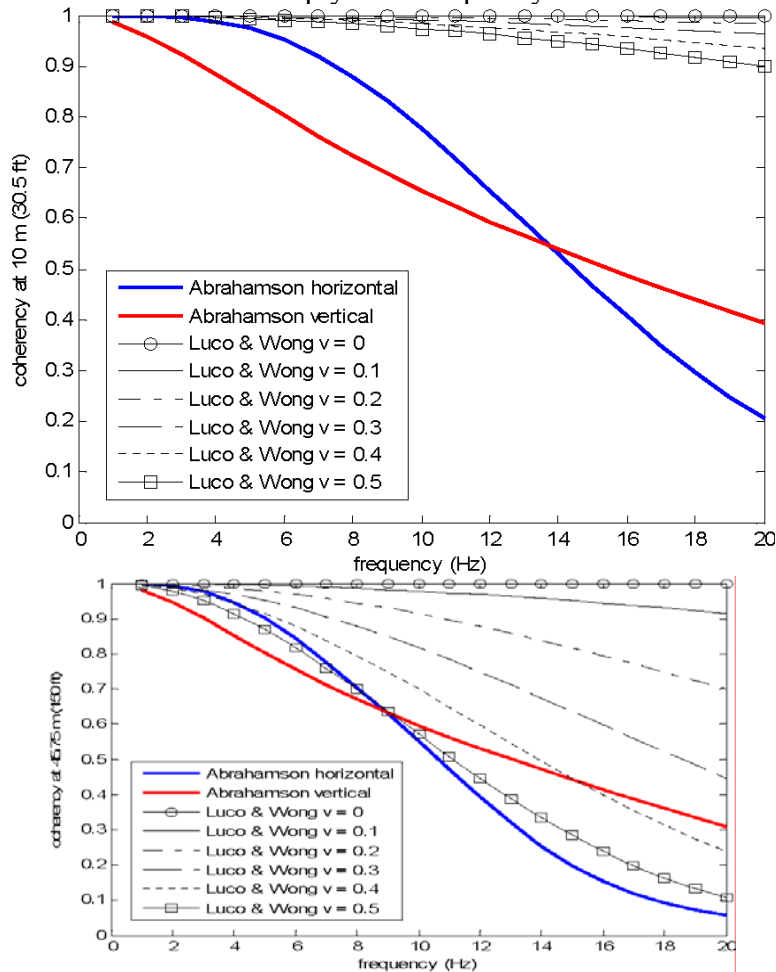
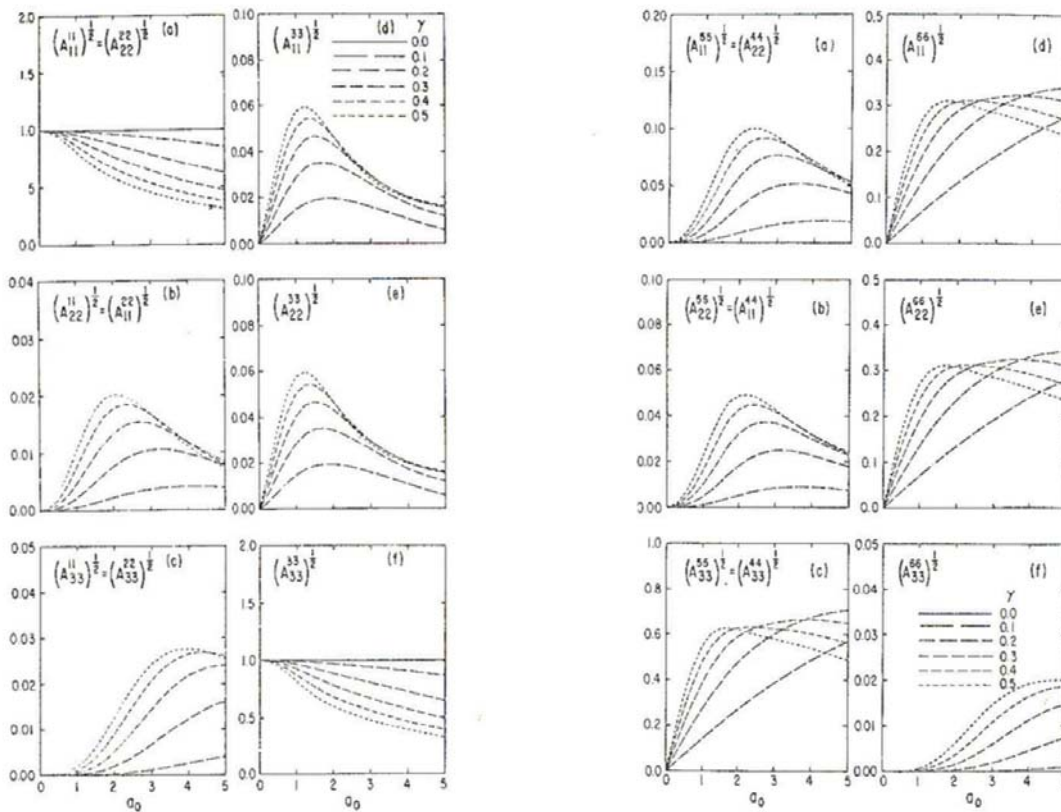


Figure I-2. Comparison of the Abrahamson and the Luco and Wong coherency models at separation distances of 10 m and 45.75 m (= 150 ft).

Luco and Wong's (1986) results for a square ( $2a \times 2a$ , Fig. I-1) foundation subjected to motions experiencing loss of coherency are presented in Fig. I-3a for the translational response components, and Fig. I-3b for the rotational response components. The results are presented as functions of the dimensional parameter  $\sigma$  and for variable values of  $\nu$ . An increase of " $\sigma$ " in the dimensional parameter in the figures, considering that  $a = 150$  ft, is equivalent to 13.37 Hz for  $\beta = 6300$  fps used in the benchmark comparison, and 9.125 Hz for  $\beta = 4300$  fps suggested on p. 2-5, yielding maximum values for the frequency at  $\sigma = 5$  of 66.85 Hz and 45.62 Hz, respectively.

According to Luco and Wong (1986),  $a_c \sqrt{A_{ij}^{ij}}$ ,  $i=1, 2, 3$  and  $j=1, 2, \dots, 6$ , can be interpreted as the amplitude of a transfer function between the  $i$ -th component of the excitation and the  $j$ -th component of the response (Fig. I-1). In this sense,  $\sqrt{A_{11}^{11}} = \sqrt{A_{22}^{22}}$  in Fig. I-3a, subplot (a), corresponds to the ITFs provided in the report in any of the two horizontal directions, and in Fig. I-3a, subplot (f), to the ITF in the vertical direction. As can be seen from Fig. I-3a, loss of coherency in a specific direction results in significant reduction of translation in the corresponding direction ( $\sqrt{A_{11}^{11}}$ ,  $\sqrt{A_{22}^{22}}$ ,  $\sqrt{A_{33}^{33}}$ ), but affects only minimally the translational response in the other directions.



(a) translational response

(b) rotational response

The decay of the transfer functions  $\sqrt{A_{11}^{11} A_{11}^{11}}$ ,  $\sqrt{A_{22}^{22}}$ ,  $\sqrt{A_{33}^{33}}$  in Fig. I-3a is much slower than the ITFs presented in the EPRI report, possibly because the Luco and Wong model produces significantly higher coherency values than the EPRI model (Fig. I-2). Figure I-3b presents the results for the rotational components of the foundation. According to Luco and Wong (1986), can be interpreted as the amplitude of the transfer function between the  $i$ -th component of the excitation and the foundation response  $\tilde{U}_{05} = a\tilde{\theta}_{05}$  (Fig. I-1), i.e., rocking about the  $x_2$  axis. Hence, and represent the rocking transfer functions due to the vertical excitation, and  $\sqrt{A_{11}^{66}}$  and  $\sqrt{A_{22}^{66}}$  the torsional response caused by the horizontal motions. Figure I-3b then suggests that the rocking response about the  $x_1$  and  $x_2$  axis are mostly associated with the vertical component of the free-field ground motion, and the torsional response about the  $x_3$  axis is associated with the  $x_1$  and  $x_2$  components of the Figure I-3. Foundation response to seismic ground motions exhibiting loss of coherence (from Luco and Wong, 1986). The coherency drop parameter “ $\gamma$ ” in the figure is referred to in the text as “ $\nu$ ” because “ $\gamma$ ” in the EPRI reports refers to the coherency function.

Figure I-3b indicates that rocking caused by the vertical motions (subfigure (c)), and torsion caused by the horizontal motions (subfigures (d) and (e)) can be significant, and increase as  $\nu$  increases (and coherency decreases, Fig. I-2). It is also noted from Fig. I-3b, subfigures (c), (d) and (e), that as  $\nu$  increases, the peaks of  $\sqrt{A_{33}^{44}}$ ,  $\sqrt{A_{33}^{55}}$ ,  $\sqrt{A_{11}^{66}}$  and  $\sqrt{A_{22}^{66}}$  shift towards the lower frequencies. On the other hand, the negligible effect of rocking discussed on p. 6-10 of the EPRI report appears to be counter-intuitive, in that the large reductions in the translational response due to incoherency presented in the report do not result in any rotational effects. Since the Abrahamson coherency model drops more rapidly with frequency and separation distance than the Luco and Wong model (Fig. I-2), this should lead to even higher values for the rotational transfer functions, but it is stated in the report that their effect is negligible. Does the rotational effect become negligible in the report’s study, because, due to the sharp decay of the Abrahamson coherency model, the peak of the rotational transfer functions shifts to such low frequencies where the ground motions do not contain much energy? How do all elements of the  $[S_{UoI}]$  matrix of Eq. 3-2 (not only the translational ITFs) behave at different frequencies?

### **Industry Response/Resolution:**

4.52 The ITFs calculated in the present study are presented in Figures 4-13, 4-14, 4-15 and 4-16. These ITFs demonstrate the same shape and trends as Figure 2 of the study by Kim and Stewart (*Kinematic Soil-Structure Interaction from Strong Motion Recordings* by Seunghyun Kim and Jonathan Stewart, Journal of Geotechnical and Geoenvironmental Engineering, April 2003). This Figure 2 depicts the amplitude of the transfer function between free-field motion and the foundation input motion for different foundation shapes based on analytical formulations from Veletsos, Prasad, Luco, Wong, etc. as described in the above reference.

In addition, as discussed within the responses to several previous RAIs, there has been an expanded treatment of both rocking and torsion within Chapters 4, 5 and 6 to reflect additional models/studies in this area.

---

---

**NRC Comment/Question:**

- 4.53 There is insufficient information provided in the report to evaluate the effect of embedment and incoherence on p. 6-17. It is stated that “It is anticipated that the effects of embedment and the effects of seismic wave incoherence are independent of each other”. This depends on whether coherency is a function of depth or not. It is also stated on p. 6-17 that Figures 6-26 and 6-27 suggest “independency of embedment and incoherency”. If the same coherency model was used for the surface and the embedded structure, then the comparison between Figs. 6-26 and 6-27 indicates only the effect of embedment, not coherency. Also, in Fig. 6-26, what is the meaning of the response at an El. -21’ for a surface structure?

**Industry Response/Resolution:**

- 4.53 The issue of embedment has been addressed in Chapters 5 and 6 and in the response to RAI 4.2.

## Enclosure 2

# APPENDIX B

## VALIDATION OF INCOHERENCY EFFECTS THROUGH RECORDED EVENTS

---

Over the course of this incoherence structural response task, the project team has utilized the talents of the Technical Review and Advisory Group (TRAG) and individual NRC staff members to provide comments and insights on the use of incoherency relative to the new plant seismic response. One goal within this task has been to research whether actual recorded data could be utilized to provide specific validation of incoherent ground motion effects on foundations and structures reflected within the studies documented in this report. During a meeting at the NRC in late 2005 discussions centered around the review of past studies by researchers in this field such as Dr. Stewart and Dr. Kim, and on the earthquake recordings that have occurred at the Diablo Canyon and the Perry nuclear power plants. To address the potential of using recorded data for validation purposes, the project team researched the technical literature for studies that reflected such validation efforts and also collected available recording data for the Deer Canyon earthquake that affected the Diablo Canyon NPP and the Leroy earthquake that affected the Perry NPP. The results of these efforts are documented in the following sections of Appendix B. The overall conclusions from these studies are contained in section B.4.

### **B.1 Technical Literature on Validation of Incoherency Effects**

Significant effort has been expended over the last three decades to validate the effects of soil-structure interaction (SSI) on structure response with one emphasis being on recorded earthquake motions. The majority of these efforts have focused on total SSI effects, i.e., the combined effects of kinematic and inertial interaction. It is well recognized that it is very difficult to separate the effects of kinematic and inertial interaction in recorded responses. The most successful attempts to separate the effects are for structures where one of the phenomena is not deemed to be important. For example, a structure such as a stiff tank embedded in soil with relatively small mass may serve to demonstrate the effects of kinematic interaction with minimal inertial interaction effects (Ishii et al., 1984).

Kinematic interaction is due to the variation in ground motion over the contact surface of the soil/rock and structure/foundation. For surface-founded structures, this variation is that at the interface of the foundation and the surface of soil or rock, and due to horizontal spatial variation of motion. Generally, this horizontal variation is due to wave passage effects and incoherence of ground motion. The effects of wave passage on nuclear power plant structures, for reasonable wave propagation parameters, have been shown to be of minimal consequence. However, the effects of incoherence of ground motion are significant for nuclear power plant structures

founded on rock sites. For embedded foundations, kinematic interaction is due to the above phenomena and due to the spatial variation of the ground motion with depth in the soil or rock. Until recently, studies where kinematic interaction has been the primary focus were performed to investigate the spatial variation of ground motion with depth in the soil or rock and its effects on the response of structures with embedded foundations and partially embedded walls. These field observations of embedment verified the physics of the problem, i.e., generally, there is a reduction in motion with depth in the soil or rock and a corresponding reduction in foundation motion of structures. Chang et al. (1985) and Johnson (2003) summarize many of the efforts to document these phenomena.

Seismic wave incoherence has been recognized as a phenomenon of particular interest to structures of large plan dimensions and for structures with multiple supports and large distances between supports, e.g., bridges. As reported by Chang et al. (1985), the horizontal variation of ground motion was observed many years ago, but only verified through very limited recorded data.

In more recent times, significant free-field data has been recorded, which illuminates the phenomena of incoherence of ground motion particularly the horizontal variation of ground motion due to incoherence (Abrahamson 2005a, 2006a). It is this significant body of data, which has permitted the development and benchmarking of the techniques in the present report.

Taking into account the effect of seismic wave incoherence on seismic response of nuclear power plant structures is particularly important given the seismic hazards calculated for rock sites in the Central and Eastern United States (CEUS). Current probabilistic seismic hazard assessments (PSHAs) for rock sites in the CEUS result in site-specific Uniform Hazard Spectra (UHS) that contain significant amplified response in the frequency range above 10 Hz. As demonstrated earlier in this report, the effects of incoherence of ground motion increase with increasing frequency and distance between observation points. The most significant effects are for frequencies greater than 10 Hz. These effects of incoherence are to reduce the effective translational motion of the foundation and induce additional rotational excitations of the foundation for frequencies greater than 10 Hz. The effect on in-structure response is to reduce the high frequency content response for high frequency input ground motion. For these current CEUS ground motions, it is important to account for all aspects of SSI in calculating structure response of these structures.

Over the last decade, Stewart and colleagues have devoted significant effort to evaluating the effects of kinematic interaction on structures through observations. This body of work includes Stewart and Stewart (1997), Stewart et al. (1999a), Stewart et al. (1999b), and Kim (2001). Kim and Stewart (2003) summarize these efforts including results and recommendations for incorporation of incoherency effects into the design of conventional structures. Key points from the Kim and Stewart (2004) study are presented below:

- The approach taken to calculate transfer functions between recorded free-field ground motion and recorded foundation motion parallels that of Chap. 3 here, i.e., at a given frequency, the transfer function is the square root of the ratio of the diagonal terms of the cross power spectral density function (CPSD) matrix divided by the PSD of the input motion.

- The complete data set included twenty-nine instrumented sites: fourteen with near surface foundations and fifteen with piles. Multiple earthquakes were recorded at some of the fourteen sites. The fourteen near surface cases were evaluated, incoherency parameters estimated, and the results compared to the transfer functions of Veletsos et al. (1997). The structure-foundations systems were conventional structures.
- The focus of the studies was on foundation response. However, an important aspect of the evaluation was to approximately account for inertial interaction effects in the data. This was achieved for cases where in-structure response was recorded. In-structure response provided information as to the soil-structure frequencies at which corrections to the data or elimination of the data could be done. As mentioned above, it is very difficult to separate the phenomena of kinematic and inertial interaction. However, attempts were made to do so in the studies cited. Other considerations in the selection of data sites to be included were foundation conditions (near surface foundations, mat foundations, etc.), relatively close proximity of free-field instruments to the structures of interest, free-field instruments not so close that their recordings were significantly affected by structure response.
- Translational response of the foundations were taken from one of three sources: foundation response recorded at or near the foundation centroid, averaged response from multiple recordings on the foundation to estimate the centroid values, or the translational response recorded at the recording station uncorrected to the centroid, if that was the only data available. Rotational motion (torsion and rocking) was calculated from differences in recorded translational motions at points on the foundation divided by the distance between the points.
- An assessment was made of the suitability of the data based on signal processing concepts and only those ordinates found to meet the criteria were included. Generally, this led to the focus being on frequencies less than 10 Hz. Further, the highest confidence in the data was for translations. Rotations being calculated as differences in translations divided by a distance measure were much less reliable. In all cases, there is a great deal of scatter in the data.

Figure B.1-1 is reproduced from Kim (2001) to demonstrate a number of points.

- The quantity plotted is transmissibility, which is consistent with the ITF calculated in the body of this report. The transmissibility is a function of the ratio of the foundation response to the free-field motion. The three plots are for two components of horizontal ground motion and torsion.
- Kim and Stewart (2003) exercised several criteria to determine the data to be included in the regression analysis as discussed in the text herein. The conclusion was to perform the regression analysis to fit the parameters of the Veletsos model for frequencies less than 10 Hz. The frequency range of main interest to this study is greater than 10 Hz.

- Inertial interaction effects were isolated to the extent possible and the data points near the soil-structure fundamental frequency were adjusted.

In conclusion, the transmissibility functions oscillate significantly over the entire plotted frequency range (0 to 25 Hz). It is clear that matching the trend of the results is achievable, but matching the ITF or transmissibility of an individual earthquake will be extremely difficult.

- For correlation with theoretical representations, in addition to the factors discussed above, a number of other factors complicated the comparisons: foundation conditions (rigidity, embedment, etc.), assumption of purely vertically incident incoherent waves is likely not strictly correct (dispersion of motion due to reflections within the site), differences in the effects as measured for the two horizontal directions, the models assumed half-space or very simplified site profiles where certainly non-homogeneity of the site is the actual situation, etc.
- The conclusions of the evaluations are that the phenomena of incoherence of ground motion exists and should be taken into account when specifying the design ground motion for structures. The approach to account for incoherence is to apply a transfer function to the free-field ground motion to develop a design ground motion for the design seismic analysis – the same concept as proposed herein but without added provisions to account for induced rotations. The recommended transfer functions to be applied are the theoretical functions of Veletsos et al. (1997) with the assumption of ground motion incoherence given by an exponential decay. Limitations or caveats of this approach are principally on the foundation, i.e., foundations that are continuous or behave in a continuous manner (mat foundations or inter-connected spread footings), foundation dimensions less than 60 m. (presumably to more closely approximate rigid foundation behavior for conventional structures), and embedment ratios less than 0.5.

The approach recommended by Kim and Stewart (2003) is identical to the simplified method proposed within the body of this report with the following exceptions:

- The assumed ground motion coherency function is distinctly different from the Abrahamson functions (Abrahamson, 2005, 2006), which are based on the extensive body of recorded data – recorded over the last decade or so.
- No additional consideration for induced rotations is included in the recommended approach. The simplified method of Chapter 5 includes an added provision to account for induced rotations.

The majority of incoherency response validation studies to date have focused on conventional structures for many reasons. At the present time, due to the number of instrumented structures and the frequency of earthquakes (particularly in California), the only extensive data base of recordings exists for conventional structures. Studies such as the body of work by Stewart and colleagues are extremely valuable in validating the effects of incoherence on structure response. However, further validation of the phenomena for nuclear power plant structures is

sought. The following two sections discuss the observed behavior of the Diablo Canyon Nuclear Power Plant and the Perry Nuclear Power Plant subjected to earthquake ground motions.

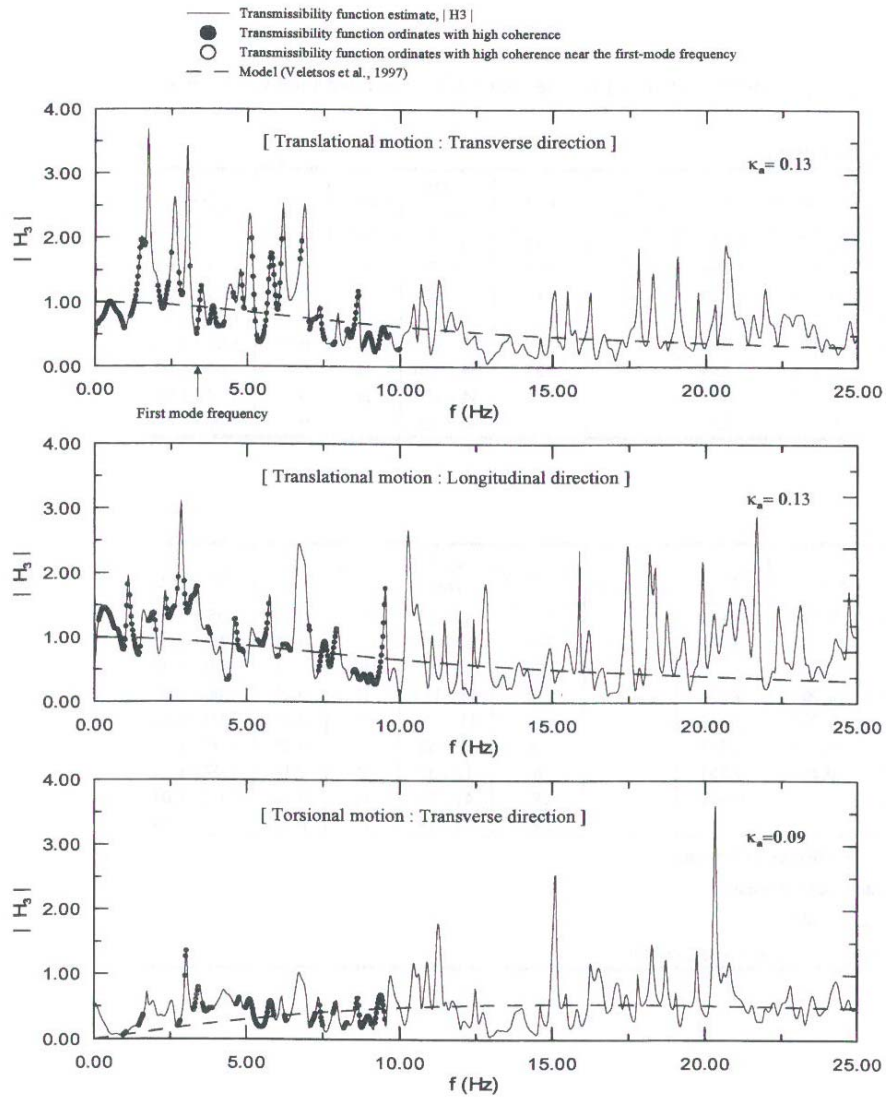


**Figure B.1-1**  
**Example of Transmissibility Functions for a Single Earthquake, Data Processed, and**  
**Estimation of Incoherence Parameter of the Free-Field Motion (Kim, 2001)**

## B.2 Diablo Canyon Earthquakes

The Diablo Canyon nuclear power plant in California has experienced recent earthquakes in which ground motion was recorded on the containment foundation and in the free-field. A magnitude 6.5 San Simeon earthquake was studied but found to have only low frequency motion (due to the high magnitude and being relatively far from the Diablo Canyon site). The Magnitude 3.4 Deer Canyon Earthquake that occurred October 18, 2003, however, provides an opportunity to compare calculated and measured incoherency effects. This relatively low magnitude earthquake ground motion is narrow banded with high frequencies in the 10 to 20 Hz range making this motion a good candidate for the study of ground motion incoherence effects. The peak ground acceleration is in the range of 0.01 and 0.02g depending on the component. Measured free-field and containment foundation motion are shown in Figure B.2-1. The containment motion is significantly reduced from the free-field motion at frequencies greater than 10 to 12 Hz.

Calculations simulating incoherent Deer Canyon foundation motion for the Diablo Canyon foundation footprint and soil conditions are compared to measured foundation and free-field Deer Canyon earthquake motion in this appendix. However, this approach does not account for SSI effects that may be a significant reason for high-frequency reductions of foundation motion relative to the free-field motion. To account for SSI effects, a transfer function relating horizontal foundation motion to horizontal free-field ground motion determined from soil-structure analyses of the Diablo Canyon plant many years ago is available in the literature (PG&E, 1988). The total transfer function between foundation and free-field motion is the product of an SSI transfer function and an incoherency transfer function. For purposes of discussion, the SSI transfer function, as used here, is comprised of two parts: the effects of vertical spatial variation of the ground motion, i.e., the combination of spatial variation with depth in the rock/soil at the site and the effects of the excavation and embedment of the foundation; and the inertial interaction effects. To compute an SSI transfer function for comparison to the transfer function from the SSI analyses, the transfer function of the total motion was estimated from the measured foundation and containment foundation motions and divided by the computed incoherency transfer function (ITF) determined by the CLASSI random vibration approach.

It should be recognized that the free-field seismic instrument at the time of the Deer Canyon earthquake was not located on the same rock type/formation as the Diablo Canyon containment foundation. A new free-field seismic instrument will be or has been installed to the north of the containment structure on the same rock type/foundation. Hence, difference in rock conditions is another difference between the free-field and containment foundation during the Deer Canyon earthquake.

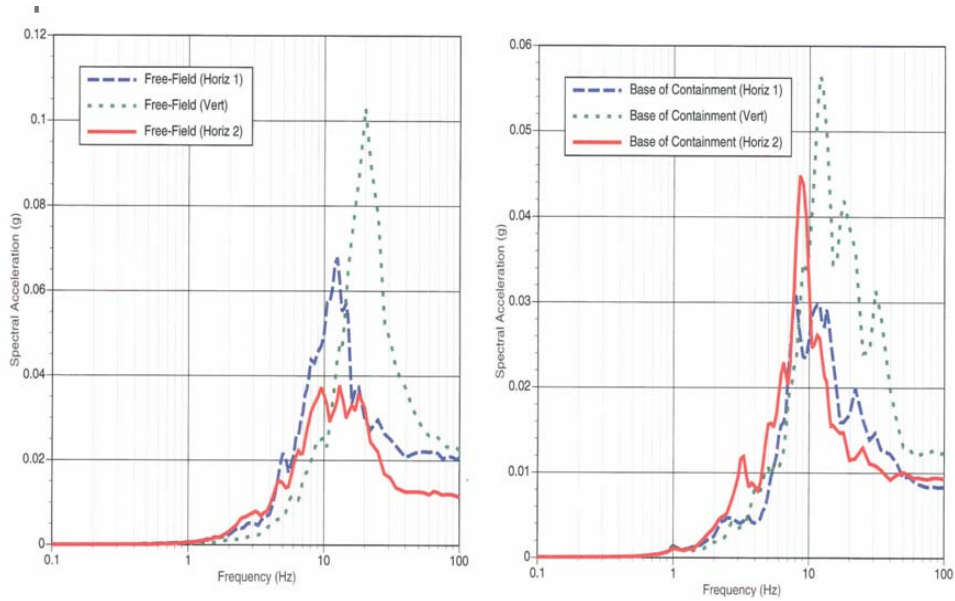
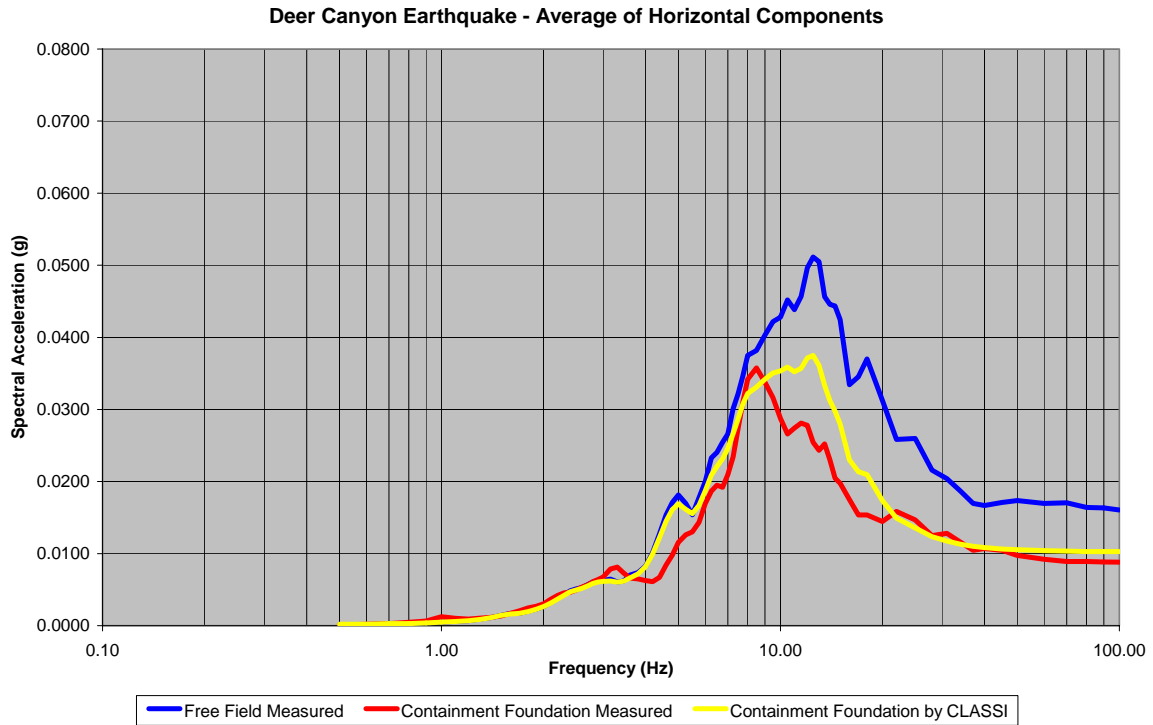
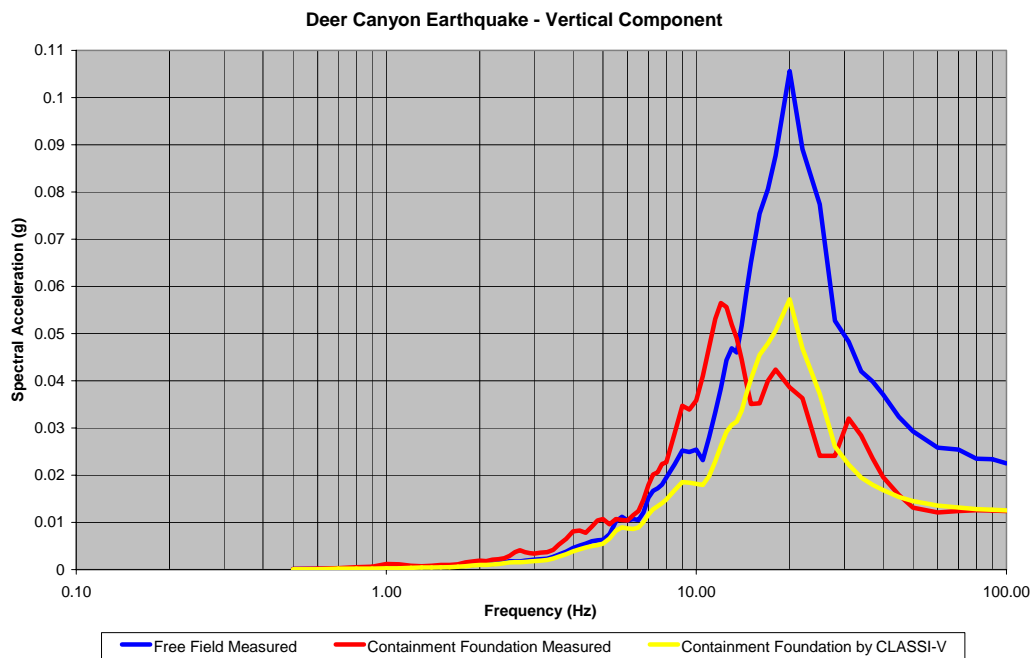


**Figure B.2-1  
Measured Earthquake Motion at Diablo Canyon from the 2003 Deer Canyon Earthquake**

The foundation of the Diablo Canyon containment structure has a 153 foot diameter circular footprint. Soil properties consist of a 3 layers over a half space. The layers are 10, 20, and 125 feet with shear wave velocities of 2600, 3300, and 4000 fps. The half space has a shear wave velocity of 4800 fps. Soil damping and densities used in the 1988 SSI analyses were also used. The free-field ground response spectra was input as a PSD using the CLASSI RVT approach in order to evaluate the containment motion PSD due to ground motion incoherence only considering the Diablo Canyon foundation as rigid and massless. The resulting PSD was then converted to a response spectra by random vibration theory for comparison to the measured foundation response spectra. The results of this calculation are shown in Figure B.2-2. The computed foundation motion is of the same amplitude as the measured motion but with slightly different frequency content. The measured motion has lower frequency content than the computed foundation motion indicating the effects of soil-structure interaction. As stated above, any difference in foundation and free-field motion is due to the combination of ground motion incoherence and soil-structure interaction. Hence, Figure B.2-2 is interesting but does not isolate the effects of ground motion incoherence and soil-structure interaction.



a. Horizontal Motion

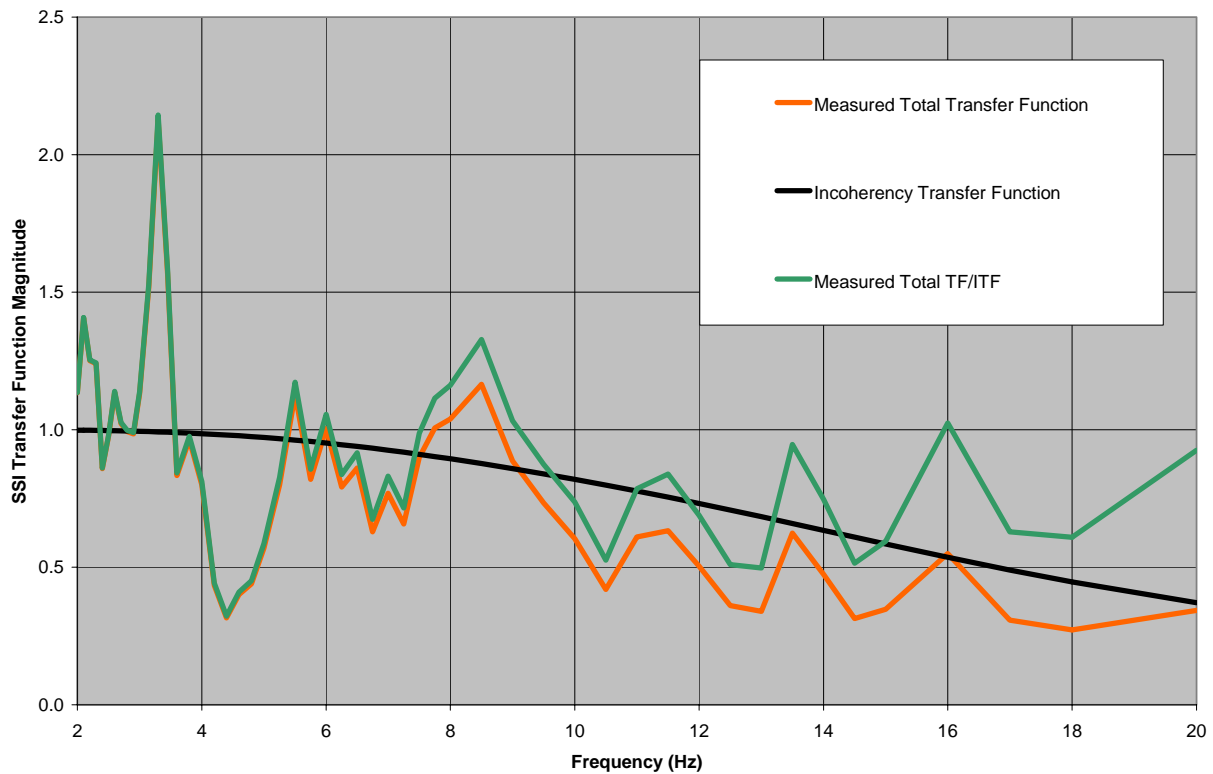


b. Vertical Motion

**Figure B.2-2**  
**Comparison of Measured and Computed Foundation Motion at Diablo Canyon**

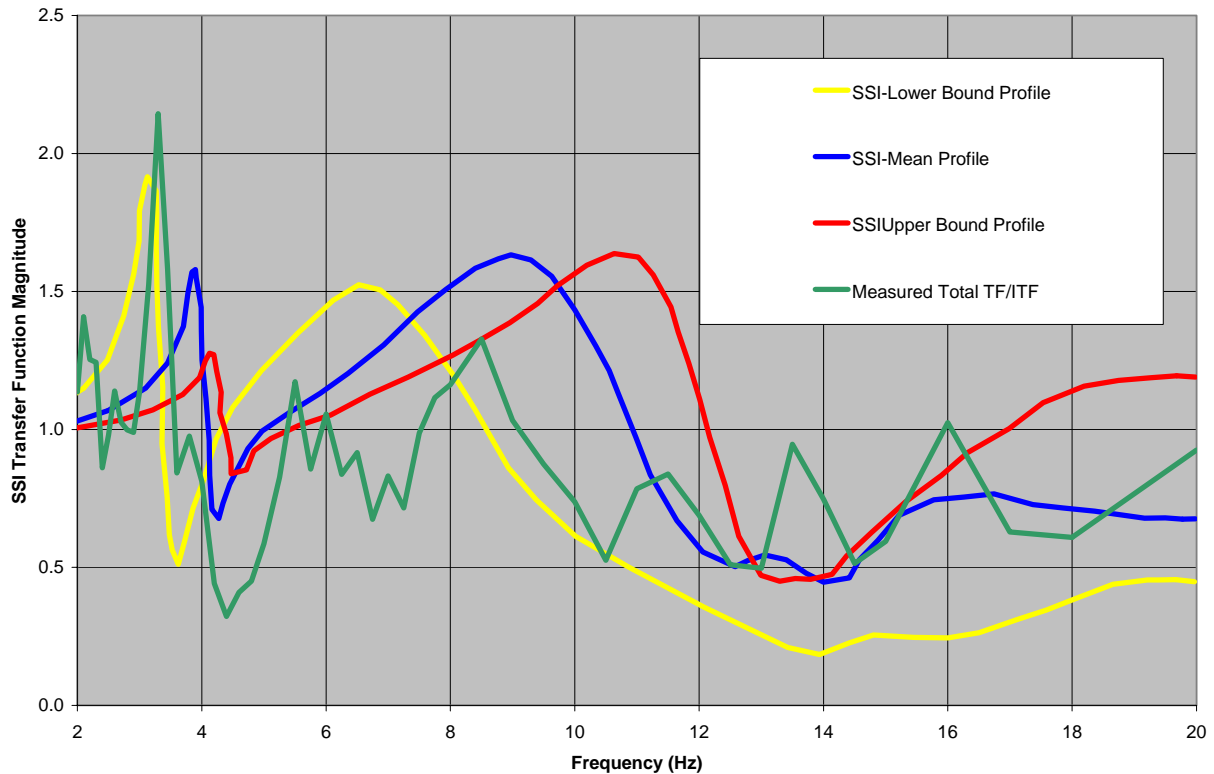
In order to isolate the effects of incoherency from other SSI effects (i.e., inertial interaction, embedment), the Diablo Canyon existing SSI transfer functions were compared to transfer

functions computed from the total motion transfer function and the incoherency transfer function. The total motion transfer function is estimated as the square root of the ratio of the foundation motion power spectral density to the free-field motion power spectral density. Each of these power spectral density functions are determined by random vibration theory using the foundation and free-field response spectra respectively. The incoherency transfer function is determined for the Diablo Canyon foundation footprint and soil properties in the same manner described in Chapter 4. The measured transfer function for the ratio of the square root of PSDs and the incoherency transfer function (ITF) are shown in Figure B.2-3. The estimated SSI transfer function is then equal to the measured transfer function divided by the incoherency transfer function and this result is also shown in Figure B.2-3.



**Figure B.2-3**  
**Total Motion, Incoherency, and Estimated SSI Transfer Functions**

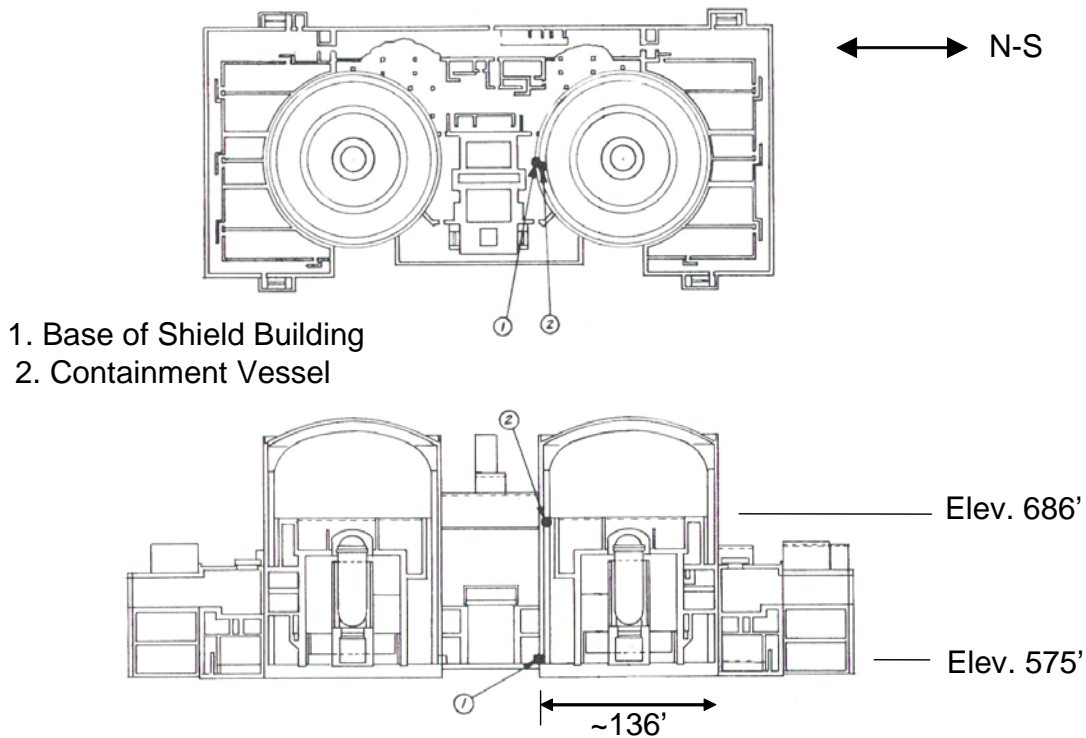
SSI transfer functions determined from the 1988 soil-structure interaction analyses are available for horizontal motion and for mean, upper bound and lower bound soil profiles. These SSI transfer functions are compared to the estimated SSI transfer function determined as the ratio of total to incoherency transfer functions in Figure B.2-4. It may be seen that the SSI transfer functions from SSI analyses are highly variable but the estimated SSI transfer function from measured ground motion and incoherence calculations lies in the same range as the SSI analyses results over a wide frequency range. The results presented in Figures B.2-2 and B.2-4 support that the differences in foundation and free-field motion at Diablo Canyon from the 2003 Deer Canyon earthquake could be due to ground motion incoherence combined with SSI effects. In the frequency range from 11 to 20 Hz the estimated SSI transfer function is reasonably close to the mean soil SSI transfer function from SSI analyses.



**Figure B.2-4**  
**Comparison of Estimated and Calculated SSI Transfer Functions**

### **B.3 Measured Response of the Perry Nuclear Power Plant during the Northeastern Ohio Earthquake of January 31, 1986**

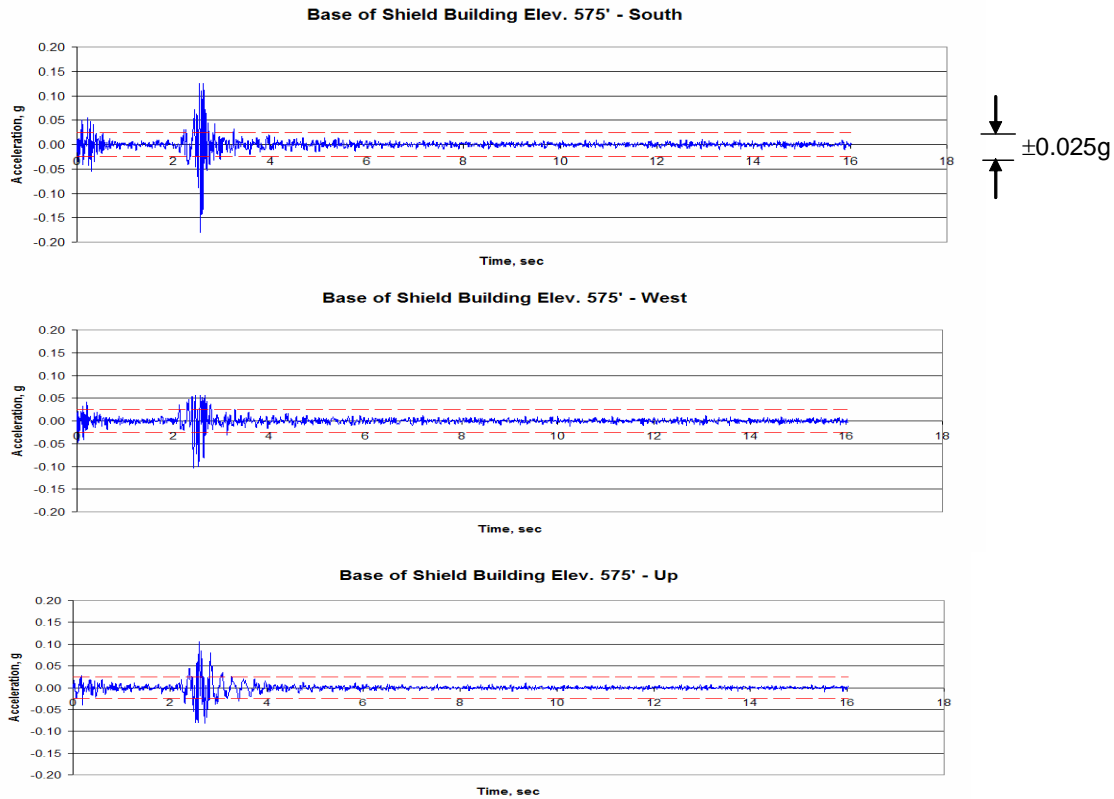
On January 31, 1986, an earthquake with an estimated moment magnitude of 4.6 occurred in the vicinity of Leroy, Ohio. The Perry Nuclear Power Plant, which was undergoing pre-operational testing (prior to fuel load), is located approximately 17 km to the north of the epicentral area. The plant is a single unit Mark III BWR with a free standing steel containment shell surrounded by a concrete shield building. The estimated epicentral intensity of the earthquake was VI (MMI scale) and the Perry site intensity was estimated to be V (MMI scale). The Perry Plant has a Kinematics SMA-3 strong recording system with two tri-axial transducer units (force balance accelerometers) mounted on cantilever steel brackets attached to the shield wall near the base mat and the steel containment shell at the approximate elevation of the operating floor. Figure B.3-1 shows the general plan and section of the two unit Perry Plant with the instrument locations identified. Note, only one unit was complete at the time of the earthquake. As can be noted, there are no free-field instruments.



**Figure B.3-1  
Perry Plant Configuration Showing Strong Motion Instrument Locations**

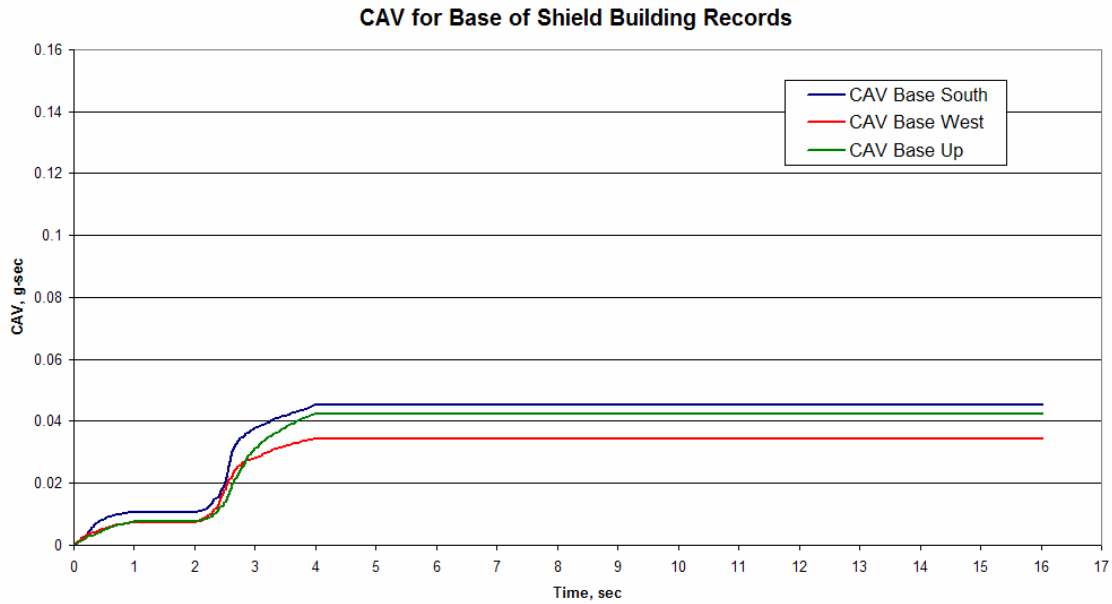
The common base mat of the containment and shield buildings is directly founded on rock with a surface shear wave velocity of 4900 fps. The containment and shield buildings are physically separated from the other plant structures. In the north-south direction, the base mat is not embedded while in the east-west direction a portion of the shield building is embedded.

Figure B.3-2 shows the recorded accelerations (processed and corrected) at the base of the shield building.



**Figure B.3-2  
Processed and Corrected Acceleration Records Obtained from the Base of Shield Building  
Instruments**

As can be noted, the duration of the strong motion response is less than one second. Since the base mat was founded on sound rock, the base record was inferred to be equivalent to a free-field record. The maximum response (peak acceleration) of the base motion is 0.18 g and occurs in the north-south direction. Walkdown inspections of the plant revealed that no damage had occurred nor were any spurious activation of the plant controls noted. However, the response spectra of the recorded base motion indicated that the OBE of the plant had been exceeded in the 20 Hz region. This evidence of a non-damaging event, which would have led to plant shutdown under the then current rules, prompted both the NRC and EPRI to initiate studies that ultimately led to the establishment of Regulatory Guides 1.166 and 1.167. One of the criteria of RG 1.166 is the CAV threshold of 0.16 g-sec, where the CAV is the integral of the absolute acceleration of the free-field motion greater than 0.025 g. Figure B.3-3 shows the calculation of the CAV for the Perry Plant records which is approximately one-fourth of the limiting value, indicating that the recorded motion (inferred to be a free-field motion) has very low damage potential.



**Figure B.3-3**  
**CAV Computation from Recorded Base of Shield Building Acceleration Records**

Figures B.3-4 through B.3-6 compare the response spectra of the recorded motions, both at the base of the Shield Building and the Containment Vessel at the operating floor elevation.

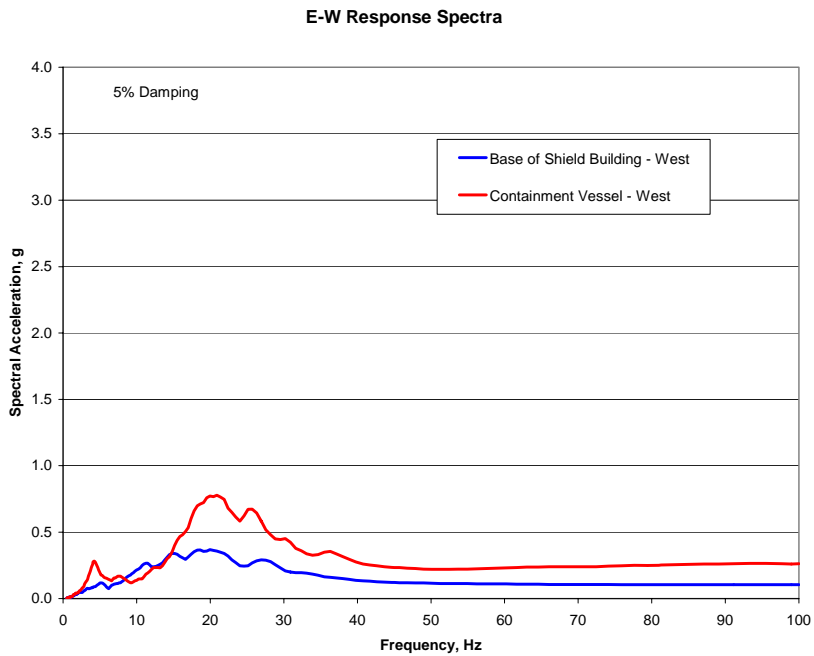


**Figure B.3-4**  
**Comparison of East-West Response Spectra**

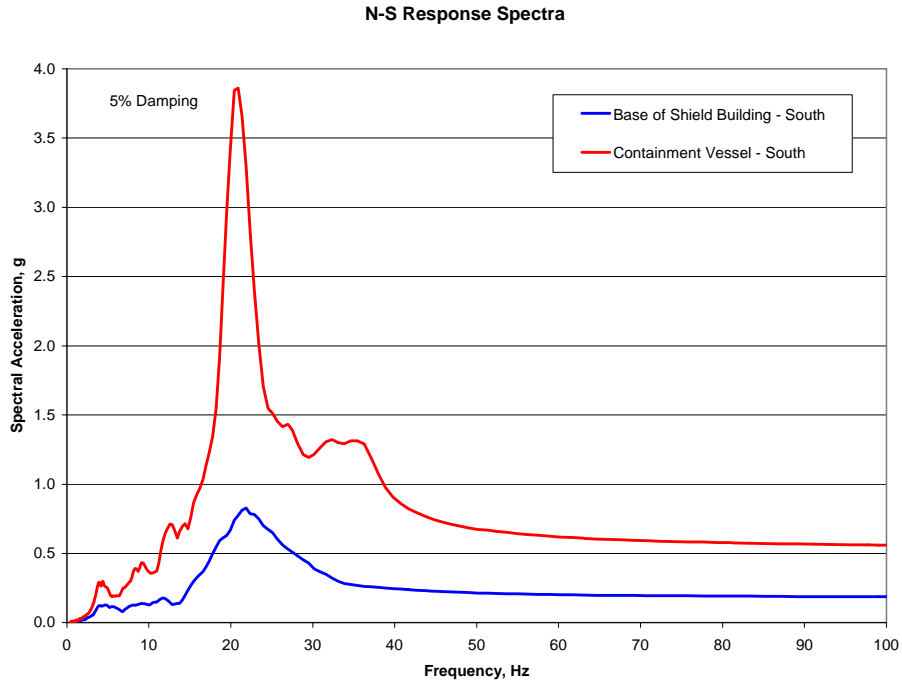


**Figure B.3-5**  
Comparison of North-South Response Spectra

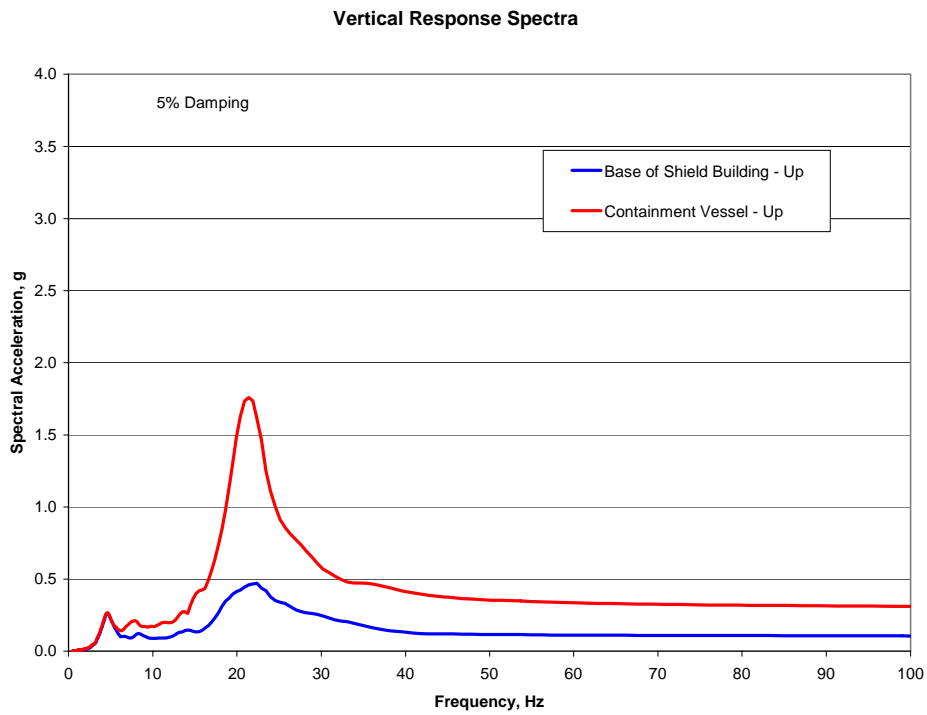


**Figure B.3-6**  
Comparison of Vertical Response Spectra

As can be noted, all three directions have a dominant response mode at 20 Hz. If a four-second record window is used to examine the north-south and vertical records from 1 to 5 seconds, as shown in Figure B.3-7, the measured response of the base of Shield Building appears to be periodic and correlated.

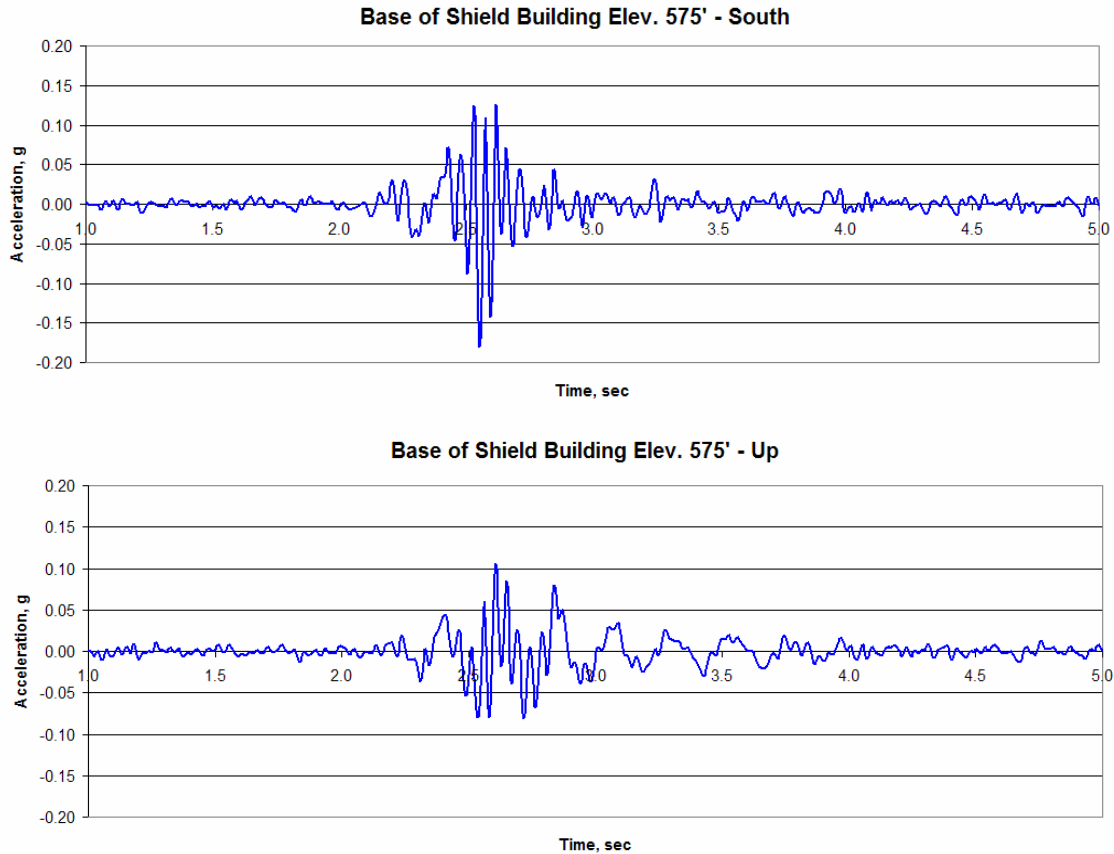


**Figure B.3-7**  
**North-South and Vertical Response Windows**

Both the plant AE (architect-engineer) and the USNRC (consultant) conducted analytical studies of the plant response. The AE used the design model which incorporated rock springs to simulate the interaction of the plant structures with the supporting media. The AE model indicated dominant modes at 4 and 19 Hz and the AE concluded that the observed response at 20 Hz was to be expected as a result of the rock-structure system. The NRC assumed a fixed base model (no rock interaction) and obtained dominant modes at 4.5 and 20 Hz. The NRC consultant concluded that base rocking was not significant but that a significant mode of response for the Containment Vessel occurs at approximately 20 Hz. The fixed base model was then used, assuming that the recorded base motion was a free-field motion, to obtain estimate of the response spectra at containment shell location.

As can be noted in Figure B.3-1, the placement of the instruments would result in coupled vertical and north-south translational response. Figures B.3-4 to B.3-7

suggest that both the vertical and translational motion of the base of Shield Building response is correlated to the structure response at the fundamental and at approximately 20 Hz. Figure B.3-8 shows the Fourier spectra modulus,  $|F_{SB}[f]|$ , computed for the windowed (Hann weighted) base of Shield Building response. The presence of the filtered translational response in the vertical motion is a clear indication that rocking of the base mat is occurring.

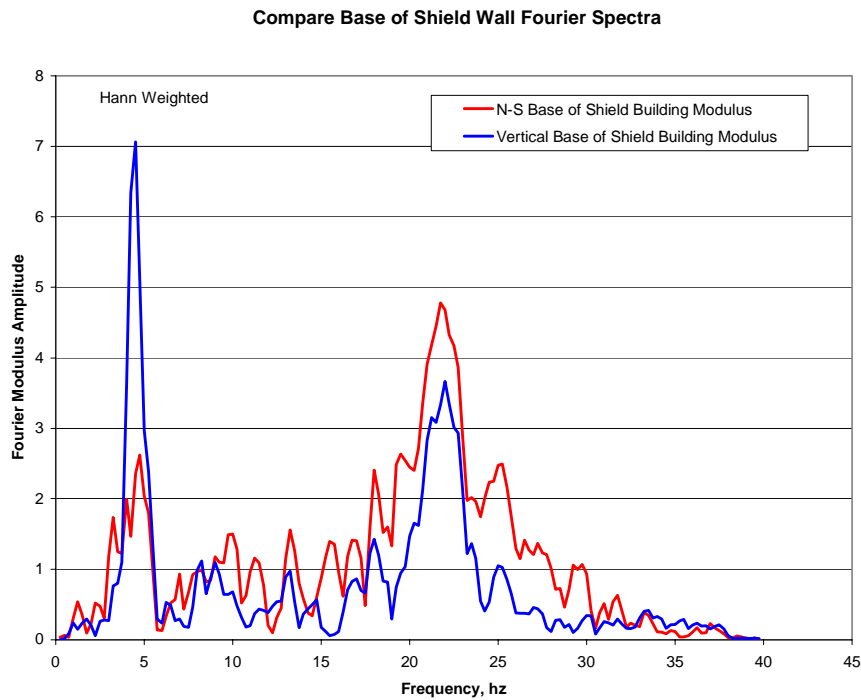


**Figure B.3-8**  
**Fourier Modulus Spectra for Base of Shield Building**

An estimate of the north-south transfer function for the translation response of containment vessel at the elevation of the operating floor may be provided by the ratio of the respective Fourier spectra moduli. Figure B.3-9 shows the ratio of Fourier spectra modulus,  $|F_{SB}[f]|/|F_{SB}[f]|$ , for the dominant frequency response regions. The bandwidth estimate of the Containment Vessel damping for the 20 Hz mode is approximately 1%.

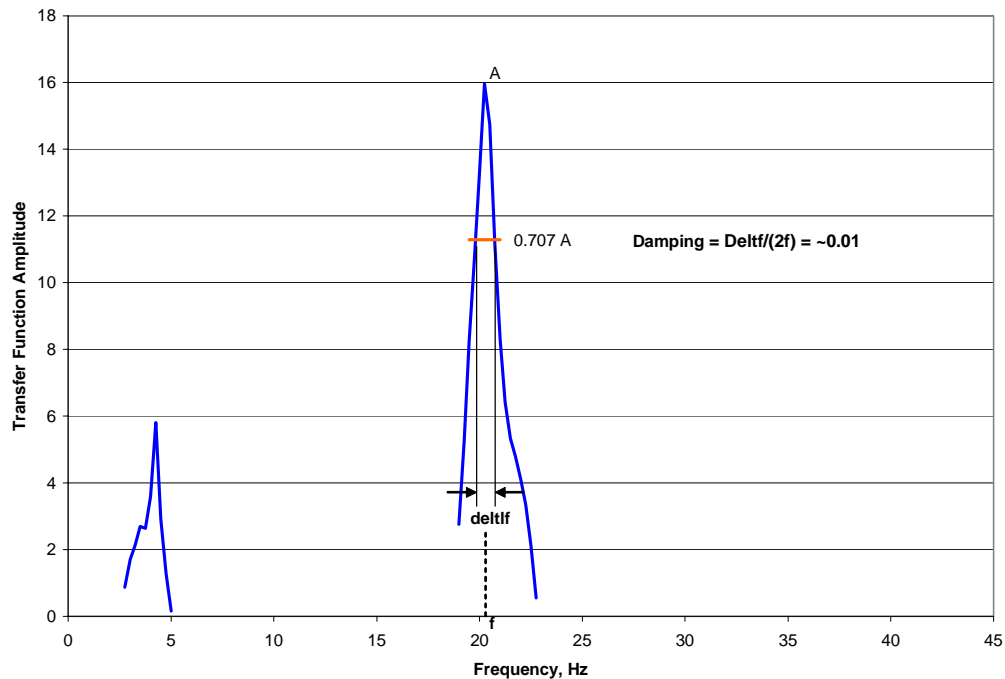


**Figure B.3-9**  
**Estimated Transfer Function for Translational Response (North-South) of Containment Vessel**

Based on the above observations, it is concluded that the recorded motions of the Perry Nuclear Power Plant due to the 1986 Northeastern Ohio earthquake have extremely short duration, less than one second, and according to current evaluation criteria would be classified as non-damaging. The resulting stresses in the freestanding containment shell (1.5-in thick) would be very low and the estimated damping associated with the second mode response (~20 Hz) of the containment shell would be approximately 1%. There was likely high-frequency content in the free-field rock motion, but the 20 Hz motion observed at the base of the Shield Building is due to both the feedback response of the rocking interaction and a compliance between the Shield Building and the Containment Vessel (i.e., lack of fixed base condition at the base mat interface). The amplified response observed for the Containment Vessel is an expected response of the system for low level input motion with very low response damping.

The Perry Plant recordings are not felt to present a valid case of proving or disproving incoherency or high-frequency response amplification. The lack of a true free-field instrument inhibits any understanding of the base mat response averaging (i.e., the effect of incoherency) and the location of the instruments coupled with a very low input motion (i.e., resulting in very low damping) causes the measured amplified vertical and horizontal response to be correlated.

## **B.4 Conclusions Regarding the Validation of Incoherency Effects Through Recorded Events**

Appendix B highlights the difficulties of validating the effects of incoherence of ground motion on nuclear power plant structures with data existing today:

- General conclusions as to the existence of the phenomena and their effects on structures are validated.
- The phenomena of most interest to the nuclear power plant community are for frequencies greater than 10 Hz. For existing recorded motions, it is possible to draw general conclusions for this frequency range, but not specific quantitative conclusions.
- The existing data bases are for conventional structures and must be extrapolated to the situation of nuclear power plant type structures. This extrapolation is performed in general terms for validation purposes.
- An on-going difficulty in evaluating recorded data for soil-structure interaction is the separation of the various elements of the phenomena – kinematic vs. inertial interaction; kinematic interaction due to vertical spatial variation of ground motion for embedded foundations vs. horizontal spatial variation of ground motion; flexible vs. rigid foundation behavior. To further validation efforts in these regards, instrumentation plans need to be developed to isolate the aspects of SSI to be studied.
- The number of nuclear power plants, their locations in regions of low seismicity, and the small number of earthquakes recorded at these facilities has led to very limited data being recorded for validation of the various aspects of SSI. Further, the instrumentation schemes have not been developed for validation of the elements of SSI. Consequently, general behavior is validated, but not specifics. Two cases in point are the Diablo Canyon and Perry nuclear power plants discussed in sections B.2 and B.3. General information is derived from these situations, but not specific validation of elements of SSI.

In conclusion, the approach taken in the present study to account for incoherence of ground motion is compatible with that taken by Stewart and colleagues to evaluate recorded data and to implement the results into the seismic design process. Recorded data at Diablo Canyon and Perry nuclear power plants highlight the difficulties in using recorded data to validate specific elements of SSI. Carefully designed instrumentation schemes will be required in the future to validate these individual elements.

## **B.5 References**

Abrahamson, N. (2006). *Spatial Coherency for Soil Structure Interaction*, Electric Power Research Institute, Final Report 1014101, Palo Alto, CA. August (Draft).

Abrahamson, N. (2005). *Spatial Coherency for Soil Structure Interaction*, Electric Power Research Institute, Technical Update Report 1012968, Palo Alto, CA. December.

Bechtel Power Corporation (1988). *Final Report on the Diablo Canyon Long Term Seismic Program, Soil-Structure Interaction Analysis*, prepared for Diablo Canyon

Power Plant Long Term Seismic Program, PG&E Company, San Francisco, CA. July.

Chang, C.-Y., M.S. Power, I.M. Idriss, P. Sommerville, W. Silva, and P.C. Chen (1985). *Engineering Characterization of Ground Motion, Task I1: Observational Data on Spatial Variations of Earthquake Ground Motion*, NUREG/CR-3805, Vol. 3.

EPRI (1997). *Soil-Structure Interaction Analysis Incorporating Spatial Incoherence of Ground Motions*, Electric Power Research Institute, Report TR-102631 2225, Palo Alto, CA. November.

Ishii, K., T. Itoh, and J. Suhara (1984). "Kinematic Interaction of Soil-Structure System Based on Observed Data," *Proc. 8<sup>th</sup> World Conference on Earthquake Engineering, San Francisco, Ca*, Vol. 3, Earthquake Engineering Research Center, Berkeley, CA, pp. 1017-1024.

Johnson, J.J. ((2003). "Soil-Structure Interaction," *Earthquake Engineering Handbook*, Chap. 10, W-F Chen, C. Scawthorn, eds., CRC Press, New York, NY.

Kim, S. (2001). *Calibration of Simple Models for Seismic Soil Structure Interaction from Field Performance Data*, PhD Dissertation, University of California, Los Angeles, CA.

Kim, S. and J.P. Stewart (2003). "Kinematic Soil-Structure Interaction from Strong Motion Recordings," *J. Geotech. Geoenviron. Eng.*, Vol. 129, No. 4, pp. 323-335.

Kohima, H., N. Fukuwa, and J. Tobita (2004), "Dynamic Response of Low and Medium-rise Building Based on Detailed Observation Considering Soil-Structure Interaction," Thirteenth World Conference on Earthquake Engineering, Vancouver, B.C., Canada, Paper No. 1243, August.

Stewart, J.P., G.L. Fenves, and R.B. Seed (1999a). "Seismic Soil Structure Interaction in Buildings I: Analytical Methods," *J. Geotech. Geoenviron. Eng.*, Vol. 125, No. 1, pp. 26-37.

Stewart, J.P., R.B. Seed, and G.L. Fenves, (1999b). "Seismic Soil Structure Interaction in Buildings II: Empirical Findings," *J. Geotech. Geoenviron. Eng.*, Vol. 125, No. 1, pp. 38-48.

Veletsos, A.S., A.M. Prasad, and W.H. Wu (1997). "Transfer Functions for Rigid Rectangular Foundations," *Earthquake Eng. Str. Dyn.*, Vol. 26, No. 1, pp.5-17.

## Enclosure 3

# APPENDIX D

## UNCERTAINTY EFFECTS OF COHERENCY FUNCTIONS

---

### Background

Chapter 2 presented the median coherency functions for horizontal and vertical ground motion as functions of frequency and distance between observation points, i.e., points on the foundation (Abrahamson, 2005a, 2006a). Equations 2-1, 2-2, and 2-3 and Table 2-1 specified the form and parameters of these functions. For this sensitivity study, Dr. Abrahamson provided an estimate of the variability in the coherency functions. The expression for the median coherency function (Equation 2-1) is reproduced here as Equation D-1. The corresponding variability in the coherency functions is defined in Equations D-2 and D-3.

The equation for median plane wave coherency is:

$$\gamma_{pw}(f, \xi) = \left[ 1 + \left( \frac{f \operatorname{Tanh}(a_3 \xi)}{a_1 f_c} \right)^{n_1} \right]^{-1/2} \left[ 1 + \left( \frac{f \operatorname{Tanh}(a_3 \xi)}{a_2 f_c} \right)^{n_2} \right]^{-1/2} \quad (\text{Equation D-1})$$

where:  $f$  is frequency and  $\xi$  is separation distance between foundation locations and

the constants  $a_1$ ,  $a_2$ ,  $a_3$ ,  $n_1$ ,  $n_2$ , and  $f_c$  are tabulated in Table 2-1.

Equations D-2 and D-3 (Abrahamson, 2005b) gives an expression for the 84<sup>th</sup> percentile plane wave coherency as the median value plus the sigma, where sigma is 0.4 for frequencies equal or greater than 20 Hz and smoothly varies to zero at zero frequency and at zero distance. Sigma is in Arctanh units.

$$\gamma_{pw,84}(f, \xi) = \tanh \left[ \tanh^{-1}(\gamma_{pw}(f, \xi)) + \sigma(f, \xi) \right] \quad (\text{Equation D-2})$$

$$\sigma_H(f, \xi) = \begin{cases} 0.4 & \text{for } f > 20\text{Hz} \\ 0.4 + (f - 20)(-0.0065 - 1.9 \times 10^{-6} \xi^2) & \text{for } f \leq 20\text{Hz} \end{cases} \quad (\text{Equation D-3})$$

## **Objective of Sensitivity Study on Coherency Uncertainty**

Perform a sensitivity study to establish a reasonable estimate of the effects of coherency uncertainty on the incoherency transfer functions. The focus is on the 84% non-exceedance probability (NEP) response of the rigid massless foundation (150 ft. square shape).

## Assumptions

The following assumptions were made to perform the analyses:

1. Coherency functions and incoherency transfer functions are assumed to be independent of frequency. Analyze each frequency of interest independently. These are common assumptions for SSI analysis in the frequency domain.
2. Point-to-point coherency functions are assumed to be independent. That is, no correlation of coherency functions for points equi-distant or for points within defined radii.

## Approach

The approach was to perform Monte Carlo simulations randomly varying the coherency functions and calculating the resulting incoherency transfer functions.

The steps in the analysis procedure were:

1. Define the normal distribution function for horizontal coherency over a sample of frequencies in the frequency range of interest (0 – 50 Hz) and over the point-to-point distances of the foundation discretization (approximately 5 ft. – 210 ft). The initial sample of frequencies was selected to be 10 Hz, 15 Hz, 20 Hz and 25 Hz. The distances of interest are based on the discretization of the 150-ft square foundation mat – the center points of the 393 sub-regions of the foundation. The key elements of the coherency functions are given in Equations D-1, D-2, and D-3. For any cumulative probability,  $p$ , the coherency may be expressed as:

$$\gamma_{pw,p}(f, \xi) = \tanh\left[\tanh^{-1}(\gamma_{pw}(f, \xi)) + t_p * \sigma(f, \xi)\right] \quad (\text{Equation D-4})$$

where  $t_p$  is the normal variate associated with cumulative probability,  $p$  (e.g.,  $t_p = 0$  for  $p = 0.50$ ,  $t_p = 1.0$  for  $p = 0.84$ , etc.). The resulting coherency,  $\gamma_{pw,p}$  was limited to be in the range of -1.0 to +1.0.

2. At each frequency of interest, generate a set of incoherency transfer function values by Monte Carlo simulation (1000 samples). The end result being the distribution of incoherency transfer function values conditional on each frequency of interest.
3. From the computed incoherency transfer function values at each frequency, evaluate the median and 84% NEP.

## Results

The sensitivity study was completed as described. All of the calculated incoherency transfer function values (1000 samples), at a given frequency, were very close to the median, i.e., the values shown in Figures 4-5 and 4-6 for the 150-ft square foundation on the rock site profile.

This led to a re-evaluation of the assumptions made. The assumption of randomly varying independent coherency function values between all points on the foundation leads to this end result. For example, given the foundation discretization of 393 sub-regions. This leads to 368 samples where the distance between center points of the sub-regions is 10.16m. Randomly sampling the coherency functions (Equation D-4) 368 times for this constant distance  $\xi$  effectively spans the distribution from minimum to maximum values, i.e., 184 of the samples are less than the median and 184 values are greater than the median as they should be. However, this leads to a median estimate of this contribution to the incoherency transfer functions and, consequently, in essence, median estimates of the resultant incoherency transfer functions.

Consultation with Dr. Abrahamson concerning these results led to concurrence that it should have been expected. Dr. Abrahamson performed a further evaluation of the recorded data to investigate whether there is correlation between coherency functions at pairs of observation points. Dr. Abrahamson's conclusion (Abrahamson, 2006b) is that the correlation is low, correlation coefficients less than 0.14 for frequencies 10 Hz and greater. The collective judgment of the Team is that incorporating this correlation into the uncertainty analysis will lead to only small variability in the incoherency transfer functions. There is no need to repeat the evaluation for these revised assumptions.

## References

Abrahamson, N. (2006a). *Spatial Coherency for Soil Structure Interaction*, Electric Power Research Institute, Final Report 1014101, Palo Alto, CA. August (Draft).

Abrahamson, N. (2006b). Personal Communication, July 7.

Abrahamson, N. (2005a). *Spatial Coherency for Soil Structure Interaction*, Electric Power Research Institute, Technical Update Report 1012968, Palo Alto, CA. December.

Abrahamson, N. (2005b). "Draft 84<sup>th</sup> Percentile Coherency Model," Memo to G. Hardy, August 10.

## Enclosure 4

# CHAPTER 3

## TECHNICAL APPROACH

---

### General

In order to incorporate seismic wave incoherence into seismic analyses, a stochastic approach has been employed as described in this chapter. This approach is described in detail in EPRI Report TR-102631 2225 (EPRI, 1997) and briefly summarized in this chapter. By this approach, incoherency transfer functions have been developed for the rigid massless foundation and validated to be appropriate by evaluating structure response for a typical NPP structure. Random vibration theory (RVT) has been employed to convert response spectra to power spectral density (PSD) functions and PSD to response spectra in order to determine spectra incoherency corrections on the rigid, massless foundation. As described in Chapter 2, coherency functions as a function of separation distance, frequency, apparent wave velocity, and direction of motion from Abrahamson, 2005 are used as the basic input for all evaluations. The incoherency transfer functions and spectra corrections have been generated for the rigid, massless foundation using the computer program, CLASSI. In addition, CLASSI has been used to evaluate seismic structural response of example soil/structure systems. The procedures used to evaluate incoherency transfer functions, to evaluate foundation response of rigid, massless foundations, and to evaluate structure and foundation response of example structural models accounting for soil-structure interaction and seismic wave incoherence are described in this Chapter.

By these procedures, all elements of incoherence are appropriately treated. These elements include the reduction of the amplitude of translational motions and the effect of induced rotations. Chapters 4, 5, and 6 investigate the procedures. Chapter 4 deals with rigid, massless foundations of varying configurations, size, and site conditions. The rock site profile and the soil site profile of Chapter 2 and their companion free-field ground response spectra are considered in Chapter 4. Chapter 5 deals with a representative structure, i.e., a simplified model of the AP1000, also described in Chapter 2. The rock site profile and associated ground response spectra of Chapter 2 are the examples considered. Chapter 6 summarizes the results and the conclusions.

### Procedure to Evaluate the Incoherency Transfer Function (ITF)

The incoherency transfer function is determined using the computer program, CLASSI following the procedure shown in Table 3-1. To run CLASSI (Wong and Luco, 1980), we must first define the foundation footprint plan dimensions, underlying soil layers with properties of density, shear wave velocity, Poisson's ratio, material damping, and layer thickness, and frequencies for analysis. The foundation footprint is divided into  $n$  sub-regions for input to CLASSI. The coherency function is evaluated at the mid-point of each of these sub-regions with the separation distance being the distance between all of the combinations of sub-region mid-points.

Based on the assumption that ground motions can be represented by a stationary random process, the coherency function between ground motions  $x_i(t)$  and  $x_j(t)$ , denoted by  $\gamma(f)$ , is a complex function of frequency,  $f$ , defined by:

$$\gamma(f) = \frac{S_{ij}(f)}{\sqrt{S_{ii}(f)S_{jj}(f)}} \quad \text{(Equation 0-1)}$$

in which  $S_{ij}$  is the cross power spectral density function between motions  $x_i(t)$  and  $x_j(t)$  and  $S_{ii}$  and  $S_{jj}$  are the power spectral density functions for motions  $x_i(t)$  and  $x_j(t)$ , respectively.

$[\gamma]$  is evaluated as a  $3n$  by  $3n$  matrix of the Abrahamson coherency function based on the separation distances between sub-regions for each selected frequency and for input apparent wave velocity or slowness.

The incoherency transfer function, ITF( $f$ ) is equal to the amplitude of the square root of the diagonal terms of  $[S_{UoI}]$  where  $[S_{UoI}]$  is the  $6$  by  $6$  cross PSD matrix of rigid massless foundation motion subjected to unit PSD input.

$$[S_{UoI}] = [F] [S_{UGI}] [FC]^T \quad \text{(Equation 0-2)}$$

where  $[F]$  is a  $6$  by  $3n$  scattering transfer function matrix relating sub-region displacements to rigid body displacements and  $[FC]$  is the complex conjugate of  $[F]$  and  $[S_{UGI}]$  is a  $3n$  by  $3n$  covariance matrix of incoherent ground motions for unit PSD input given by  $[I] [\gamma] [I]$  where  $[I]$  is an identity matrix.  $[F]$  is determined by:

$$[F] = [C] [T]^T \quad \text{(Equation 0-3)}$$

where  $[C]$  is the  $6$  by  $6$  compliance matrix (equal to the inverse of the impedance matrix  $[K]^{-1}$ ); and  $[T]$  is a  $3n$  by  $6$  traction matrix representing contact tractions on all  $n$  sub-regions subjected to unit rigid body motions.

$$[T] = [G]^{-1} [\alpha_b] \quad \text{(Equation 0-4)}$$

$[G]$  is the  $3n$  by  $3n$  Green's function matrix containing responses of the foundation to unit harmonic point loads and  $[\alpha_b]$  is a  $3n$  by  $6$  rigid foundation mode shape matrix. One of the program modules to CLASSI uses soil profile properties to determine the Green's function.

Even though the scattering transfer function matrix  $[F]$  is a function of the compliance matrix  $[C]$  and the traction matrix  $[T]$ , both of which are dependent on the soil properties, it may be shown that  $[F]$  is independent of the soil conditions. As a result, the incoherency transfer function (ITF) is independent of the soil conditions. The independence of the scattering transfer function  $[F]$  from soil properties is a direct result of the CLASSI formulation which considers the SSI response of a rigid surface inclusion on a layered half-space (i.e., a rigid massless foundation).

Let the modification of the field-field surface motion due to the presence of the rigid surface inclusion be represented by six component vector  $\{U_0\}$ . The average free-field surface motion of each of  $n$  sub-regions that represents the interface of the rigid foundation area with the half-space surface is represented by the  $3n$  component vector  $\{U_n\}$ . The motion of a reference point of the rigid inclusion  $\{U_0\}$  in terms of the set of sub-region motions  $\{U_n\}$  is related by the  $6 \times 3n$  scattering transfer function  $[F]$ :

$$\{U_0\} = [F] \{U_n\} \quad \text{(Equation 0-5)}$$

It may be noted that the  $3n \times 6$  rigid body transformation array  $[\alpha_b]$  is defined by:

$$\{U_n\} = [\alpha_b]\{U_0\} \quad \text{(Equation 0-6)}$$

$[\alpha_b]$  is only a function of the foundation footprint geometry and the location of the  $n$  sub-regions and not of the properties of soil layers. As a result, comparison of Equations 3-5 and 3-6 shows that  $[F]$  must be independent of the soil conditions.

The  $6 \times 6$  impedance matrix  $[K]$  relates the driving forces applied to the rigid inclusion,  $\{P_0\}$  to the displacements of the rigid inclusion,  $\{U_0\}$  by:

$$\{P_0\} = [K]\{U_0\} \quad \text{(Equation 0-7)}$$

The impedance matrix may also be expressed in terms of the  $3n \times 3n$  array  $[G]$  of Green's functions integrated over each sub-region, and the  $3n \times 6$  rigid body transformation array  $[\alpha_b]$  by:

$$[K] = [\alpha_b]^T [G]^{-1} [\alpha_b] \quad \text{(Equation 0-8)}$$

Combining Equations 3-6, 3-7, and 3-8, it may be noted that  $\{P_0\} = [\alpha_b]^T [G]^{-1} [\alpha_b] \{U_0\} = [\alpha_b]^T [G]^{-1} \{U_n\}$ . The array  $[G]^{-1} [\alpha_b]$  may be identified as the  $3n \times 6$  traction array  $[T]$  from Equation 3-4. Transposing Equation 3-4 gives  $[T]^T = [\alpha_b]^T [G]^{-1}$ . As a result:

$$\{P_0\} = [T]^T \{U_n\} \quad \text{(Equation 0-9)}$$

Equating Equations 3-7 and 3-9 so that  $\{P_0\} = [K]\{U_0\} = [T]^T \{U_n\}$ , we may write express  $\{U_0\}$  in terms of  $\{U_n\}$  as:

$$\{U_0\} = [K]^{-1} [T]^T \{U_n\} = [C][T]^T \{U_n\} = [F] \{U_n\} \quad \text{(Equation 0-10)}$$

where  $[C] = [K]^{-1}$  is the  $6 \times 6$  compliance array of the rigid inclusion reference point. The scattering transfer function,  $[F]$  is equal to  $[C][T]^T$  in accordance with Equation 3-3.

From Equation 3-6,  $\{U_n\} = [\alpha_b]\{U_0\}$ . Multiplying both sides to this equation gives  $[\alpha_b]^T \{U_n\} = [\alpha_b]^T [\alpha_b] \{U_0\}$ .  $\{U_0\}$  can then be related to  $\{U_n\}$  by  $\{U_0\} = ([\alpha_b]^T [\alpha_b])^{-1} [\alpha_b]^T \{U_n\}$  which may be identified as the least squares solution for the average motion of the rigid surface inclusion given the over-determined free-field motion of the  $n$  sub-regions  $\{U_n\}$ . Hence, from Equation 3-5, it may be seen that the scattering transfer function  $\{F\}$  is given by:

$$[F] = ([\alpha_b]^T [\alpha_b])^{-1} [\alpha_b]^T \quad \text{(Equation 0-11)}$$

Equation 3-11 shows that the scattering transfer function is independent of any soil properties, being determined only by the rigid body kinematics of the rigid foundation motion. The use of the identity  $[F] = [C][T]^T$  is actually equivalent to the least squares solution, and is a convenient means of computation for the scattering transfer function given the CLASSI computation of  $[K]$  and  $[T]$  for solution of the SSI problem.

CLASSI is used to evaluate the impedance matrix  $[K]$  and the traction matrix  $[T]$  at each selected frequency. Normal outputs are impedance and scattering matrices. Also,  $[T]$ , a Green's function matrix  $[G]$ , and  $[\alpha_b]$  are generated internally by the program. Input is the foundation footprint and the definition of sub-regions along with soil properties. For this study, the foundation footprint was divided into 10-ft square sub-regions. Around the periphery of the foundation, the outside 10-ft was further divided into 5-ft square sub-regions.

Based on CLASSI determined  $[K]$ ,  $[T]$ ,  $[G]$ , and  $[\alpha_b]$  the  $6 \times 6$  cross PSD,  $[S_{U_0I}]$  of the rigid massless foundation to unit PSD input due to incoherent input motion is generated. For this

purpose, the coherency matrix,  $[\gamma]$ , the covariance matrix for unit PSD input,  $[S_{UGI}]$  and the scattering transfer function,  $[F]$  are evaluated. Also, incoherency transfer function, ITF, which is equal to the amplitude of the square root of the diagonal terms of  $[S_{UoI}]$  is calculated.

**Table 0-1  
Procedure to Evaluate Incoherency Transfer Function**

<ul style="list-style-type: none"> <li>Define Soil Profile and Specify Properties by Soil Layers Define Foundation Footprint and Specify as n Sub-Regions</li> </ul>
<ul style="list-style-type: none"> <li>Input coherency function, <math>\gamma(f,s)</math> as a function of Frequency, f and Separation Distance, s</li> </ul>
<ul style="list-style-type: none"> <li>Run CLASSI modules to Evaluate the Impedance Matrix and Green's Function Matrix</li> </ul>
<ul style="list-style-type: none"> <li>From Green's Function Matrix and Rigid Foundation Assumption, Evaluate the Traction Matrix, <math>[T]</math>. Invert the Impedance Function to Evaluate the Compliance Function, <math>[C]</math></li> </ul>
<ul style="list-style-type: none"> <li>Evaluate <math>[S_{UoI}]</math>, the Cross PSD matrix of Rigid Massless Foundation Motion Subjected to Unit PSD Input  <math display="block">[S_{UoI}] = [F] [S_{UGI}] [FC]^T</math>           where <math>[F] = [C] [T]^T</math>            and <math>[S_{UGI}] = [I] [\gamma] [I]</math> </li> </ul>
<ul style="list-style-type: none"> <li>Evaluate the Incoherency Transfer Function, ITF(f) as the Amplitude of the Complex Square Root of <math>[S_{UoI}]</math></li> </ul>

### Procedure to Evaluate the Rigid Massless Foundation Incoherent Response Spectra

In order to evaluate the foundation response spectra for the rigid massless foundation, it is necessary to input ground motion response spectra for CEUS rock sites,  $[RS_o]$  as described in Chapter 2. These response spectra are converted to power spectral density (PSD) functions, and procedures similar to that described in the previous sub-section are employed to evaluate the PSD of the foundation response. These output PSDs are then converted to response spectra. This process is shown in Table 3-2.

The PSD for a component of ground response spectrum,  $S_o(f)$ , is evaluated by random vibration theory as discussed below. Standard relationships of stationary random vibration theory are used to convert response spectra (RS) into power spectral density (PSD) functions, and vice versa. To calculate a PSD from a RS, an iterative process is used. A starting PSD uniform function (white noise) is used and iterations performed until the RS calculated from the new PSD matches the target RS. To calculate a RS from a PSD, a direct integral relationship exists. Numerical integration is performed to calculate the moments of the PSD and the peak factors relating the standard deviation of the maximum response to the mean of the maximum peak response (RS). Der Kiureghian, A., "Structural Response to Stationary Excitation," Journal of the Engineering

Mechanics Division, American Society of Civil Engineers, December 1980 is the basic reference followed (Der Kiureghian, 1980).

The PSD of the rigid massless foundation to actual incoherent input motion is determined using  $[S_{UG}]$ , a  $3n$  by  $3n$  covariance matrix of actual incoherent ground motions as determined by Equation 3-12.

$$[S_{UG}] = [S_o^{1/2}] [\gamma] [S_o^{1/2}] \quad \text{(Equation 0-12)}$$

where  $[S_o^{1/2}]$  is a  $3n$  by  $3n$  on-diagonal PSD matrix on the input ground motion and  $S_o(f)$  is the power spectral density of the input ground motion. The difference between  $[S_{UG}]$  and  $[S_{UGI}]$  is that  $[S_o^{1/2}]$  is used instead of identity matrix,  $[I]$ .

$[S_{Uo}]$ , the 6 by 6 cross PSD of rigid massless foundation motion is determined from:

$$[S_{Uo}] = [F] [S_{UG}] [FC]^T \quad \text{(Equation 0-13)}$$

$[F]$  the 6 by  $3n$  scattering transfer function matrix relating sub-region displacements to rigid body displacements and its complex conjugate  $[FC]$  are determined in exactly the same manner as described in the previous sub-section.

The response spectrum for the foundation response,  $[RS_{Uo}]$  is then determined from the PSD defined by the diagonal terms of the  $[S_{Uo}]$  matrix using the random vibration approach.

**Table 0-2**  
**Procedure to Evaluate the Rigid Massless Foundation Incoherent Response Spectra**

<ul style="list-style-type: none"> <li>Define Free Field Ground Response Spectra, <math>[RS_o]</math></li> </ul>
<ul style="list-style-type: none"> <li>Evaluate the PSD for each Component of Ground Response Spectrum, <math>S_o(f)</math>, by random vibration theory. Evaluate <math>[S_o^{1/2}]</math>, a <math>3n</math> by <math>3n</math> On-Diagonal PSD Matrix of the Input Ground Motion</li> </ul>
<ul style="list-style-type: none"> <li>Evaluate <math>[S_{Uo}]</math>, the Cross PSD matrix of Rigid Massless Foundation Motion <math>[S_{Uo}] = [F] [S_{UG}] [FC]^T</math> where <math>[S_{UG}] = [S_o^{1/2}] [\gamma] [S_o^{1/2}]</math></li> </ul>
<ul style="list-style-type: none"> <li>Response Spectrum of Foundation Response, <math>[RS_{Uo}]</math> is determined from the PSD Defined by the Diagonal Terms of the <math>[S_{Uo}]</math> Matrix using random vibration theory.</li> </ul>

### Procedure to Evaluate the Foundation and Structure Incoherent Response Spectra by Random Vibration Theory

The 6 by 6 cross PSD of foundation response motion,  $[S_{UF}]$  may be determined by pre-multiplying  $[S_{Uo}]$ , the 6 by 6 cross PSD of rigid massless foundation motion by  $[H_F]$  a 6 by 6 transfer function matrix between foundation response and the scattered foundation input motions and post-multiplying by  $[H_FC]$ , the complex conjugate of  $[H_F]$ :



function matrix between structural response and the scattered foundation input motions) and post-multiplying by  $[H_T C]$ , the complex conjugate of  $[H_T]$ :

$$[S_{Us}] = [H_T] [S_{Uo}] [H_T C]^T \quad \text{(Equation 0-20)}$$

The structure transfer function matrix is given by:

$$[H_T] = ([\alpha_s] + [\phi_s] [D] [\Gamma_s]) [H_F] \quad \text{(Equation 0-21)}$$

Where all matrices and terms have been previously defined.

The response spectrum for the foundation response,  $[RS_{Us}]$  is then determined from the PSD defined by the diagonal terms of the  $[S_{Us}]$  matrix using the random vibration approach described above.

### **Procedure to Evaluate the Foundation and Structure Incoherent Response Spectra by CLASSI**

The complete random vibration approach described above could have been employed herein. However, the formulation of CLASSI and its ease of use permitted implementation of a more direct approach to the SSI analysis of structure/foundation. The procedure used is shown in Table 3-3.

CLASSI program modules generate the complex impedance and scattering matrices at each frequency considered. The impedance matrix represents the stiffness and energy dissipation of the underlying soil medium. The foundation input motion is related to the free-field ground motion by means of a transformation defined by a scattering matrix. The term “foundation input motion” refers to the result of kinematic interaction of the foundation with the free-field ground motion. In general, the foundation input motion differs from the free-field ground motion in all cases, except for surface foundations subjected to vertically incident waves. The soil-foundation interface scatters waves because points on the foundation are constrained to move according to its geometry and stiffness. Modeling of incoherent ground motions is one aspect of this phenomena and the focus of this study.

In essence, the incoherency transfer function is the scattering matrix accounting for the effects of seismic wave incoherency over the dimensions of the foundation. For this application, a 6 by 6 complex incoherency transfer function matrix [ITF] is evaluated by taking the square root of  $[S_{UoI}]$ , the 6 by 6 complex cross PSD matrix of rigid massless foundation motion to unit PSD input for each direction of translational input. Each column of the scattering matrix for vertically propagating waves is replaced by the diagonal terms from the incoherency transfer function matrix at each frequency of interest that correspond to each direction of input excitation. CLASSI SSI analyses are then performed in a conventional manner to evaluate the structure and foundation in-structure response spectra. CLASSI solves the SSI problem in the frequency domain. Ground motion time histories are transformed into the frequency domain, SSI parameters (impedances and scattering matrices) are complex-valued, frequency-dependent, and the structure is modeled using its fixed-base eigensystems. SSI analyses are performed—output are time histories of response of interest from which in-structure response spectra are computed. The resulting in-structure response spectra at structure and foundation locations of interest include the effects of soil-structure interaction and seismic wave incoherence.

**Table 0-3**  
**Procedure to Evaluate the Foundation and Structure Incoherent Response Spectra by CLASSI**

<ul style="list-style-type: none"> <li>• Define Free-Field Ground Motion Time Histories Compatible with Response Spectra, <math>[RS_0]</math></li> </ul>
<ul style="list-style-type: none"> <li>• Define Soil Profile and Specify Properties by Soil Layers</li> <li>• Define Foundation Footprint and Specify as n Sub-Regions</li> <li>• Define Foundation Thickness and Mass Properties</li> <li>• Define a Fixed Base Structural Model</li> </ul>
<ul style="list-style-type: none"> <li>• Input coherency function, <math>\gamma(f,s)</math> as a function of Frequency, f and Separation Distance, s</li> </ul>
<ul style="list-style-type: none"> <li>• Run CLASSI modules to Evaluate the Impedance Matrix</li> </ul>
<ul style="list-style-type: none"> <li>• Evaluate the Scattering Matrix as the Incoherency Transfer Function. Each Column of the Scattering Matrix Corresponds to a Direction of Input Excitation and is Given by the Diagonal Terms from the Incoherency Transfer Function Matrix at Each Frequency of Interest.</li> </ul>
<ul style="list-style-type: none"> <li>• Evaluate Fixed Base Modal Properties of the Structure</li> </ul>
<ul style="list-style-type: none"> <li>• Run CLASSI modules that Combine the Structure Properties, Impedance Matrix, Scattering Matrix, and Input Time Histories and Evaluates Output Time Histories</li> </ul>
<ul style="list-style-type: none"> <li>• Run Standard Response Spectrum Evaluation Program to Determine In-Structure Response Spectra for the Foundation and Structure Locations</li> </ul>

## Enclosure 5

# CHAPTER 4

## RIGID, MASSLESS FOUNDATION RESPONSE

---

### General

The effect of seismic wave incoherence is demonstrated in this chapter for the seismic response of a rigid massless foundation. Analyses reported in this chapter represent the essence of Task 2.1 developing the incoherency transfer functions that enable the effects of incoherence to be implemented into seismic analyses.

For most analyses the soil properties and foundation areas presented in Chapter 2 are used. These properties include the rock and soil profiles along with the corresponding high and low frequency content site-specific ground response spectra.

A study of the effects of wave passage phenomena was performed to separate the effects of wave passage and local wave scattering. The wave passage study was performed for the 150-ft square foundation footprint and a rock half-space site condition of shear wave velocity of 6300 fps; the same site condition used in the benchmark comparison analyses documented in Appendix C.

### Wave Passage Effects

The Abrahamson coherency function accounts for horizontal spatial variation of ground motion from both wave passage effects and local wave scattering.

- Wave passage effects: Systematic spatial variation due to difference in arrival times of seismic waves across a foundation due to inclined waves.
- Local wave scattering: Spatial variation from scattering of waves due to the heterogeneous nature of the soil or rock along the propagation paths of the incident wave fields.

For the detailed efforts of this project, only local wave scattering of ground motion was considered. Local wave scattering results in large reductions in foundation motion and wave passage effects produce minimal further reductions. However, to take advantage of these further reductions in foundation motion due to wave passage, an apparent wave velocity must be assigned to the site. The apparent wave velocity is dependent on many parameters including earthquake source parameters, travel paths, and the earthquake source location relative to the site. Assigning an appropriate and defensible apparent wave velocity for free-field ground motion developed from probabilistic seismic hazard assessments is difficult and possibly controversial.

The effects of wave passage are demonstrated in terms of incoherency transfer functions and spectral corrections as shown in Figures 4-1, 4-2, 4-3, and 4-4. These results were generated for

the 150-ft square foundation on a rock half-space of shear wave velocity of 6300 fps. The free-field ground motion was defined by site-specific ground response spectra, with high-frequency amplification, itemized in Appendix C. Earthquake ground motion recorded with adequate instruments to identify wave passage effects leads to the estimate of apparent wave velocities greater than 2 km/sec and more justifiably at 4 km/sec.

The wave passage analyses considered are:

- Apparent wave velocity of 2000 m/s (Slowness of 0.00050 s/m)
- Apparent wave velocity of 4000 m/s (Slowness of 0.00025 s/m)
- No wave passage effects (Apparent wave velocity = infinity - Slowness of 0 s/m)

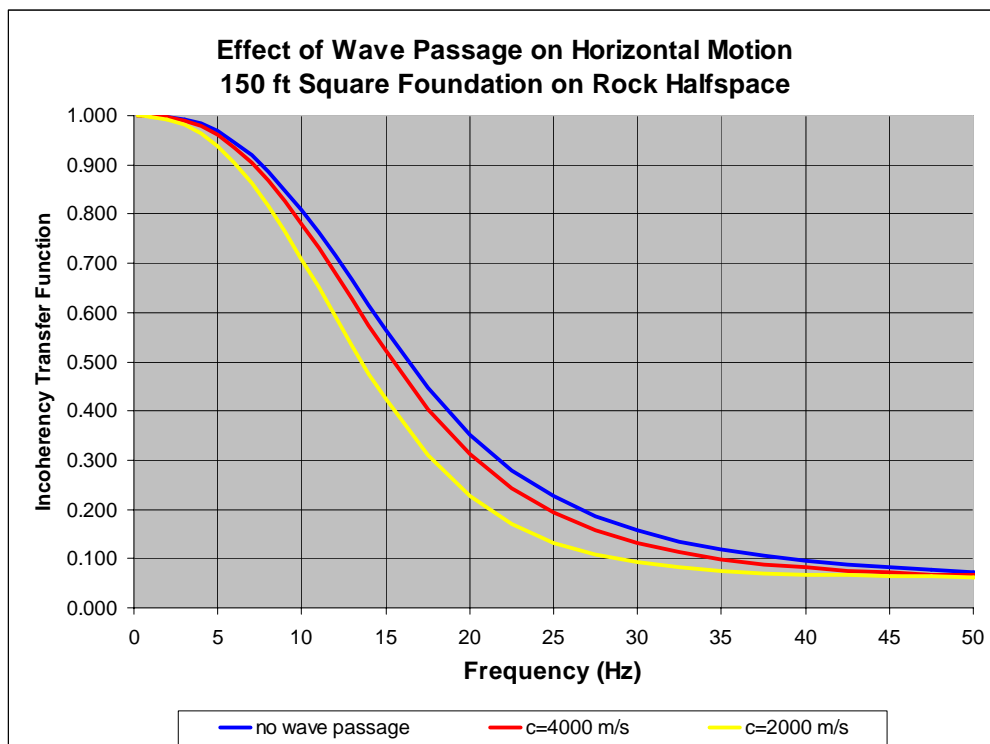


**Figure 0-1**  
**Effect of Wave Passage on Incoherency Transfer Function for Horizontal Motion**

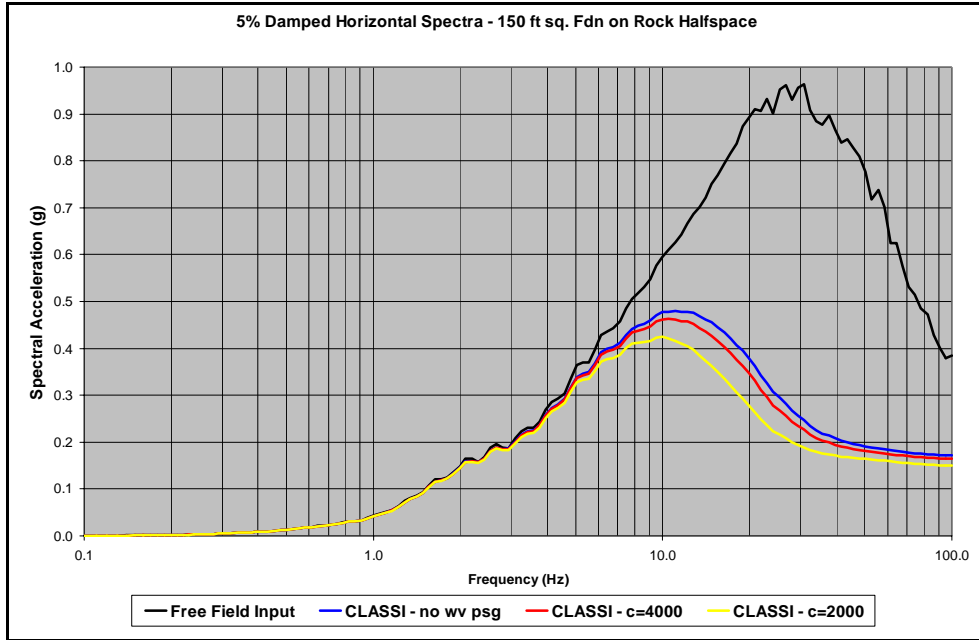


**Figure 0-2**  
**Effect of Wave Passage on Foundation Horizontal Response Spectra**

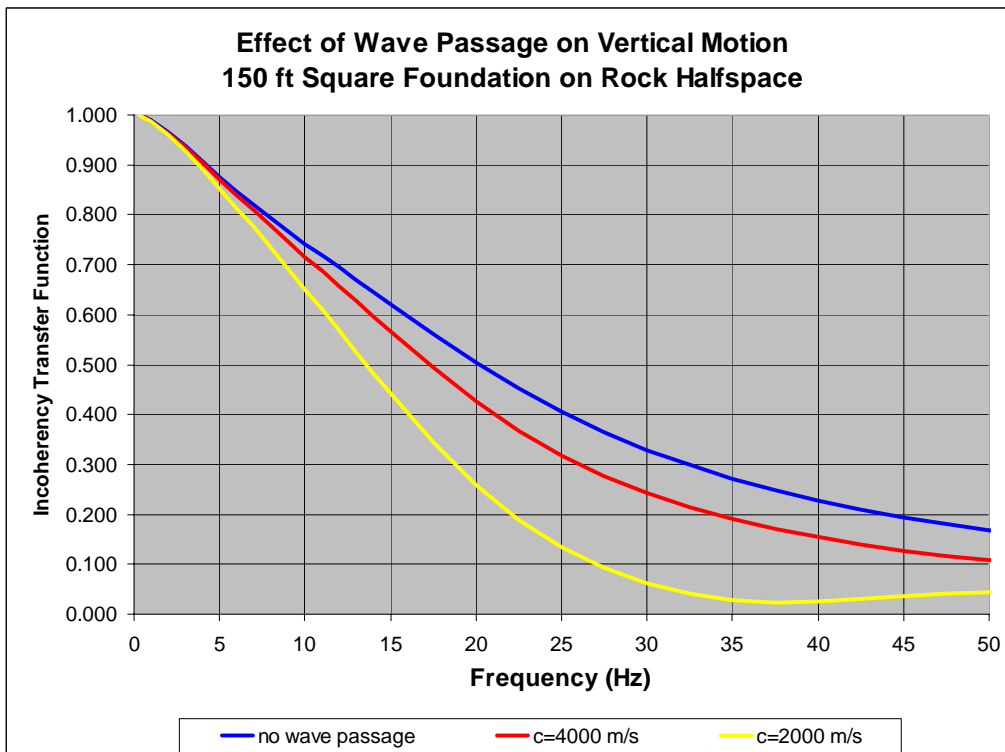


**Figure 0-3**  
**Effect of Wave Passage on Incoherency Transfer Function for Vertical Motion**

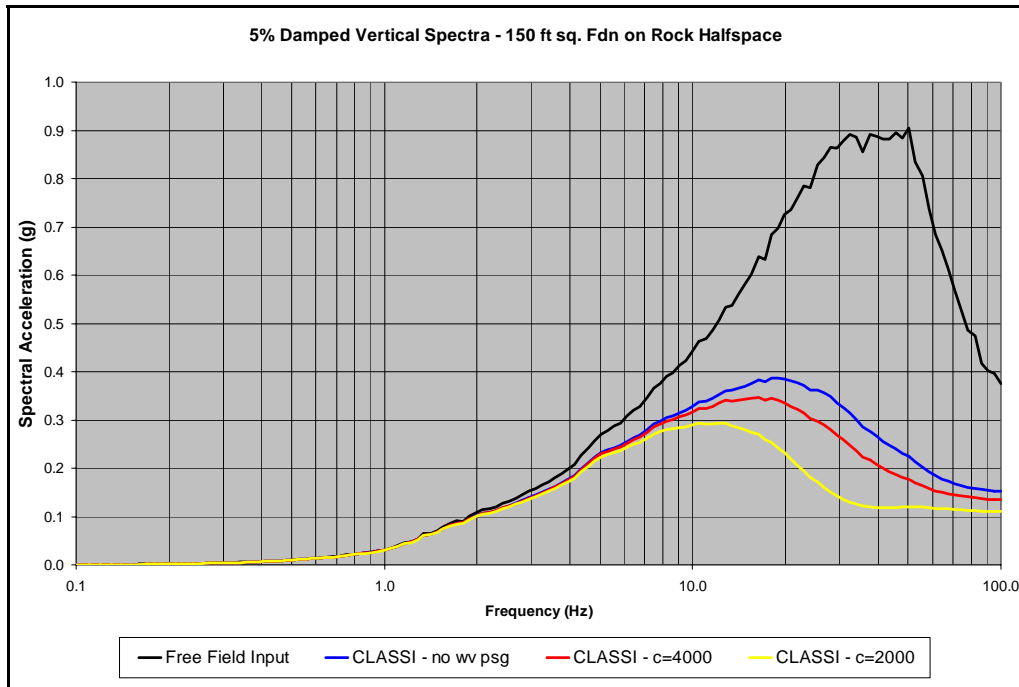


**Figure 0-4**  
**Effect of Wave Passage on Foundation Vertical Response Spectra**

### Incoherency Transfer Function

Incoherency transfer functions or wave scattering due to seismic wave incoherence have been computed in the manner described in Chapter 3. The incoherency transfer function demonstrates the effects of seismic wave incoherence as a function of frequency for the foundation footprint considered. Parametric studies have been performed for:

- Foundation Shape (Constant Area)
  - 150-ft square footprint
  - 100 by 225-ft rectangle footprint
  - 84.63-ft radius circle footprint
- Foundation Area (Constant Shape)
  - 75-ft square footprint
  - 150-ft square footprint
  - 300-ft square footprint

Calculations have been performed for local wave scattering effects only; wave passage effects have not been considered.

Soil profile. Chapter 3 demonstrated that the incoherency transfer functions are independent of site conditions. Hence, incoherency transfer functions as calculated for the rock site are presented. Foundation response is presented for the rock and soil site profiles since they are dependent on the site-specific ground motion, which differs for the two site conditions.

Foundation shape. The effects of foundation shape on the incoherency transfer functions for translational foundation motion are shown in Figures 4-5 and 4-6 for the horizontal and vertical directions, respectively. On these figures, the lines of different colors lie on top of each other so only one color is visible. The conclusion is that for these variations in foundation shape, i.e., square vs. rectangle (with reasonable aspect ratio of 2:1) vs. circle, the incoherency transfer function is independent of foundation shape. This conclusion applies only to the foundation shapes considered in this study and may change when foundations of different shapes (e.g., L shape) or larger aspect ratios are considered.

Foundation area. The effect of foundation area on the incoherency transfer function for translational foundation motion is presented in Figures 4-7 and 4-8. Square foundation footprints with area varying by a factor of 4 are considered. Although the variation on the plots appears small, the actual difference amounts to about 30 to 45 percent for an area difference of a factor of 4. Going from the 75-ft square foundation footprint to the 300-ft square foundation footprint results in an increased reduction from about 0.45 at 20 Hz and 0.23 at 30 Hz to about 0.27 at 20 Hz and 0.12 at 30 Hz.

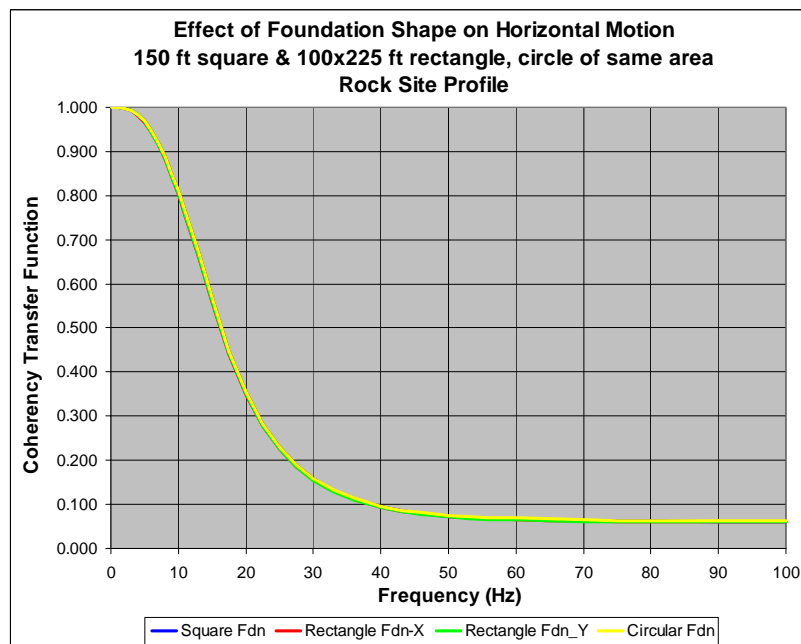


**Figure 0-5**  
**Horizontal Motion Incoherency Transfer Function – Effect of Foundation Shape**

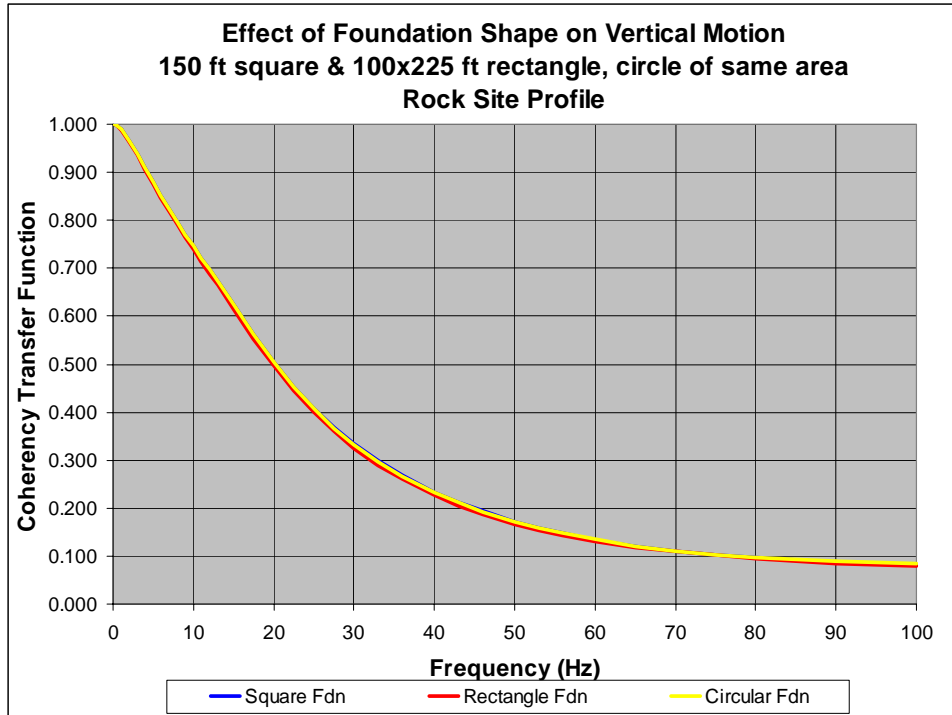


**Figure 0-6**  
**Vertical Motion Incoherency Transfer Function – Effect of Foundation Shape**

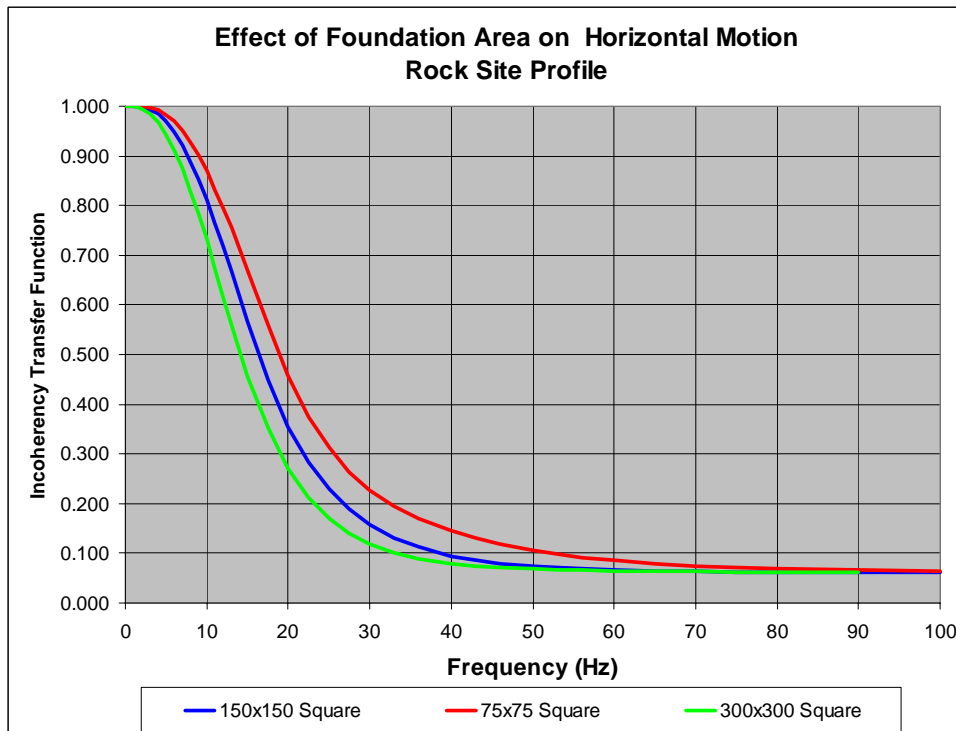


**Figure 0-7**  
**Horizontal Motion Incoherency Transfer Function – Effect of Foundation Area**

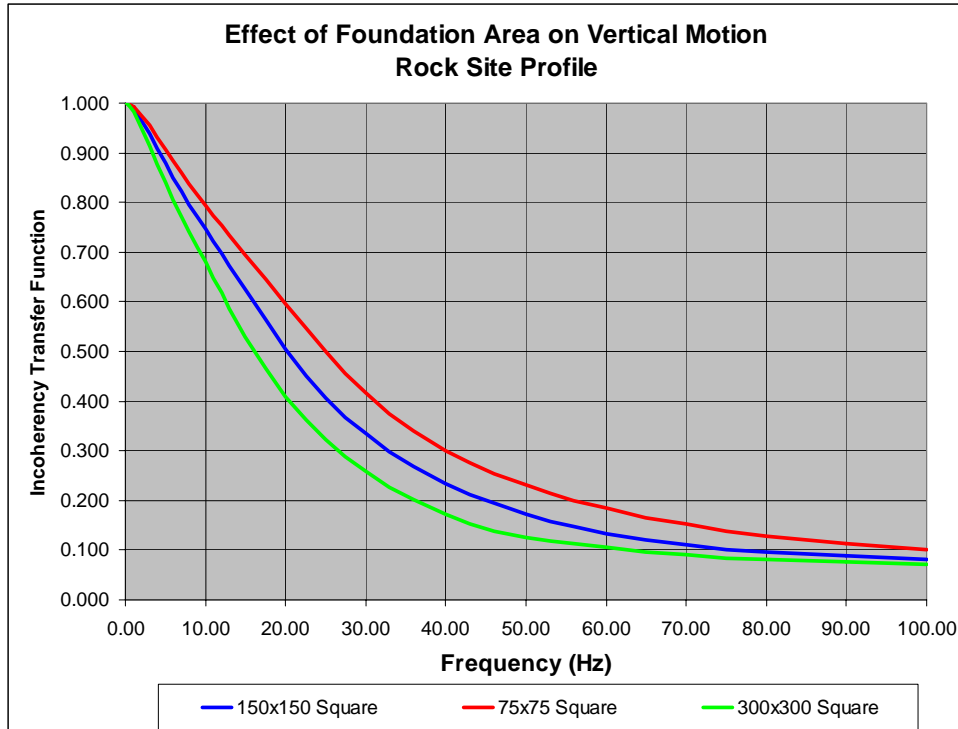


**Figure 0-8**  
**Vertical Motion Incoherency Transfer Function – Effect of Foundation Area**

## Spectral Corrections

Foundation response spectra accounting for seismic wave incoherence have been computed in the manner described in Chapter 3. By this approach, the PSD is computed from the response spectra of the free-field input motion and input to CLASSI. The program then evaluates the PSD of the foundation motion including the effects of seismic wave incoherence. The resulting response PSD is then converted to foundation response spectra by random vibration theory. Foundation response spectra have been developed for both the rock and soil site profiles described in Chapter 2 using the compatible free-field high-frequency rock and lower frequency soil ground response spectra, respectively. Parametric studies have been performed for:

- Foundation Shape (Constant Area)
  - 150-ft square footprint
  - 100 by 225-ft rectangle footprint
  - 84.63-ft radius circle footprint (spectra are identical to the square and rectangle and are not presented herein)
- Foundation Area (Constant Shape)
  - 75-ft square footprint
  - 150-ft square footprint
  - 300-ft square footprint

Results are shown in Figures 4-9 through 4-12.

Rock site. Figures 4-9 and 4-10 display response spectra for free-field ground motion and foundation response for the rock site. Figure 4-9 shows horizontal motion; Figure 4-10 shows vertical motion. Two free-field ground motion response spectra are plotted: the site-specific ground response spectra for the rock site and for reference, the US NRC Regulatory Guide 1.60 design response spectra (modified in the high-frequency region) anchored to a Peak Ground Acceleration of 0.3g (called the AP1000 SSE in the figures). Foundation response spectra for the four cases listed above are super-imposed on the free-field ground motion. It may be seen from these figures that the foundation spectra for the 150-ft square footprint, the 100 by 225-ft rectangle footprint, and the circle of the same area are the same. This is expected since the incoherency transfer functions are the same. These figures also show the effects of foundation area on response spectra for the 75-ft, 150-ft, and 300-ft square foundation footprint.

Soil site. Figures 4-11 and 4-12 display response spectra for the soil site in a similar manner to the data shown in Figures 4-9 and 4-10 for the rock site. Note however, that the site-specific free-field ground motion is significantly different than the site-specific rock motion. The same comparisons of foundation response spectra for the soil site are made. Note, there are reductions in response spectral values due to incoherence, but the most significant of those occurs in the frequency range above 10 Hz. The response spectra reductions as a function of foundation area are much more significant for the rock site than for the soil site. The effect of seismic wave incoherence is primarily a high-frequency phenomenon. Hence, the observed reductions in foundation response spectra are much less for the soil site since the soil site-specific ground motion is deficient in high frequencies. For the rock site, the peak of the horizontal spectra is reduced from 0.85g for the 75-ft square foundation to 0.76g for the 150-ft square foundation to 0.67g for the 300-ft square foundation. All of these peak spectra values are much less than the 1.48g peak of the free-field input spectra in the horizontal direction. Similar behavior is observed for the vertical ground motion.

Approximate Treatment of Incoherency of Ground Motions. Spectral corrections taken from the figures are shown in Tables 4-1 and 4-2 for horizontal and vertical motion, respectively; along with the spectral corrections that are given in ASCE 4. Reductions are shown for the foundation dimensions of 75, 150, and 300 feet. It may be seen that spectral reductions are significantly greater than the ASCE 4 values for the rock site, but are actually somewhat similar for the soil site. This demonstrates that spectral reductions are not a proper way to account for seismic wave incoherence as they strongly depend on the frequency content of the free-field input ground response spectra. An approach based on the incoherency transfer function (ITF), modified to account for induced rotations, is more appropriate. The ITFs are independent of the input motion. However, the approximate rules to be applied differ depending on the predominant frequency content of the input motion.

**Table 0-1  
Spectral Corrections for Horizontal Motion**

Frequency	ASCE 4		Rock-H			Soil-H		
	150	300	75	150	300	75	150	300
<b>5.00</b>	1.00	1.00	0.95	0.93	0.89	0.98	0.97	0.95
<b>10.00</b>	0.90	0.80	0.84	0.78	0.71	0.90	0.85	0.79
<b>15.00</b>	0.86	0.71	0.68	0.59	0.49	0.78	0.71	0.63
<b>20.00</b>	0.82	0.65	0.50	0.41	0.33	0.68	0.62	0.56
<b>25.00</b>	0.80	0.60	0.38	0.30	0.24	0.64	0.60	0.55
<b>30.00</b>	0.80	0.60	0.32	0.25	0.20	0.64	0.60	0.56
<b>40.00</b>	0.80	0.60	0.27	0.22	0.19	0.65	0.62	0.59
<b>50.00</b>	0.80	0.60	0.26	0.22	0.19	0.68	0.66	0.63

**Table 0-2  
Spectral Corrections for Vertical Motion**

Frequency	ASCE 4		Rock-V			Soil-V		
	150	300	75	150	300	75	150	300
<b>5.00</b>	1.00	1.00	0.88	0.85	0.80	0.91	0.89	0.86
<b>10.00</b>	0.90	0.80	0.78	0.73	0.66	0.83	0.79	0.74
<b>15.00</b>	0.86	0.71	0.69	0.62	0.54	0.76	0.71	0.62
<b>20.00</b>	0.82	0.65	0.61	0.52	0.43	0.69	0.63	0.54
<b>25.00</b>	0.80	0.60	0.53	0.44	0.36	0.64	0.57	0.50
<b>30.00</b>	0.80	0.60	0.46	0.38	0.30	0.59	0.52	0.46
<b>40.00</b>	0.80	0.60	0.36	0.29	0.23	0.53	0.48	0.43
<b>50.00</b>	0.80	0.60	0.31	0.25	0.20	0.50	0.46	0.42

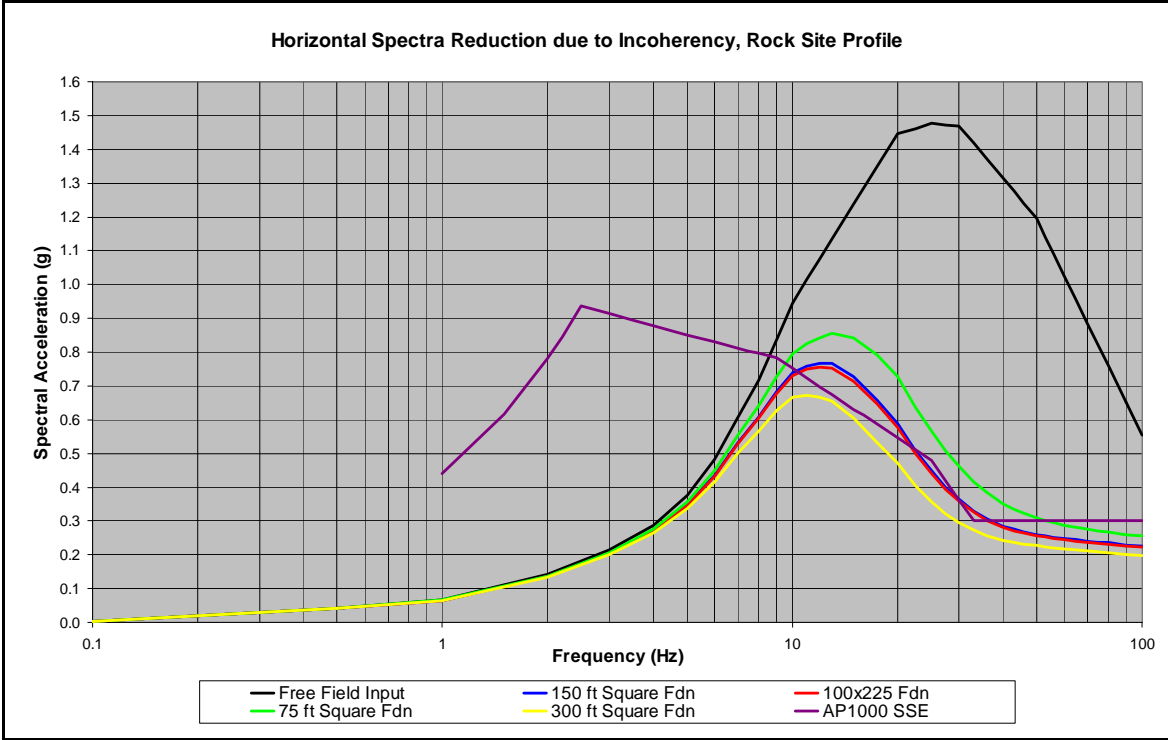


**Figure 0-9**  
**Horizontal Motion Foundation Response Spectra, Rock Site**

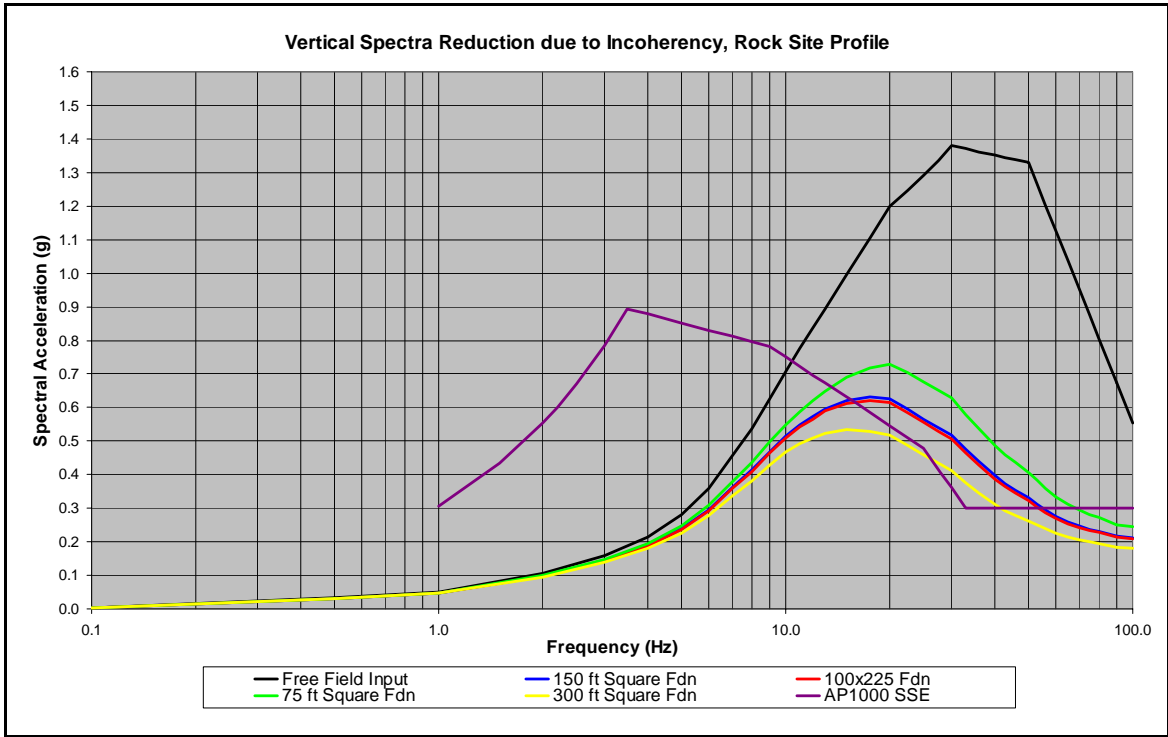


**Figure 0-10**  
**Vertical Motion Foundation Response Spectra, Rock Site**

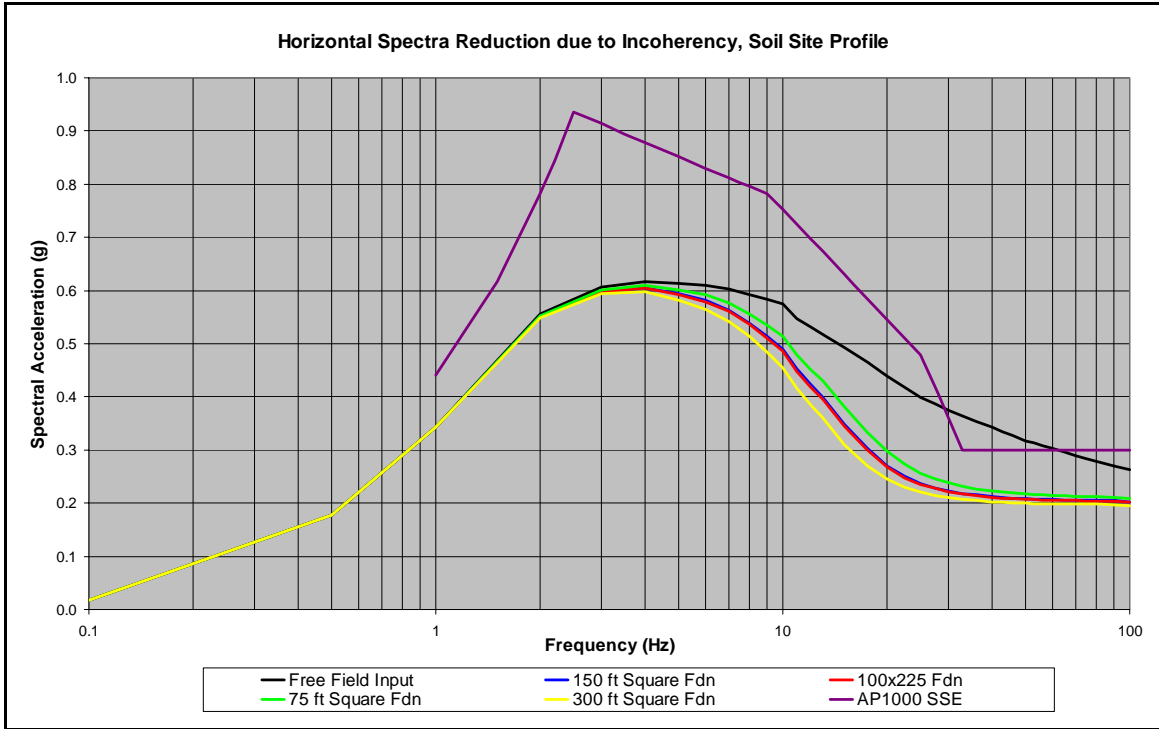


**Figure 0-11**  
Horizontal Motion Foundation Response Spectra, Soil Site

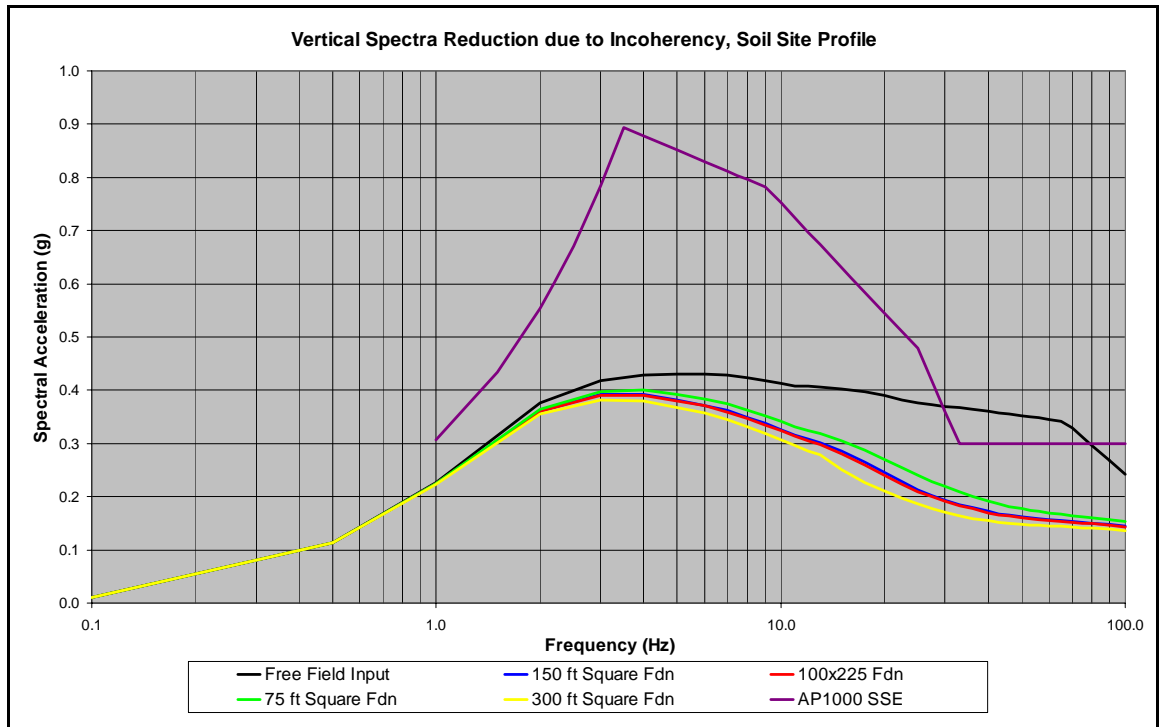


**Figure 0-12**  
Vertical Motion Foundation Response Spectra, Soil Site

## Rotations Induced by Incoherence

Thus far in this chapter it has been demonstrated that ground motion incoherence produces a reduction in the translational motion of the foundation relative to the free-field motion. It is known that incoherence can induce rotation due to the variability of the ground motion over the foundation footprint. For a rigid massless foundation, as is considered in this chapter, incoherent horizontal motion can induce torsional motion and incoherent vertical motion can induce rocking motion. To demonstrate the amplitude of induced rotations, the incoherency transfer function and the response spectrum for translational motion at the edge of the foundation caused by rotation are evaluated. These translational motions due to incoherence-induced rotations are compared to translational motions at the center of the foundation from the translational input to assess the effect of rotations.

As demonstrated in Chapter 3, the ITF is equal to the amplitude of the square root of the diagonal terms of the 6 by 6 cross PSD matrix of rigid massless foundation motion subjected to unit PSD input. The first three ITF terms are for translational motion and the last three ITF terms are for rotational motion. To quantify the maximum effect of the rotational terms on the response of the rigid massless foundation, the rotational ITF terms are converted to translational motions on the extreme edges of the foundation. To do so, they are scaled by the distance from the center of the foundation to the edge of the foundation of interest. Translations at these extreme points due to rotations induced by incoherence are evaluated for the 150-ft square foundation and the 100 by 225-ft rectangular foundation. The rock and soil site profiles described in Chapter 2 were considered for the evaluation of response spectra on the foundation.

For the 150-ft square foundation, the translation due to rotation is determined by multiplying the rotation by 75-ft, the distance from the foundation center to a wall at the edge of the foundation. Torsion due to horizontal motion and rocking due to vertical motion are illustrated in Figures 4-13 and 4-14.

For the 100 by 225-ft rectangular foundation, the 225-ft side is along the x or H1 axis and the 100-ft side is along the y or H2 axis. Vertical motion is in the z or V direction. For the rectangular foundation, H1 translation due to torsion is determined by multiplying the rotation by 50-ft, the distance from the foundation center to a wall at the edge of the foundation, and H2 translation due to torsion is determined by multiplying the rotation by 112.5-ft, the distance from the foundation center to a wall at the edge of the foundation. Vertical translation due to rocking is determined by multiplying the rotation by 112.5-ft, the largest distance from the foundation center to a wall at the edge of the foundation. Torsion due to horizontal motion and rocking due to vertical motion are illustrated in Figures 4-15, 4-16, and 4-17.

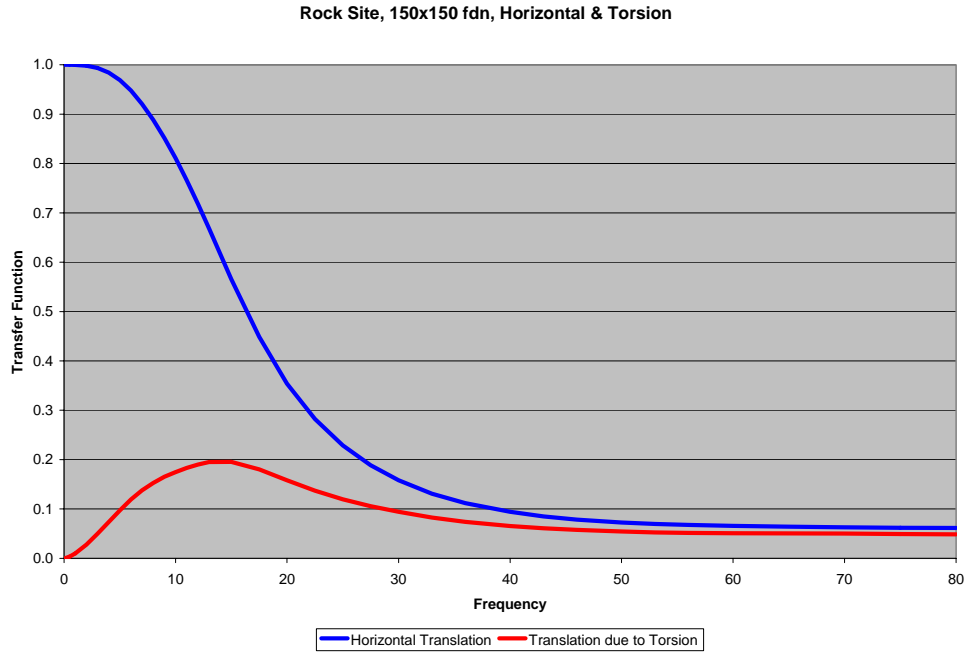


**Figure 0-13**  
**Torsion Induced by Incoherent Horizontal Input, Square Foundation**

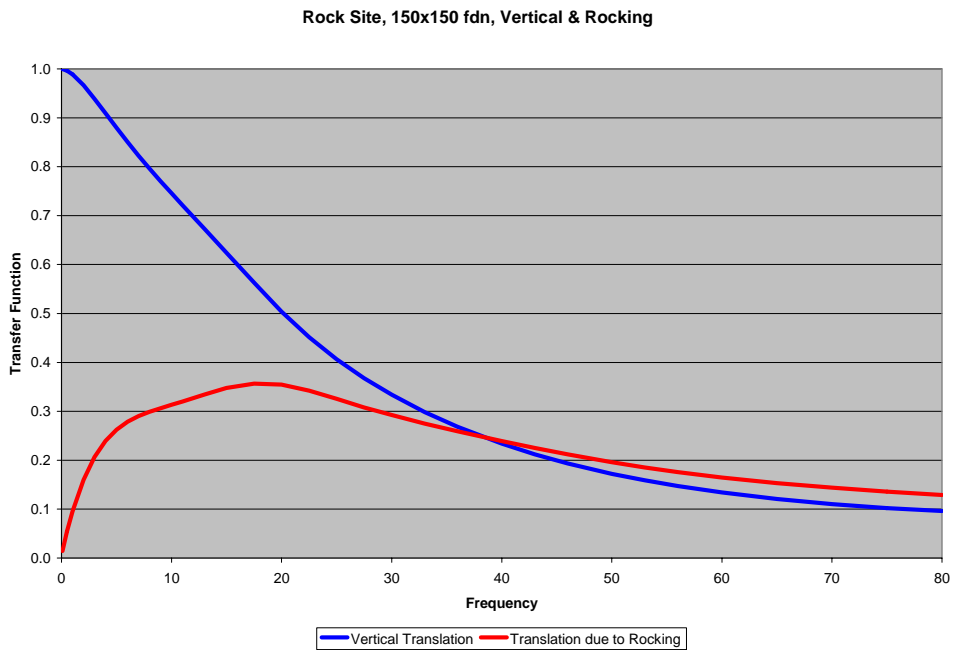


**Figure 0-14**  
**Rocking Induced by Incoherent Vertical Input, Square Foundation**

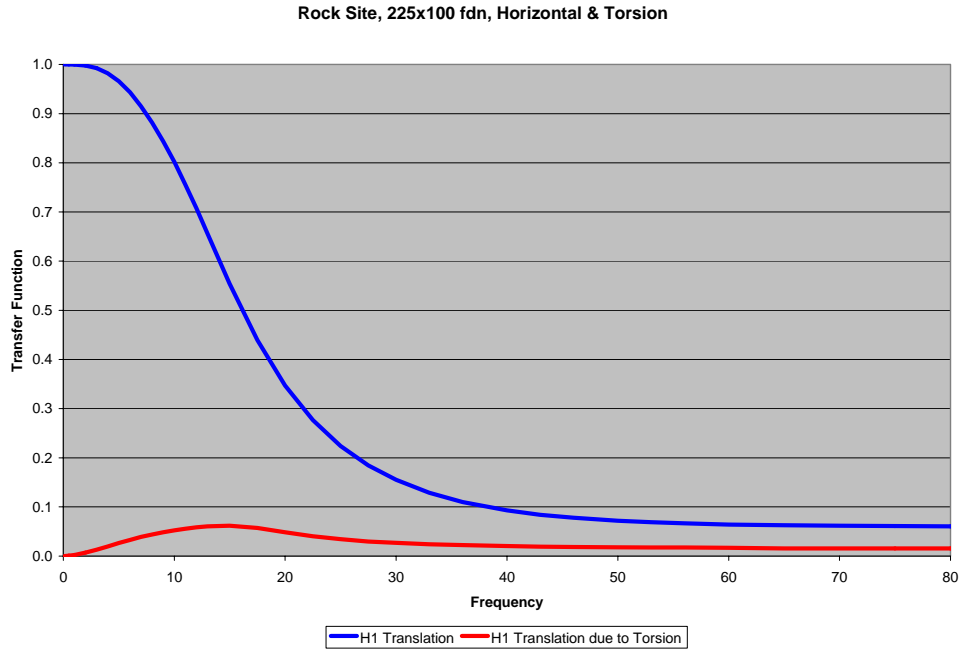


**Figure 0-15**  
**H1 Torsion Induced by Incoherent Horizontal Input, Rectangle Foundation**

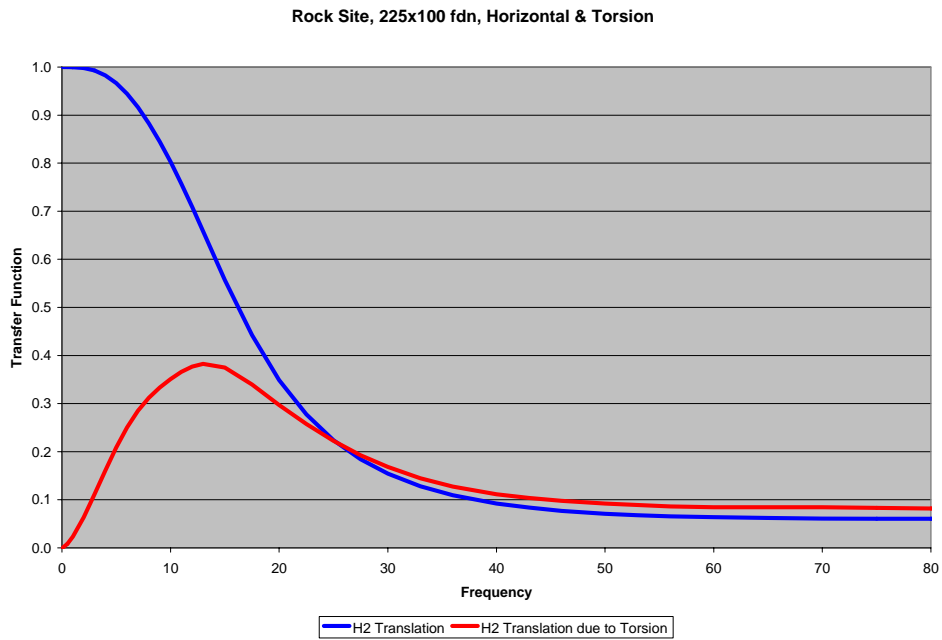


**Figure 0-16**  
**H2 Torsion Induced by Incoherent Horizontal Input, Rectangle Foundation**

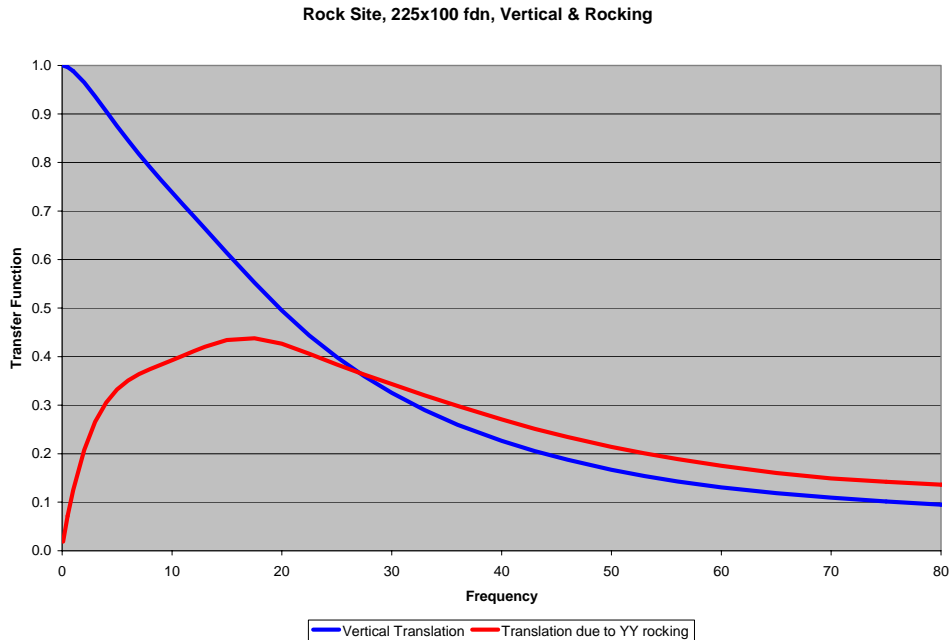


**Figure 0-17**  
**Rocking Induced by Incoherent Vertical Input, Rectangle Foundation**

Vertical motion due to rocking caused by incoherent vertical input appears to be more significant relative to vertical translation at the foundation center than the horizontal motion due to torsion caused by incoherent horizontal input relative to translational motion at the foundation center. The reason for this phenomenon is that the vertical coherency function is greater than the horizontal coherency function at the same frequencies and separation distances as demonstrated in Chapter 2.

The transfer functions shown above provide an indication of the effects of rotations and can be compared to results in the literature (Kim and Stewart, 2003). To gain a better understanding of the effect of rotation on structural response, foundation response spectra evaluated at the center and edge of the foundation were computed. In this manner, the effect of rotation on structural response can be better quantified.

Foundation response spectra accounting for seismic wave incoherence and including both translation and rocking effects have been computed in the manner described in Chapter 3. By this approach, the PSD is computed from the response spectra of the free-field input motion and input to CLASSI. The program then evaluates the PSD of the foundation motion including the effects of seismic wave incoherence. The resulting response PSD is then converted to foundation response spectra by random vibration theory. Foundation response spectra have been developed for both the rock and soil site profiles described in Chapter 2 using the compatible free-field high-frequency rock and lower frequency soil ground response spectra, respectively. Parametric studies have been performed for both the 150-ft square footprint and the 100 by 225-ft rectangular footprint. The resulting foundation response spectra for the square foundation are presented in Figures 4-18 through 4-21. Foundation spectra for the rectangular foundation are presented in Figures 4-22 through 4-25.

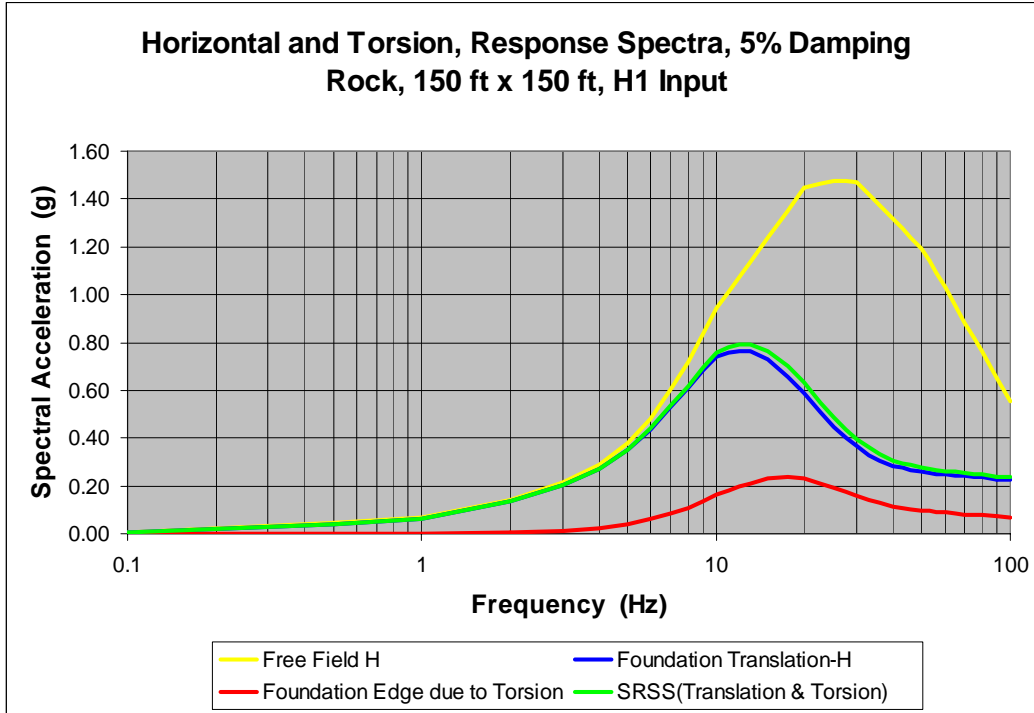


**Figure 0-18**  
Response Spectra Including Torsion, Square Foundation, Rock Site

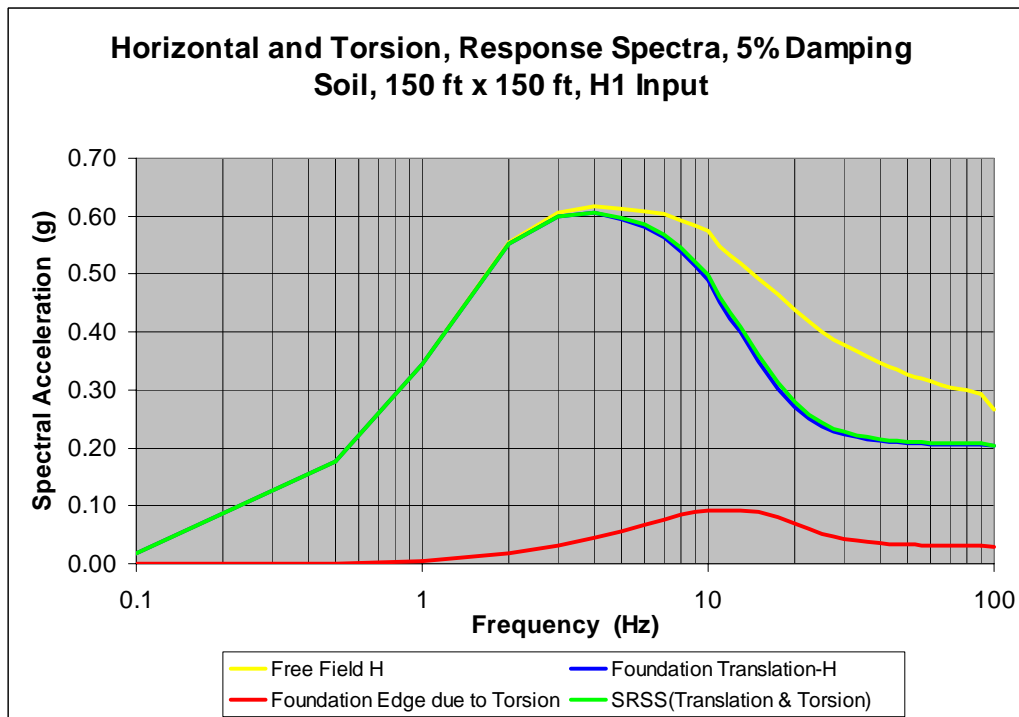


**Figure 0-19**  
Response Spectra Including Torsion, Square Foundation, Soil Site

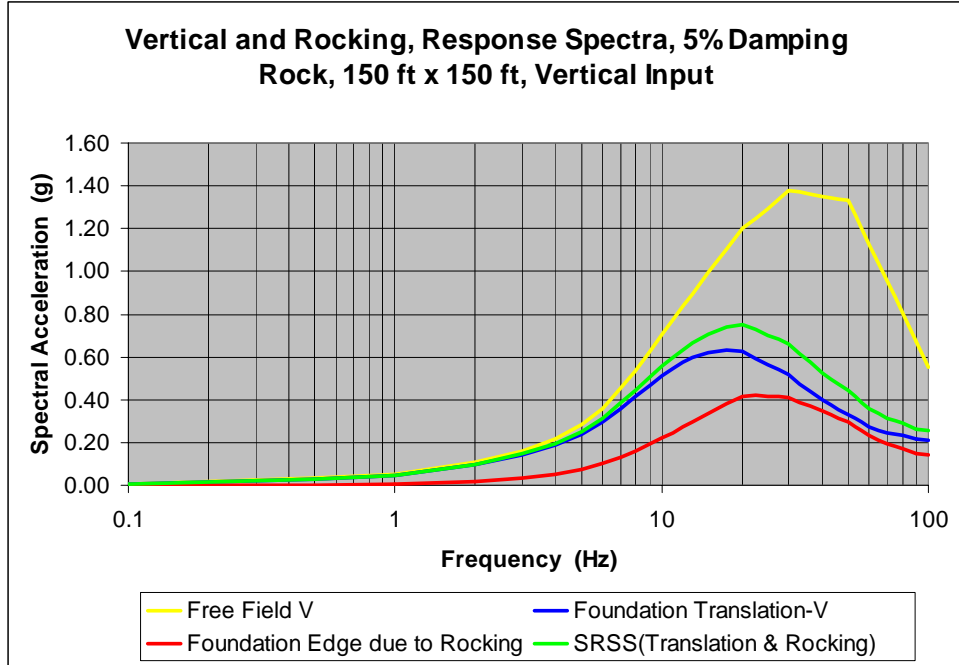


**Figure 0-20**  
Response Spectra Including Rocking, Square Foundation, Rock Site

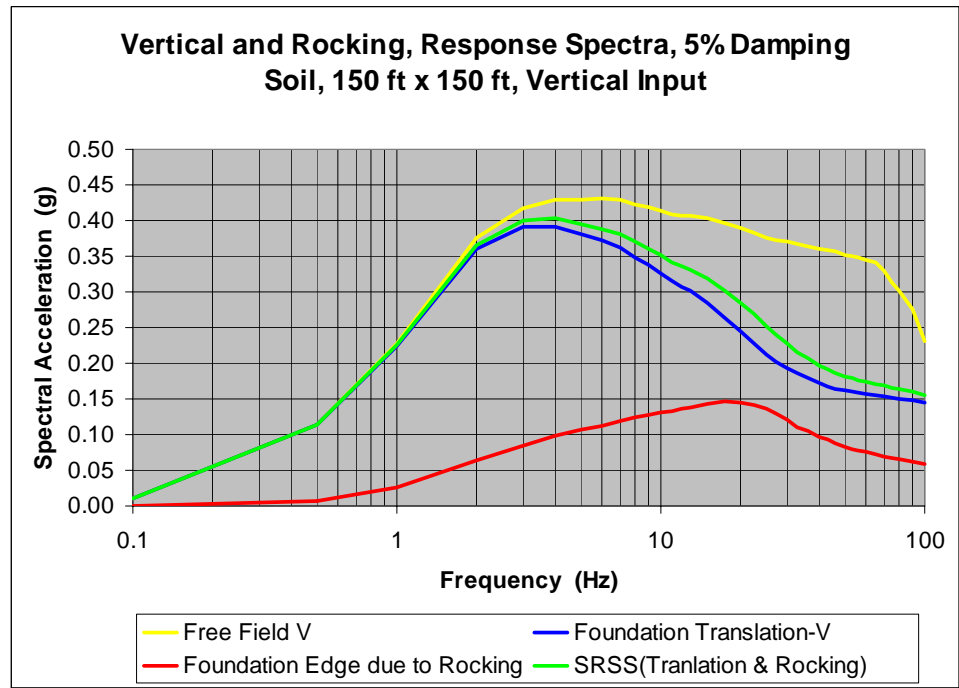


**Figure 0-21**  
Response Spectra Including Rocking, Square Foundation, Soil Site

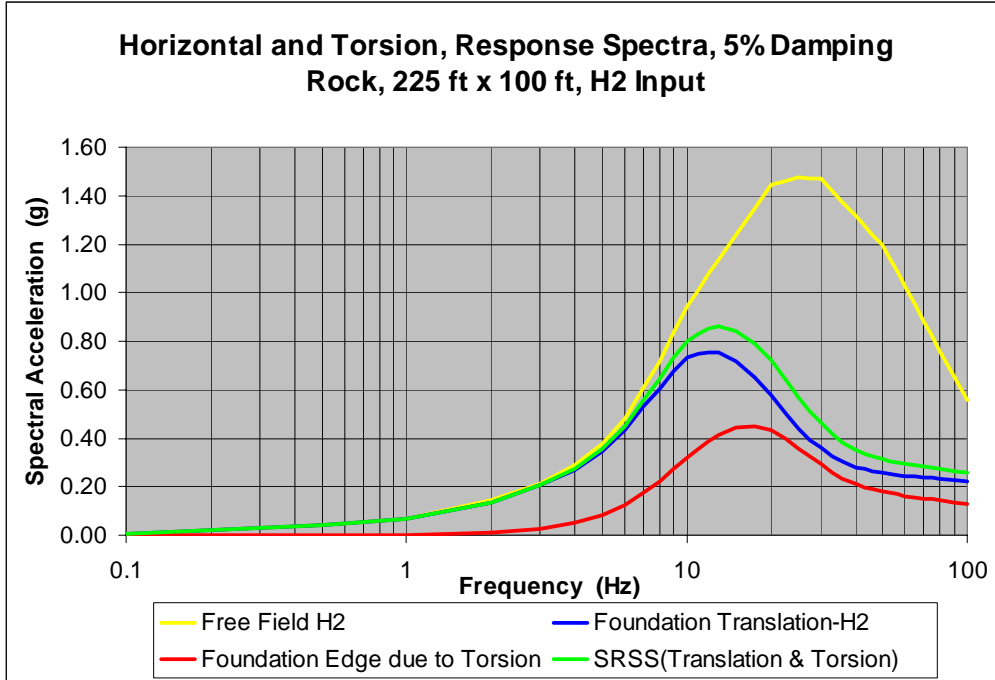


**Figure 0-22**  
**Response Spectra Including Torsion, Rectangle Foundation, Rock Site**

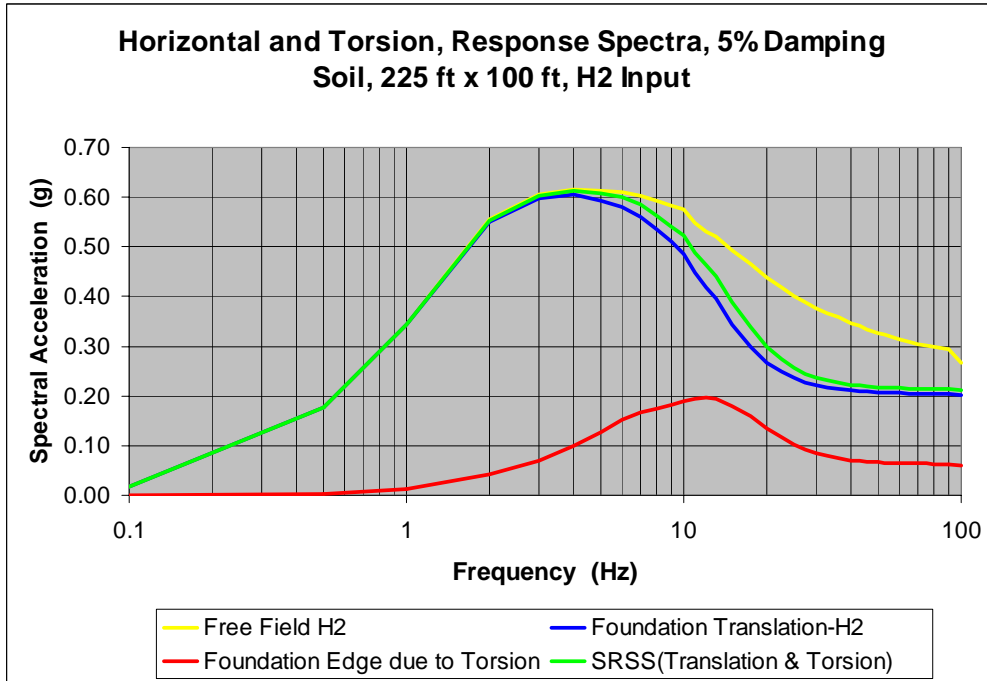


**Figure 0-23**  
**Response Spectra Including Torsion, Rectangle Foundation, Soil Site**

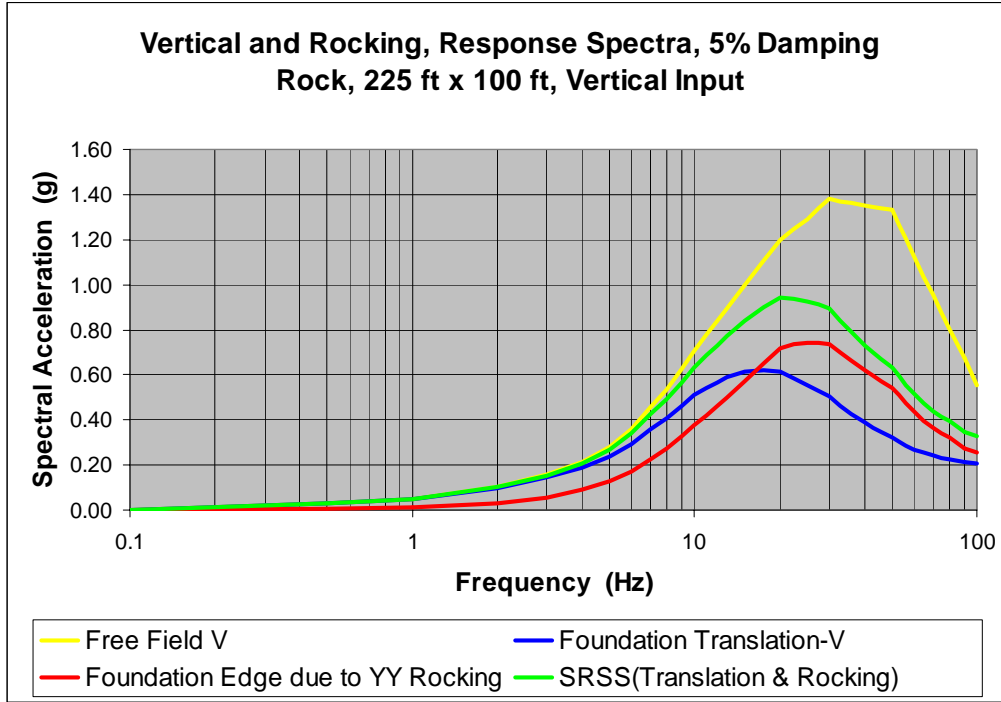


**Figure 0-24**  
Response Spectra Including Rocking, Rectangle Foundation, Soil Site

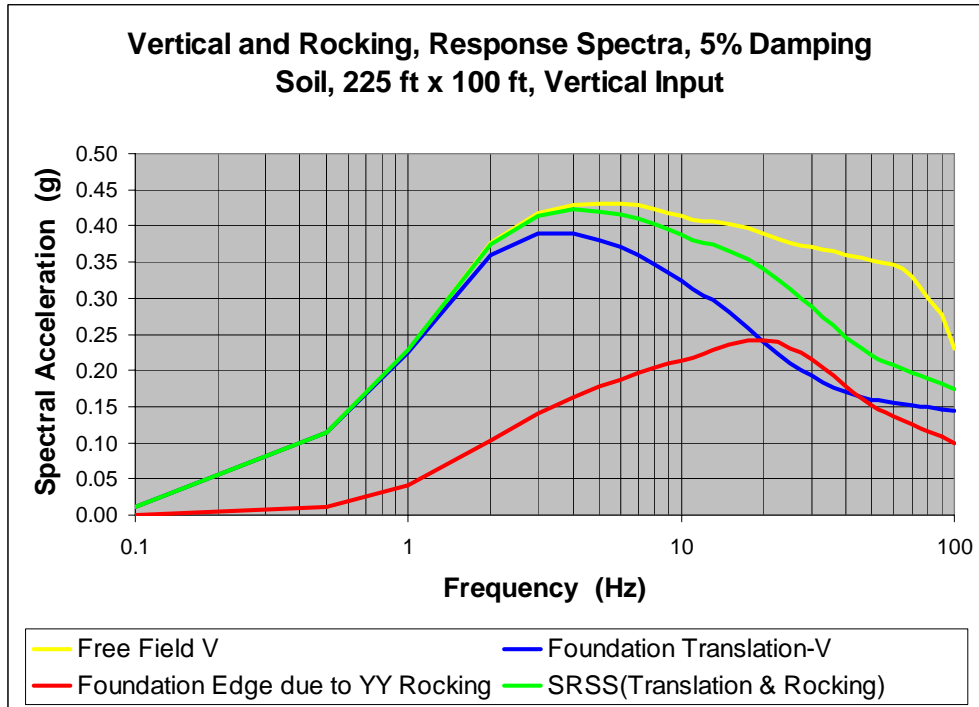


**Figure 0-25**  
Response Spectra Including Rocking, Rectangle Foundation, Soil Site

Effect of Torsion – The effect of incoherence-induced torsion on the foundation response is illustrated in Figures 4-18 and 4-19 for the square foundation, and Figures 4-22 and 4-23 for the rectangular foundation. For the rectangle foundation, torsion response was maximized by looking at the foundation edge that is 112.5-ft away from the foundation centerline. The effects of torsion are quantified by comparing the horizontal translation spectra at the foundation center with the SRSS of translation and torsion at the foundation edge. This approach is used to evaluate the random effect of torsion relative to horizontal response due to horizontal ground motion.

For the square foundation on the rock site, the ZPA is about 5% greater due to the effect of incoherence-induced torsion. For this case, the SRSS spectrum is no greater than 9% higher than the translation only spectra at any frequency. For the square foundation on the soil site, the ZPA is about 1% greater due to the effect of incoherence-induced torsion. For this case, the SRSS spectrum is no greater than 3% higher than the translation only spectra at any frequency.

For the rectangular foundation, Figures 4-22 and 4-23 show the maximum effects from the two directions, i.e., the combined effect of the motion in the two directions due to horizontal translation at the center of the foundation and that due to the induced torsion due to H2 input motion. For the rectangular foundation on the rock site, the ZPA is about 16% greater due to the effect of incoherence-induced torsion. For this case, the SRSS spectrum is no greater than 29% higher than the translation only spectra at any frequency. For the rectangle foundation on the soil site, the ZPA is about 4% greater due to the effect of incoherence-induced torsion. For this case, the SRSS spectrum is no greater than 13% higher than the translation only spectra at any frequency.

Figures 4-18, 4-19, 4-22, and 4-23 demonstrate that there are significant reductions due to incoherence even considering the added translational response at extreme locations due to torsion. This conclusion is apparent by comparison of the free-field spectra to the SRSS of translation and torsion spectra. Even so, the contribution of additional torsion due to ground motion incoherence appears to be greater, in some cases, than what can be accommodated by considering 5% accidental eccentricity per ASCE 4.

Effect of Rocking - The effect of incoherence-induced rocking on the foundation vertical response is illustrated in Figures 4-20 and 4-21 for the square foundation, and Figures 4-24 and 4-25 for the rectangular foundation. For the rectangular foundation, rocking response was also maximized by looking at the foundation edge that is 112.5-ft away from the foundation centerline. The effects of rocking are quantified by comparing the vertical translation spectra at the foundation center with the SRSS of translation and rocking at the foundation edge. This approach is used for evaluating the random effect of vertical displacements due to rocking vs. vertical displacements due to vertical ground motion only.

For the square foundation on the rock site, the vertical ZPA is about 21% greater due to the effect of incoherence-induced rocking. For this case, the SRSS spectrum is no greater than 34% higher than the translation only spectra at any frequency. For the square foundation on the soil site, the vertical ZPA is about 9% greater due to the effect of incoherence-induced rocking. For this case, the SRSS spectrum is no greater than 19% higher than the translation only spectra at any frequency.

For the rectangular foundation on the rock site, the effect at the extreme location on the foundation (112.5-ft. from the center) is significantly greater. The vertical ZPA is about 60% greater due to the effect of incoherence-induced rocking when compared to the vertical response only. For this case, the SRSS spectrum is higher by up to a factor of 2-in higher frequency ranges. For the rectangular foundation on the soil site, the ZPA is about 22% greater due to the effect of incoherence-induced rocking. For this case, the SRSS spectrum is no greater than 51% higher than the translation only spectrum at any frequency.

Figures 4-20, 4-21, 4-24, and 4-25 demonstrate that there are significant reductions due to incoherence even considering the added translational response at extreme locations due to rocking. This conclusion is based on the comparison of the free-field spectra to the SRSS of vertical translation due to translational ground motion alone and the vertical motion due to induced rocking. This is especially true for the rock site with the relative high-frequency free-field ground response spectra.

Even so, the contribution of additional rocking due to ground motion incoherence produces a significantly higher foundation motion at the extremities of the foundation than the vertical motion of the foundation center. These results demonstrate that it is still worthwhile to pursue high-frequency reductions of ground motion due to incoherence but the effects of incoherence-induced rotations must be considered. Further evaluations of this point are presented in Chapter 5.

## Enclosure 6

# CHAPTER 5 SSI & STRUCTURE RESPONSE

---

### General

The effect of ground motion incoherence on the response of rigid, massless foundations was treated in Chapter 4. These effects were presented as transfer functions between the free-field ground motion and the response of the rigid, massless foundations. In addition, the effect of incoherence was demonstrated by comparison of the response spectra on the foundation to the free-field ground response spectra. The transfer functions were denoted Incoherency Transfer Functions (ITFs).

Chapter 5 investigates the effects of incoherence of ground motion on the response of a nuclear power plant structure. The structure being analyzed is a simplified model of the AP1000 (itemized in Chapter 2). Note the structure model is comprised of three sticks with limited inter-connectivity at upper elevations. The structure is anchored to a 15-ft thick, 150-ft square foundation. For the cases including soil-structure interaction (SSI), the rock site profile described in Chapter 2 was used. The free-field ground motion of interest is that motion compatible with the rock site profile, i.e., exhibiting significant high-frequency motion. For all analyses, the spectrum compatible time histories defined the free-field ground motion. All analyses considered 3 directions of simultaneous earthquake input motion.

In addition to evaluating the effects of incoherence on the response of the structure, a simplified method to incorporate seismic wave incoherence into seismic analysis of NPP structures, including SSI was investigated. Simplified analyses described in this chapter are performed to demonstrate that the approach of multiplying the Fourier amplitude of the input ground motion by a function related to the ITF that captures translational and rotation effects of incoherency to form an engineering modified input motion is a promising approach to account for incoherency of ground motion.

Four sets of analyses have been performed for the AP1000 structural model:

1. SSI analysis with coherent input motion (blue curves in all Chapter 5 response spectra figures)
2. SSI analysis with incoherent input motion
  - a. Rigorous (direct) approach including all components of foundation input motion (three translations and three rotations) ( green curves in all Chapter 5 response spectra curves)
  - b. Rigorous (direct) approach excluding rotational foundation input motion (red curves in all Chapter 5 response spectra figures)
3. SSI analysis with input motion modified by Incoherency Transfer Function (Simplified Approach)

It is recognized that rotations (torsion and rocking) are induced by incoherence as discussed in Chapter 4. To assess the impact of these rotations on structure response in a full SSI analysis as is conducted in this chapter, the rigorous SSI analysis with incoherent input motion is performed in two ways, Analyses 2a and 2b. In Analysis 2a, the effect of rotations will be realized in the SSI analysis. In Analysis 2b, the effect of rotations is deliberately eliminated for the purpose of assessing the rotation effects.

To evaluate the effects of incoherency on in-structure response, response spectra were calculated and compared for the various analyses at the tops of the structure sticks, at lower elevations on the structure sticks, and on outriggers extending 65 or 75-ft. from the top of each stick in the X direction. To evaluate the effects of induced rocking, the responses on the structure mass center and on the outrigger were used; to evaluate the effects of induced torsion, the responses on the outriggers were used.

Induced rocking due to vertical ground motion incoherence and induced torsion due to horizontal ground motion incoherence are considered. Their effect on vertical and horizontal response in the structure is presented.

## **SSI and Incoherence – Direct Method**

The results of Analyses 1 and 2 are presented here including SSI coherent and incoherent evaluations. The SSI incoherent analyses incorporate seismic wave incoherency through the scattering matrix populated by the incoherency transfer functions generated for the rock site and for the rigid massless foundation of 150-ft square. In this manner, incoherence is directly incorporated into the seismic analysis. In Analysis 2a, all terms of the scattering matrix are included, translations and rotations. In Analysis 2b, the rotational terms of the scattering matrix are set to zero.

As discussed more fully in Chapter 2, the fixed-base modes of the three structure sticks provide some insight into the dynamic behavior. The ASB has predominate modes with frequencies less than 10 Hz with fundamental modes in the horizontal directions of 3.2 Hz (X-direction) and 3.0 Hz (Y-direction); the fundamental mode in the vertical direction of frequency 9.9 Hz (Z-direction). Many modes participate in the response of the ASB. The predominate modes of the SCV in the horizontal directions also have frequencies less than 10 Hz – the lowest frequency of an important X-direction mode being 5.5 Hz; Y-direction mode being 6.14 Hz; the lowest frequency of an important vertical mode being 16 Hz. As with the ASB, many modes participate in the response of the SCV. The predominant modes of the CIS have frequencies greater than 10 Hz. Many modes participate in the response of the CIS.

The total mass of the structures is apportioned approximately ASB – 86%, CIS – 11%, and SCV – 3%, i.e., ignoring the mass of the foundation. The dynamic behavior of the three stick model is coupled through the inter-connectivity of the sticks and natural torsion is induced throughout the three structures due to the eccentricities assumed in the ASB and CIS structures.

Results presented are in-structure response spectra (5% damping) at the foundation and at points on each of the three models (ASB, SCV, CIS) as shown in Figure 5-1. Responses at the top of each model and at approximately mid-height (referred to as “low on” a particular structure within Figure 5-1), are calculated and compared. The near mid-height locations were selected to investigate the potential effect of incoherence on points where higher modes more fully

participate in the response. Note that the ASB stick represents both the auxiliary building and the shield building. The combined auxiliary and shield building extends up to the top of the auxiliary building at Node 120. Above this node and elevation the ASB stick only represents the shield building. Hence, in addition to the top of the shield building and low in the combined ASB model, output was calculated and is presented at the top of the auxiliary building at the centerline (Z-direction), at the center of mass for the horizontal directions (X and Y), and at the outrigger (X, Y, Z).

In addition to foundation response, results are presented at Nodes 310, 310out, 120mc, 120out, and 80mc on the ASB, Nodes 417, 417out and 406 on the SCV, and Nodes 538mc, 538out, and 535mc on the CIS where node locations are illustrated in Figures 5-1 and 2-8. The “mc” designation added to the node number indicates that the mass and shear centers are not coincident and response is given at the mass center. The “out” designation added to the node number indicates an outrigger location used to display torsional response at the periphery of the structure. In-structure response spectra at these twelve locations for two horizontal, X and Y, and the vertical direction, Z, of ground motion are presented in Figures 5-2 through 5-37. Again, all analyses considered 3 directions of simultaneous earthquake input motion.

### ***Foundation Response***

Foundation response is presented in Figures 5-2, 5-3, and 5-4. Comparing the foundation response spectra due to incoherency effects (Analysis 2a) with those of Analysis 1, generally shows significant reductions over those due to coherent SSI effects at frequencies greater than 10 Hz. Spectral accelerations are reduced by a factor of 1.5 to 3 over significant frequency ranges.

Comparison of the full incoherent results (Analysis 2a – green curve) with those excluding rotational effects (Analysis 2b – red curve) provides an indication of the effects of induced rotations on foundation response at its center. Any observed change in foundation response is due to the effects of the complete SSI phenomena (kinematic and inertial effects) of the rock structure system. For the foundation response, induced rotations have minimal effects on the horizontal response spectra. Relatively small perturbations about the full incoherent results are present for frequencies between 8 and 30 Hz where Analyses 2a and 2b ZPA values are coincident. In the vertical direction, there is no significant effect of rotations on the foundation response.

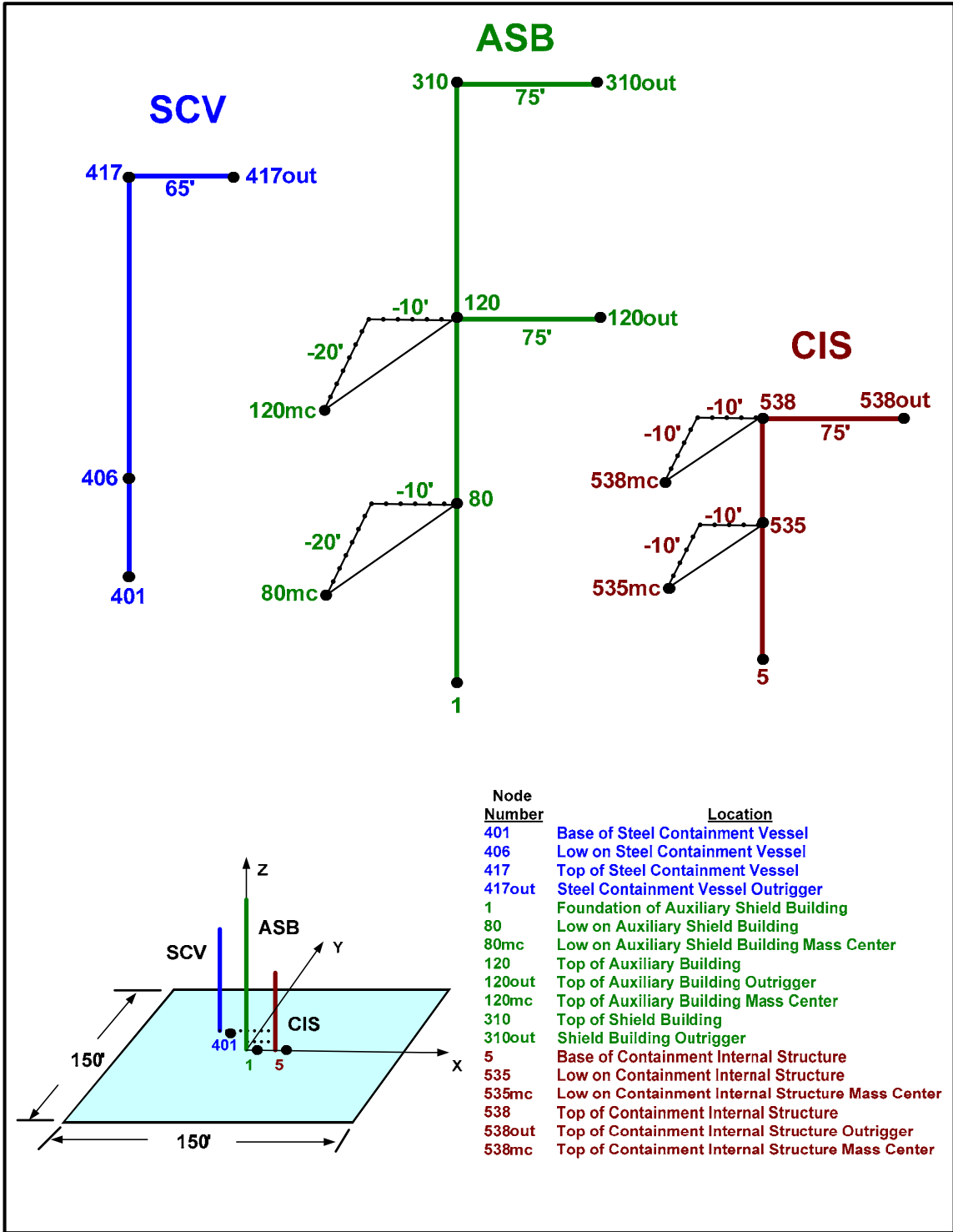


Figure 0-1  
Locations on the AP1000 Stick Model where In-Structure Response Spectra are Computed

## **Auxiliary and Shield Building (ASB)**

- **Top of Shield Building.** Responses at the top of the coupled auxiliary and shield building (ASB) are presented in Figures 5-5, 5-6, and 5-7. Comparing the response spectra due to incoherency effects (Analysis 2a) with those of Analysis 1, generally, shows significant reductions due to incoherency for frequencies greater than 12 Hz. For horizontal directions, the reductions are, generally, greater than 30% up to 30 Hz and less as one approaches the ZPA frequency. For the vertical direction, substantial reductions are observed in the frequency range above 10 Hz, including at the ZPA frequency.

At frequencies of peak amplification less than 10 Hz (X-direction 3.2 and 6.5 Hz; Y-direction 3 Hz and 6 Hz), slight increases in spectral accelerations of the incoherent case above the coherent case are observed. Comparing Analyses 2a and 2b, one concludes this effect is due to induced rotations.

The responses of the outrigger, extending 75 ft. in the X-direction, are presented in Figures 5-14, 5-15, and 5-16. The reductions in response spectral accelerations generally follow the trend of the values on the centerline, but the reductions are observed to be less. The effects of incoherence induced torsion are shown in Figure 5-15 Y-direction response, where the responses calculated due to coherence and incoherence (blue and green curves) are relatively close for frequencies above 12 Hz. The specific effect of induced torsion can be observed by comparing the no rotation case (red curves) with the full incoherence case (green curves).

For this relatively low-frequency structure, additional horizontal response induced by rocking is observed only in the low frequency range, i.e., at about 3 Hz. At frequencies of peak amplification less than 10 Hz (X-direction 3.2 and 6.5 Hz; Y-direction 3 Hz and 6 Hz), slight increases in spectral accelerations of the incoherent case above the coherent case are observed. The same phenomena observed above for frequencies less than 10 Hz is present on the outrigger, i.e., at frequencies of peak amplification, the incoherent response exceeds the coherent response. This is due to induced torsional response.

- **Top of Auxiliary Building.** Responses at the top of the auxiliary building are presented in Figures 5-8, 5-9, 5-10. In the X-direction, significant reductions due to incoherence are observed for frequencies greater than about 14 Hz to the ZPA frequency where the coherent and incoherent responses are the same. In the Y-direction, very significant reductions in the response are observed for frequencies greater than 10 Hz up to and including the ZPA. There are no observed low frequency exceedances of the incoherent responses at this location.

The responses of the outrigger, extending 75 ft. in the X-direction, are presented in Figures 5-17, 5-18, and 5-19. The reductions in response spectral accelerations generally follow the trend of the values of the points at the mass centers, but the reductions are observed to be less. The effects of incoherence induced rocking and torsion is observed for the X-direction in Figure 5-15 and in Figure 5-16 for the Y-direction response.

- **Low in ASB.** Responses at a lower elevation of the coupled auxiliary and shield building (ASB) are presented in Figures 5-11, 5-12, and 5-13. These spectra demonstrate similar behavior to that seen at other locations in the ASB. Generally, the response reductions in the vertical direction are significant for frequencies greater than 10 Hz.

## ***Steel Containment Vessel (SCV)***

- **Top of SCV.** Response at the top of the steel containment vessel (SCV) at the centerline is presented in Figures 5-20, 5-21, and 5-22. Comparing the response spectra due to incoherency effects (Analysis 2a) with those of Analysis 1, generally, show significant reductions in response for frequencies greater than about 12 Hz with less reductions at the ZPA. In the vertical direction, significant reductions are observed for all frequencies greater than 10 Hz. There are also no significant effects of induced rocking observed from these spectra.

The responses of the outrigger extending 75 feet in the X direction from the top of the steel containment vessel (SCV) are presented in Figures 5-26, 5-27, and 5-28. Significant reductions in response spectral accelerations are observed for frequencies greater than about 12 Hz in the X-direction and about 15 Hz in the Y-direction. Significant reductions in the vertical direction are observed for frequencies greater than about 12 Hz.

The effects of induced rotations are observed in the response spectra of Figure 5-27 when comparing the results due to Analyses 2a and 2b. Induced torsion is significant in the response for frequencies greater than 10 Hz. There are no rotational effects seen in the X-direction as the response spectra in Figures 5-20 and 5-26 are nearly identical. This is expected since the outrigger is placed on the X-axis and is considered to be representative of results away from the centers of mass of the structure. There are no effects of torsion seen in Z-direction response in Figure 5-28. Z direction outrigger response in Figure 5-28 is higher than center of mass response due to rocking. This rocking is structural seismic response and not due to incoherence.

- **Low in the SCV.** Responses at lower elevations of the steel containment vessel (SCV) are presented in Figures 5-23, 5-24, and 5-25. These spectra demonstrate similar behavior to that seen for the top of the SCV.

## ***Containment Internal Structure (CIS)***

- **Top of CIS.** Responses at the top of the containment internal structure (CIS) at the center of mass are presented in Figures 5-29, 5-30, and 5-31. Comparing the response spectra due to incoherency effects (Analysis 2a) with those of Analysis 1, generally, shows significant reductions over those due to coherent SSI effects at frequencies greater than about 12 Hz. These reductions are 50% or greater. Compared to the SSI coherent ground motion case.

Responses of the outrigger extending 75-ft in the X direction from the top of the containment internal structure (CIS) are presented in Figures 5-35, 5-36, and 5-37. Significant reductions in response spectral accelerations are observed in all three directions at this location at frequencies greater than about 12 Hz. Reductions on the order of 40% and greater are observed.

Comparing the full incoherent results (Analysis 2a - green curve) with those excluding rotational effects (Analysis 2b – red curve) provides an indication of the effects of induced rotations on the CIS response. At the center of mass, the effect of induced rocking is observed to be significant in the frequency range of 12-25 Hz. These phenomena are due to induced rocking exciting horizontal modes. At the outrigger location, in the X- and Z-directions, the effects of induced rotations are observed in the frequency range above 10 Hz;

in the Y-direction, the effect of induced rotations is due to the combination of torsion and rocking for frequencies greater than 10 Hz. Ignoring induced rotations under-estimates the response.

- **Low in the CIS.** Responses at lower elevations of the containment internal structure (CIS) are presented in Figures 5-32, 5-33, and 5-34. Generally, responses due to incoherence are significantly less than the case of coherent ground motions at frequencies greater than about 12 Hz. The importance of induced rotations is also evident from these plots.

### ***Summary***

Figures 5-2 through 5-34 demonstrate significant reductions in high-frequency response as a result of seismic wave incoherence. In the horizontal response directions, these reductions in response spectra are tempered due to incoherency induced rocking and torsion. Even with this phenomena of incoherency induced rocking and torsion, the fundamental conclusion remains that there are significant reductions in high-frequency response due to seismic wave incoherence.

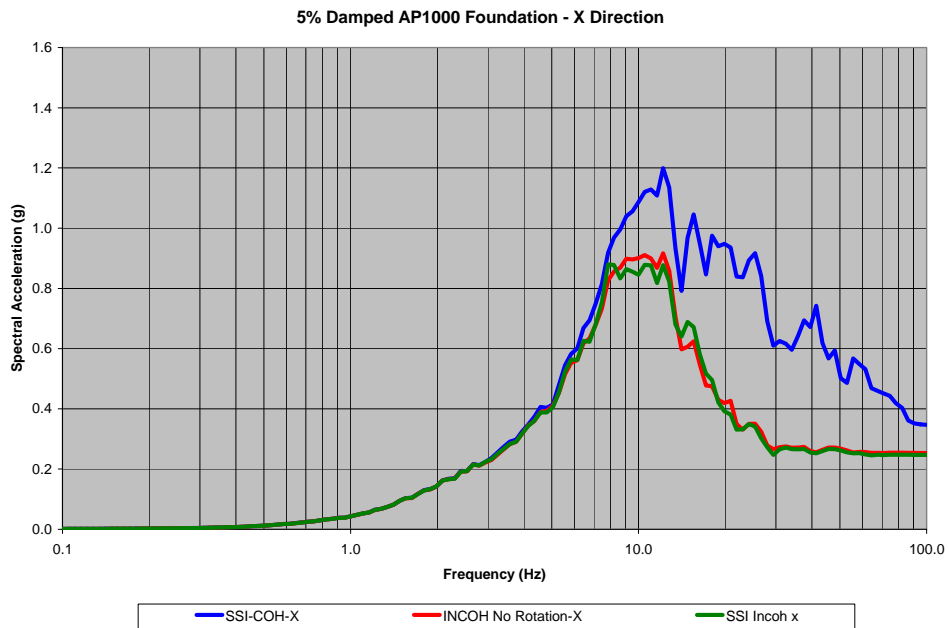


**Figure 0-2**  
**Foundation Response Spectra – X Direction –SSI Coherent, SSI Incoherent, SSI Incoherent with no Rotations (Node 1)**

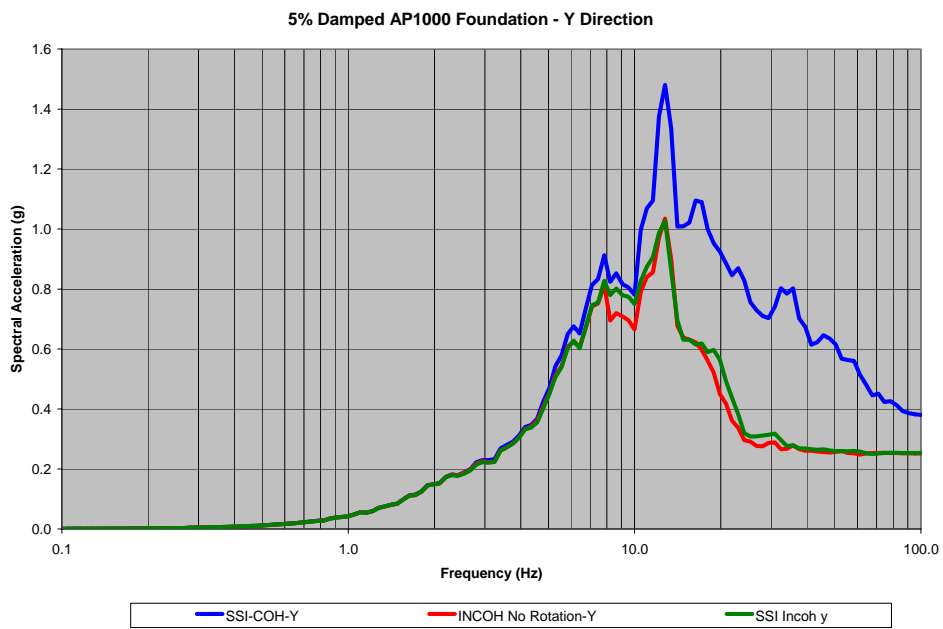


**Figure 0-3**  
**Foundation Response Spectra – Y Direction –SSI Coherent, SSI Incoherent, SSI Incoherent with no Rotations (Node 1)**

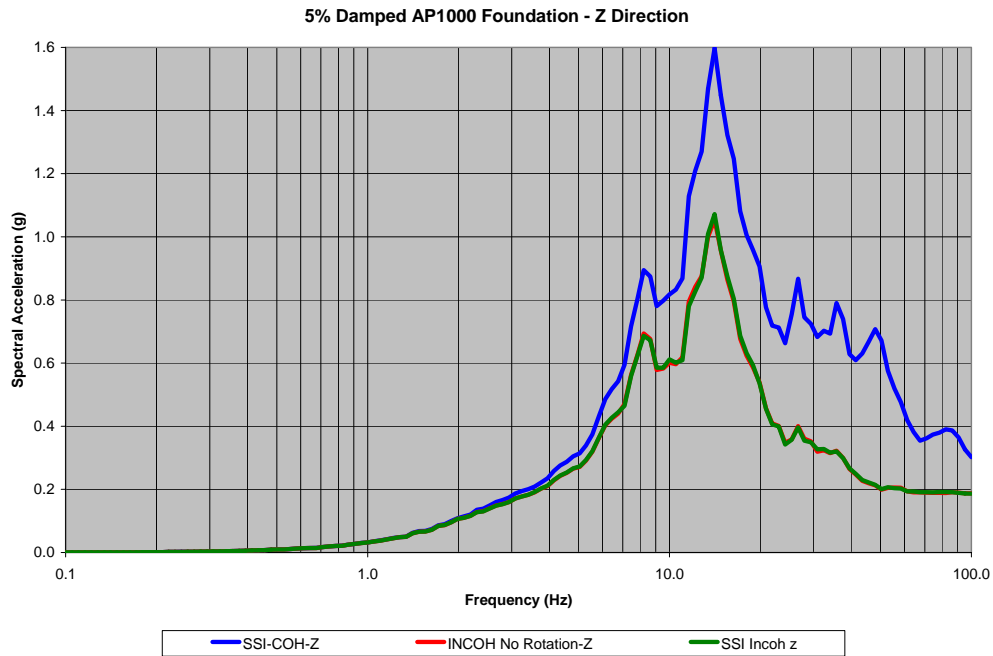


**Figure 0-4**  
**Foundation Response Spectra – Z Direction –SSI Coherent, SSI Incoherent, SSI Incoherent with no Rotations (Node 1)**

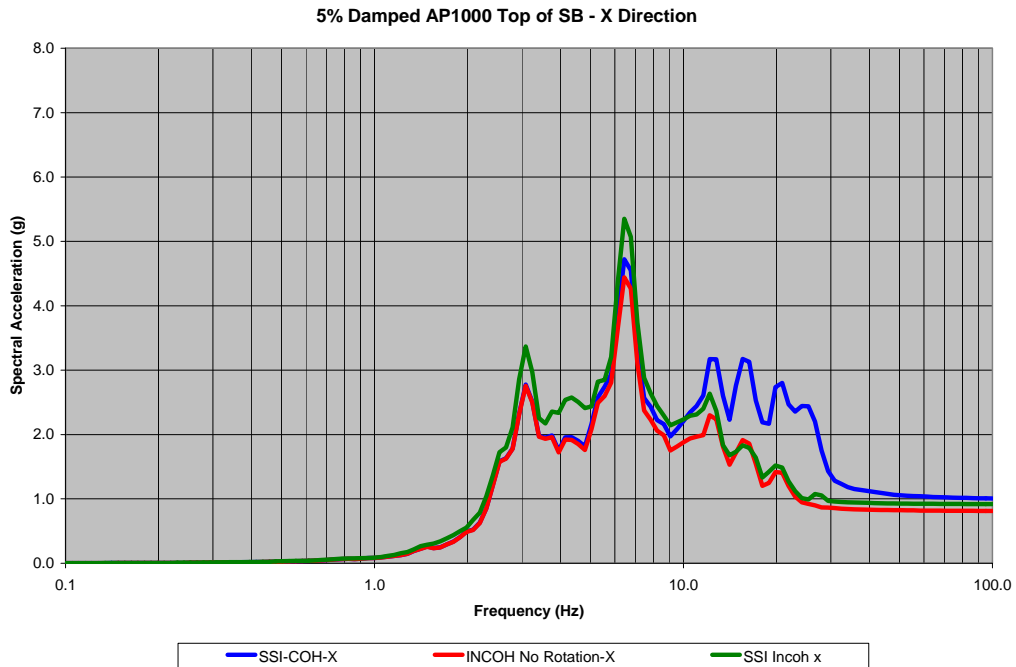


**Figure 0-5**  
**Top of Shield Building Response Spectra – X Direction –SSI Coherent, SSI Incoherent, SSI Incoherent with no Rotations (Node 310)**

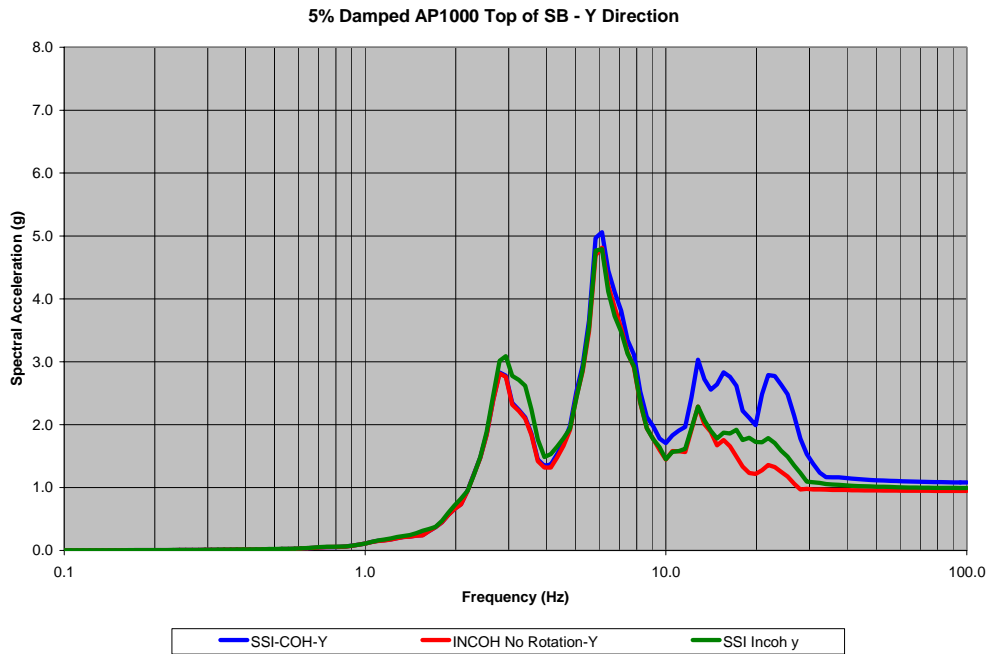


**Figure 0-6**  
**Top of Shield Building Response Spectra – Y Direction –SSI Coherent, SSI Incoherent, SSI Incoherent with no Rotations (Node 310)**

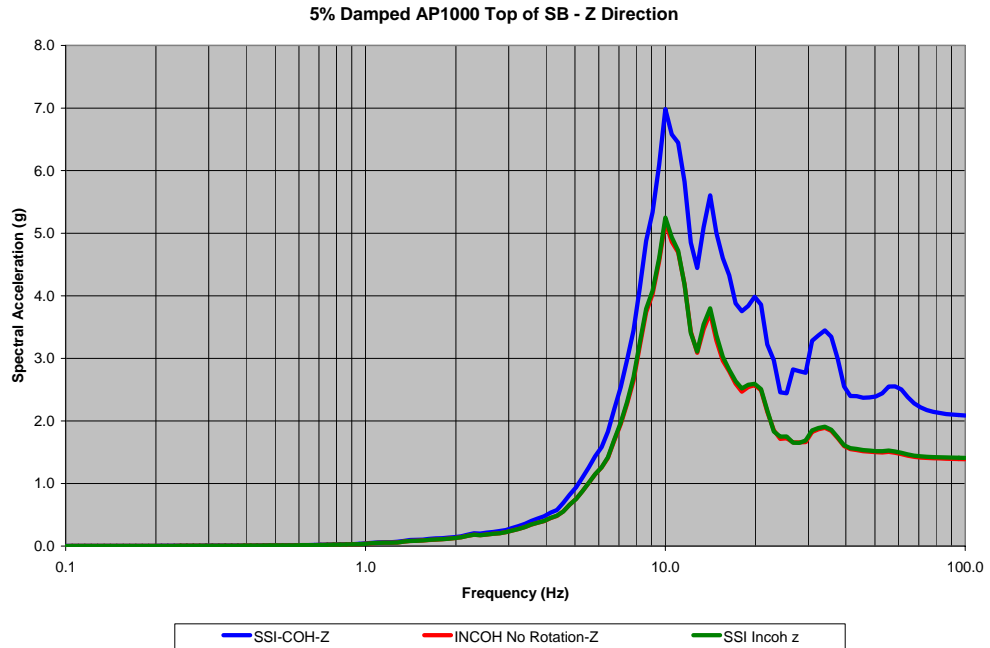


**Figure 0-7**  
**Top of Shield Building Response Spectra – Z Direction –SSI Coherent, SSI Incoherent, SSI Incoherent with no Rotations (Node 310)**

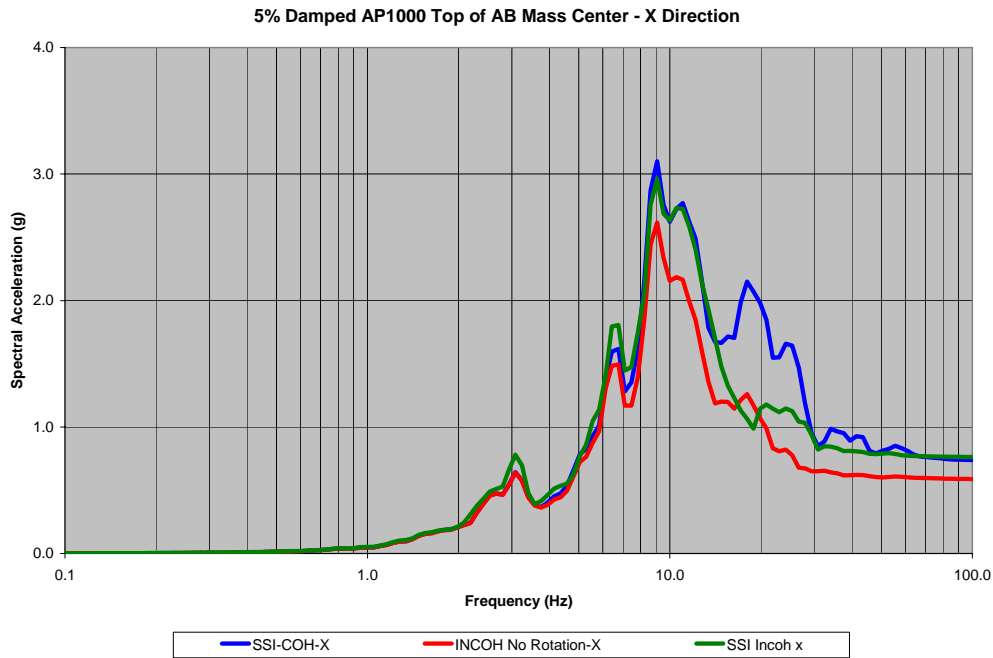


**Figure 0-8**  
**Top of Auxiliary Building Response Spectra – X Direction –SSI Coherent, SSI Incoherent, SSI Incoherent with no Rotations (Node 120mc)**

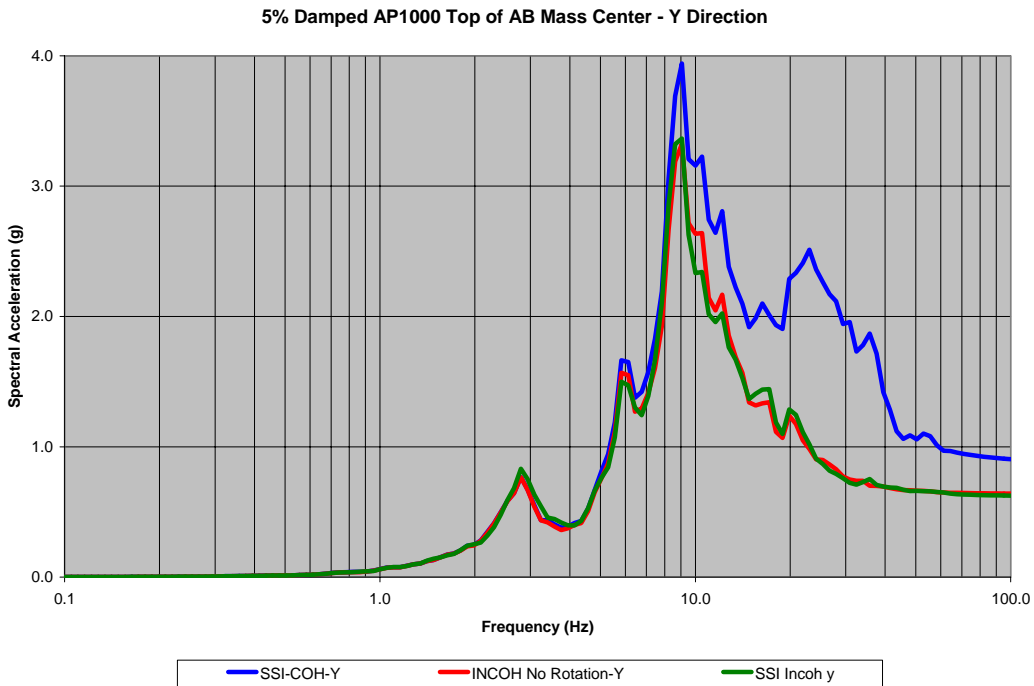


**Figure 0-9**  
**Top of Auxiliary Building Response Spectra – Y Direction –SSI Coherent, SSI Incoherent, SSI Incoherent with no Rotations (Node 120mc)**

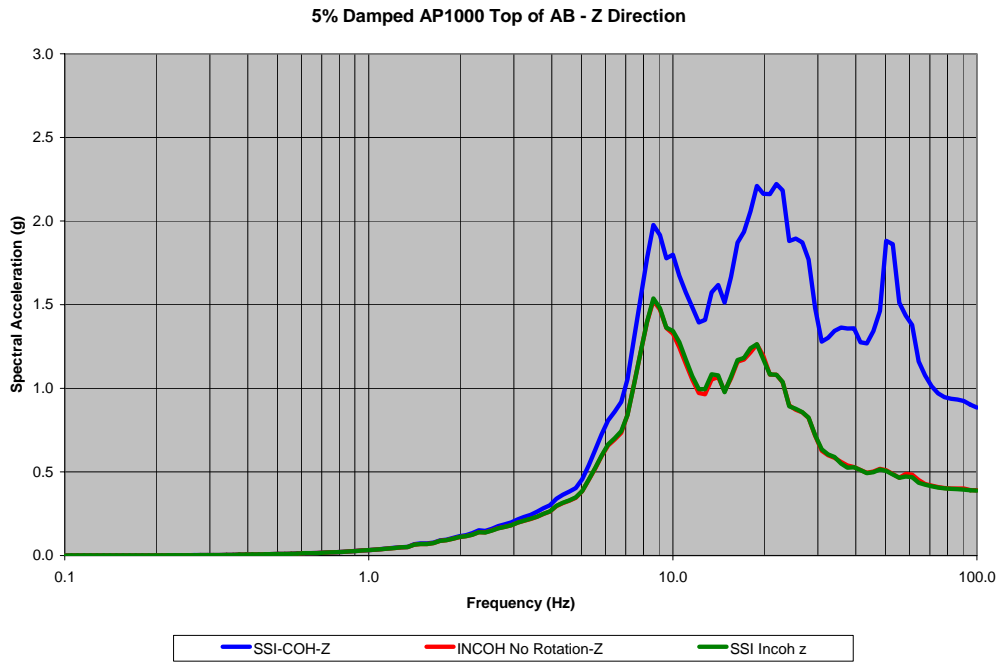


**Figure 0-10**  
**Top of Auxiliary Building Response Spectra – Z Direction – SSI Coherent, SSI Incoherent, SSI Incoherent with no Rotations (Node 120)**

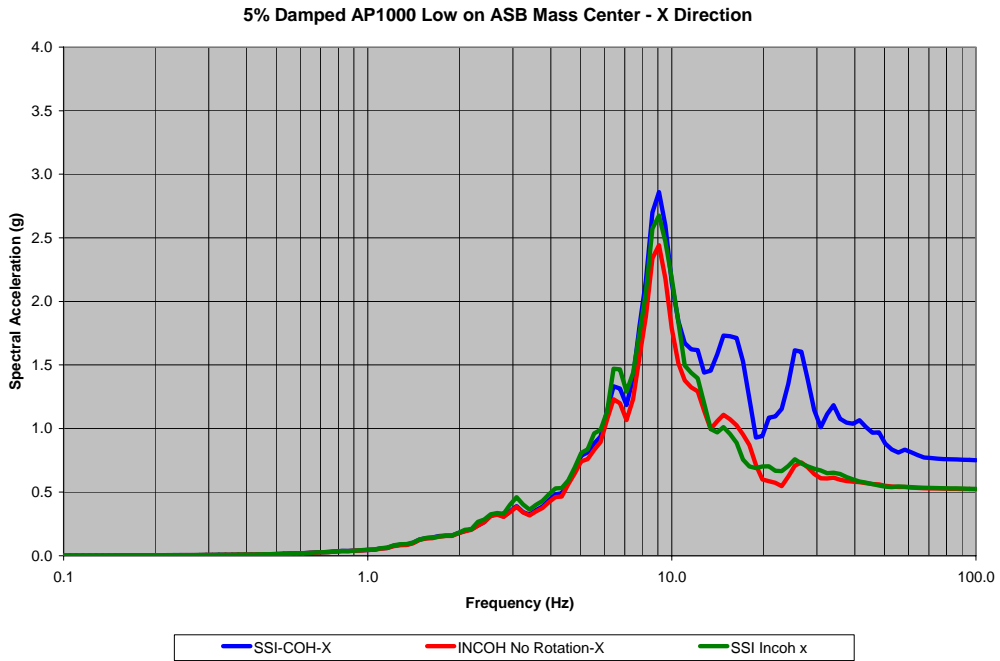


**Figure 0-11**  
**Low on ASB Response Spectra – X Direction – SSI Coherent, SSI Incoherent, SSI Incoherent with no Rotations (Node 80mc)**

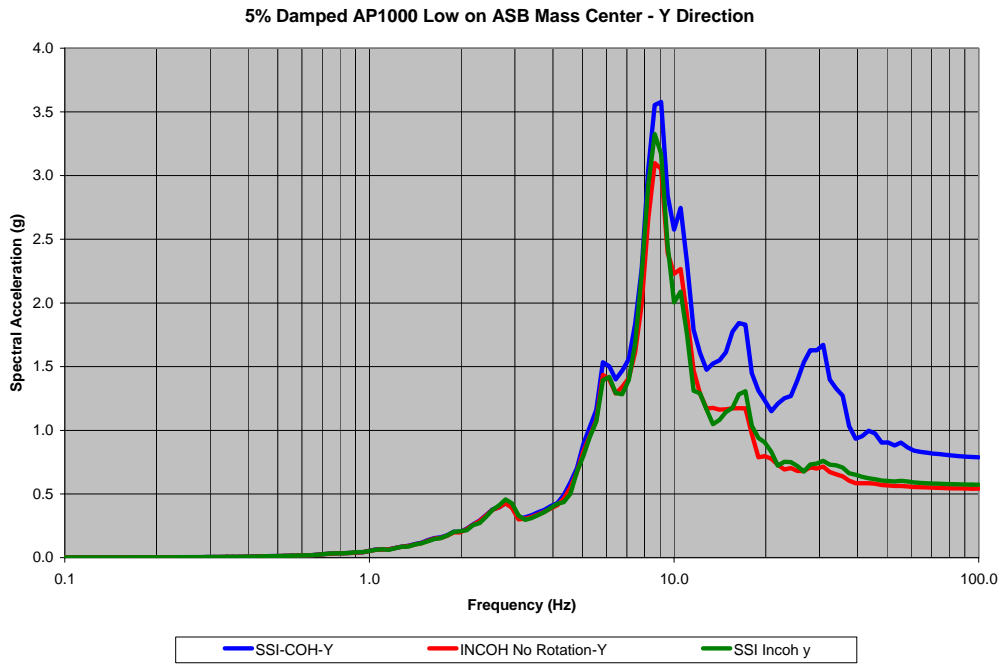


**Figure 0-12**  
**Low on ASB Response Spectra – Y Direction – SSI Coherent, SSI Incoherent, SSI Incoherent with no Rotations (Node 80mc)**

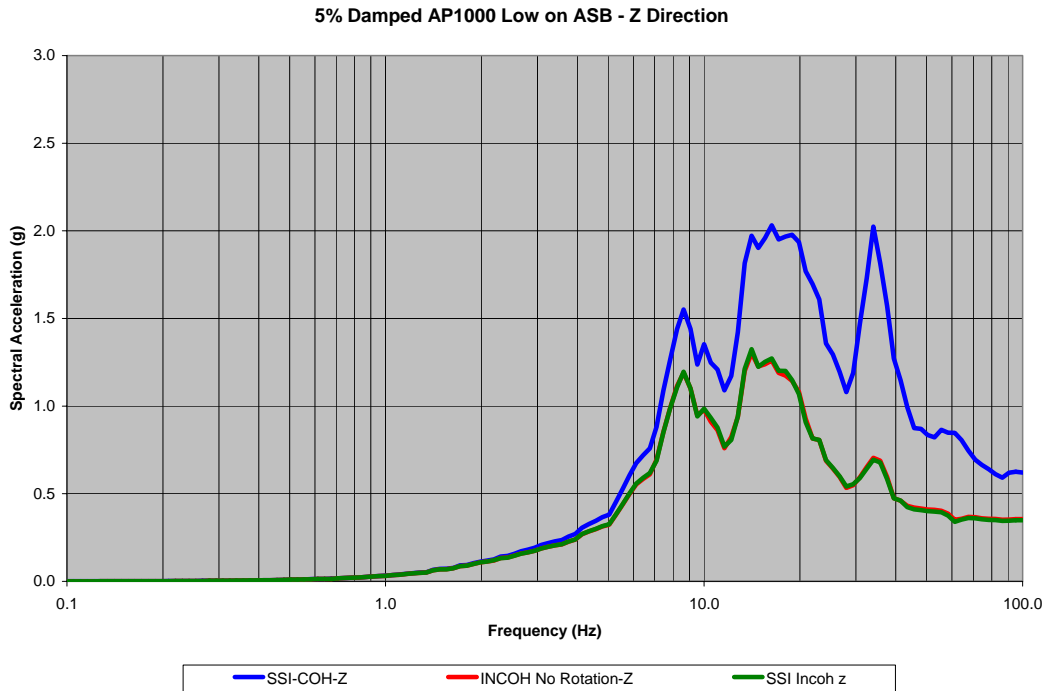


**Figure 0-13**  
**Low on ASB Response Spectra – Z Direction – SSI Coherent, SSI Incoherent, SSI Incoherent with no Rotations (Node 80)**

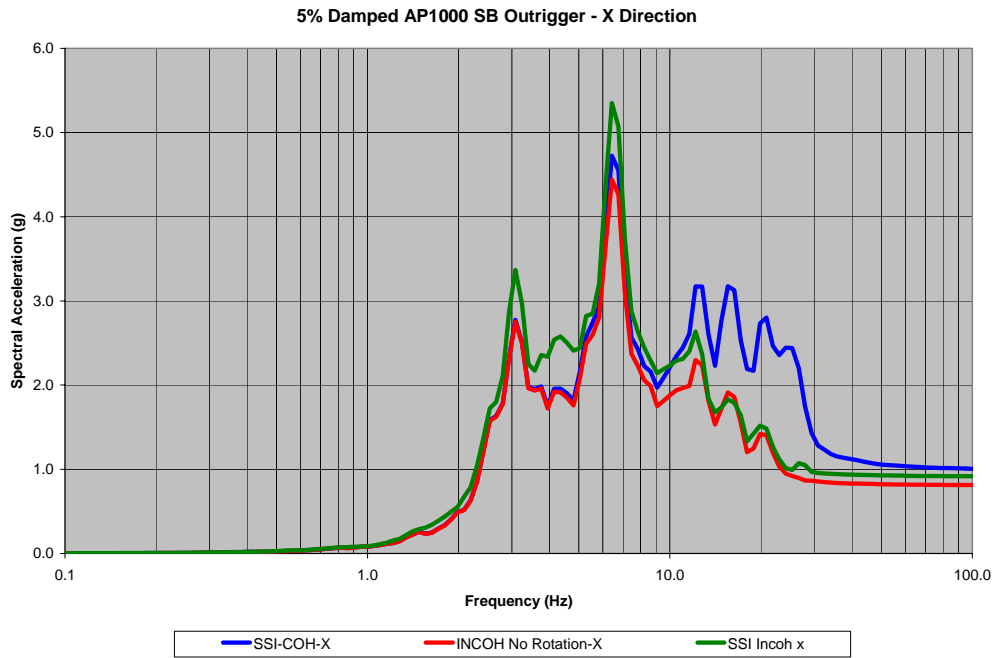


**Figure 0-14**  
**Shield Building Outrigger Response Spectra – X Direction – SSI Coherent, SSI Incoherent, SSI Incoherent with no Rotations (Node 310out)**

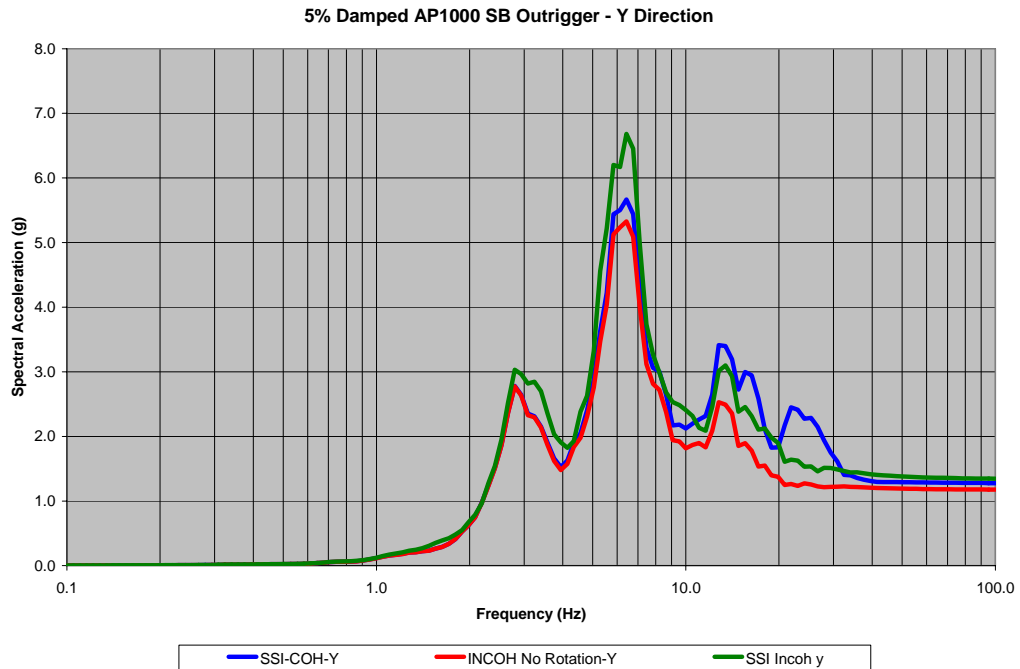


**Figure 0-15**  
**Shield Building Outrigger Response Spectra – Y Direction – SSI Coherent, SSI Incoherent, SSI Incoherent with no Rotations (Node 310out)**

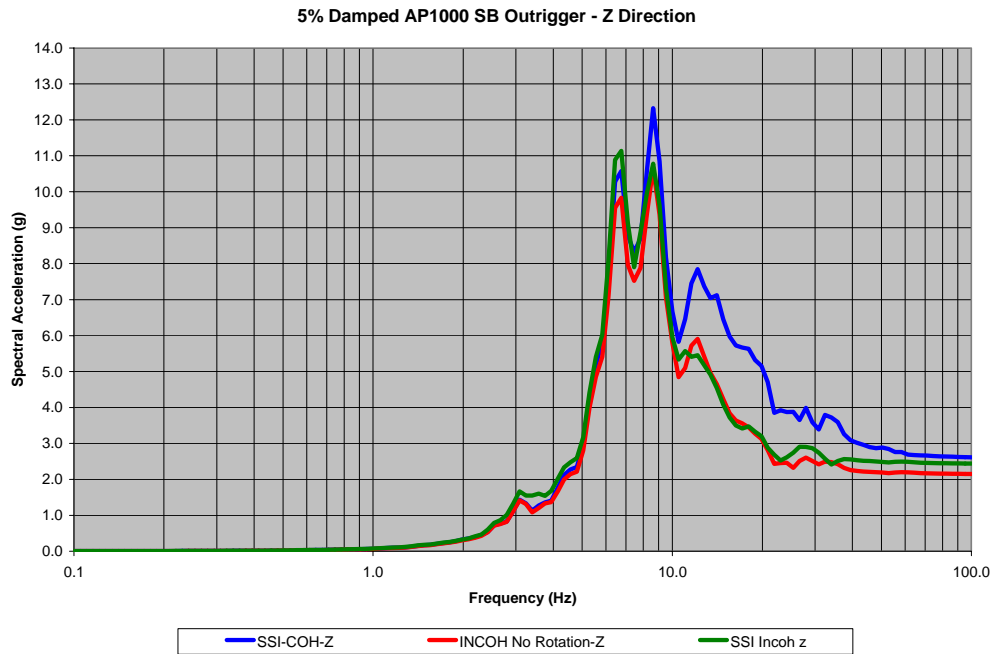


**Figure 0-16**  
 Shield Building Outrigger Response Spectra – Z Direction – SSI Coherent, SSI Incoherent, SSI Incoherent with no Rotations (Node 310out)

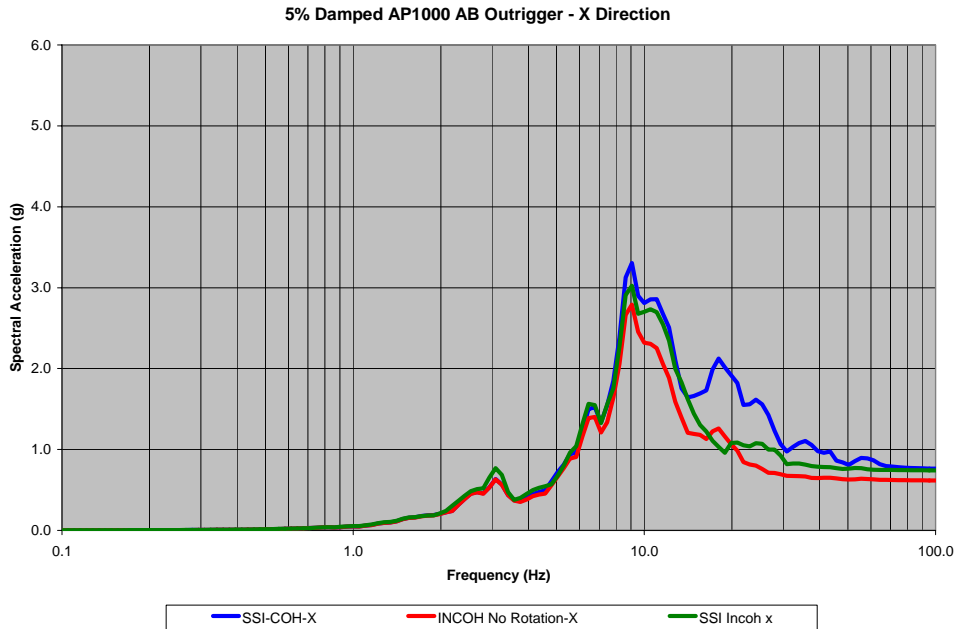


**Figure 0-17**  
 Auxiliary Building Outrigger Response Spectra – X Direction – SSI Coherent, SSI Incoherent, SSI Incoherent with no Rotations (Node 120out)

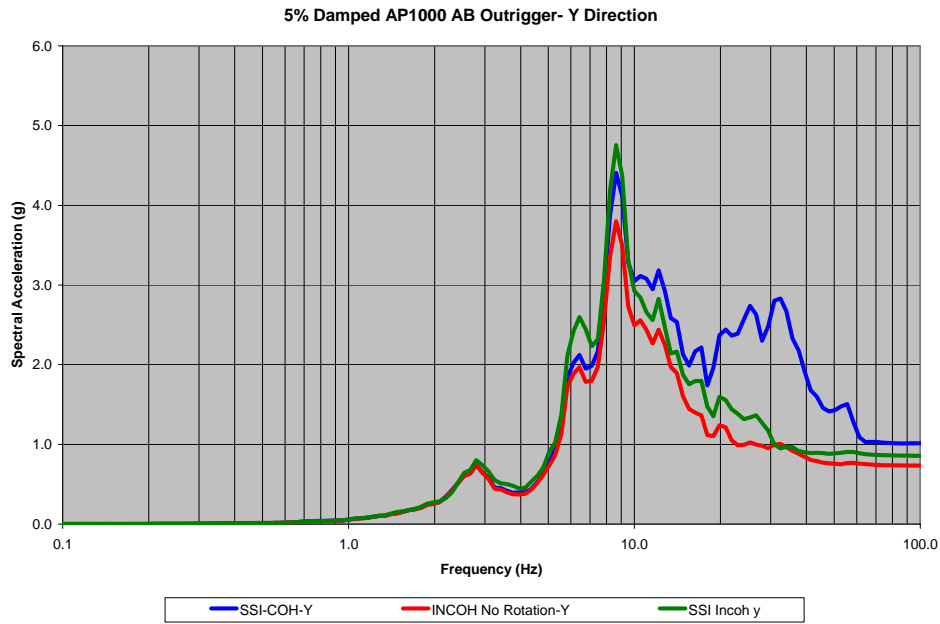


**Figure 0-18**  
**Auxiliary Building Outrigger Response Spectra – Y Direction – SSI Coherent, SSI Incoherent, SSI Incoherent with no Rotations (Node 120out)**

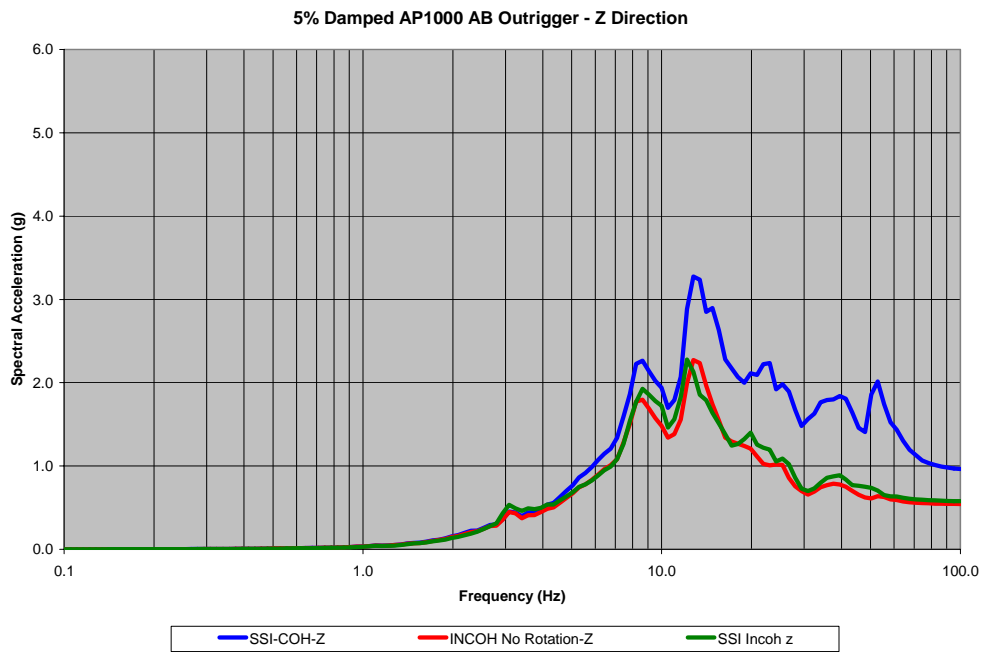


**Figure 0-19**  
**Auxiliary Building Outrigger Response Spectra – Z Direction – SSI Coherent, SSI Incoherent, SSI Incoherent with no Rotations (Node 120out)**

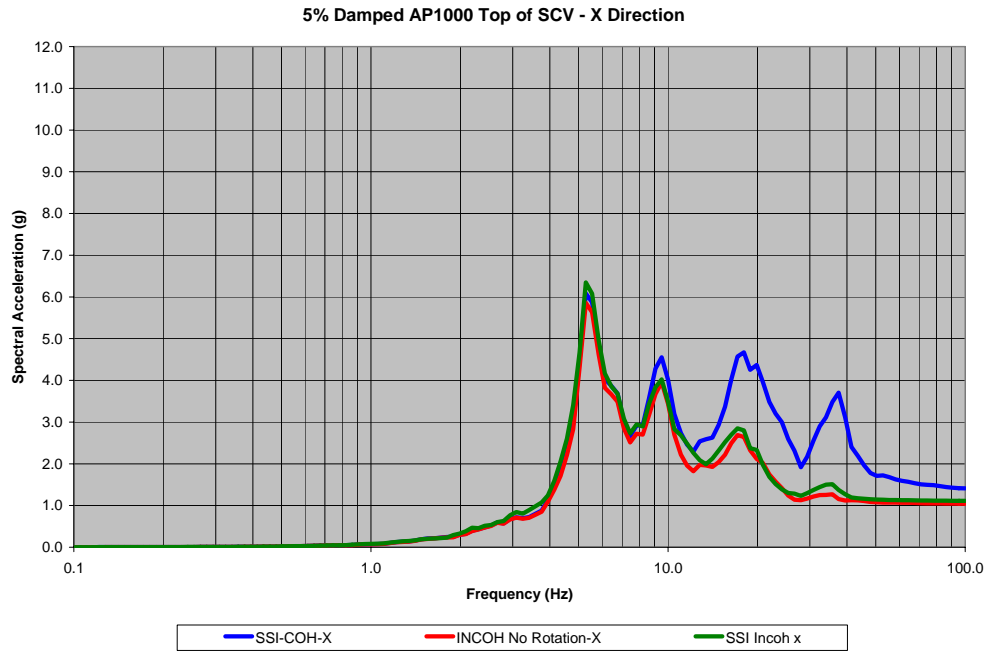


**Figure 0-20**  
**Top of SCV Response Spectra – X Direction –SSI Coherent, SSI Incoherent, SSI Incoherent, SSI Incoherent with no Rotations (Node 417)**

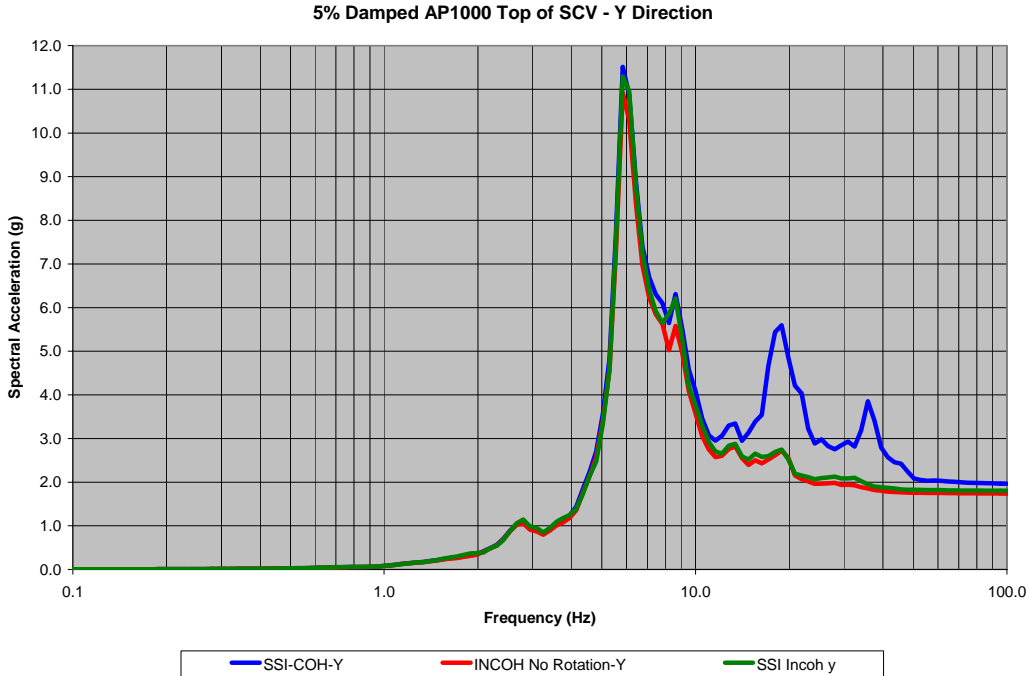


**Figure 0-21**  
**Top of SCV Response Spectra – Y Direction –SSI Coherent, SSI Incoherent, SSI Incoherent with no Rotations (Node 417)**

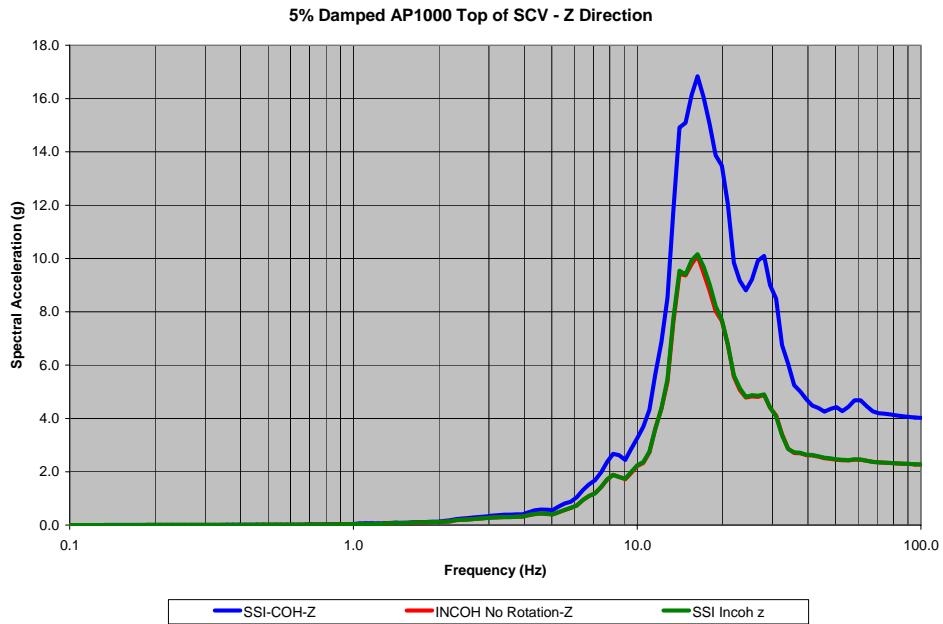


**Figure 0-22**  
**Top of SCV Response Spectra – Z Direction – SSI Coherent, SSI Incoherent, SSI Incoherent with no Rotations (Node 417)**

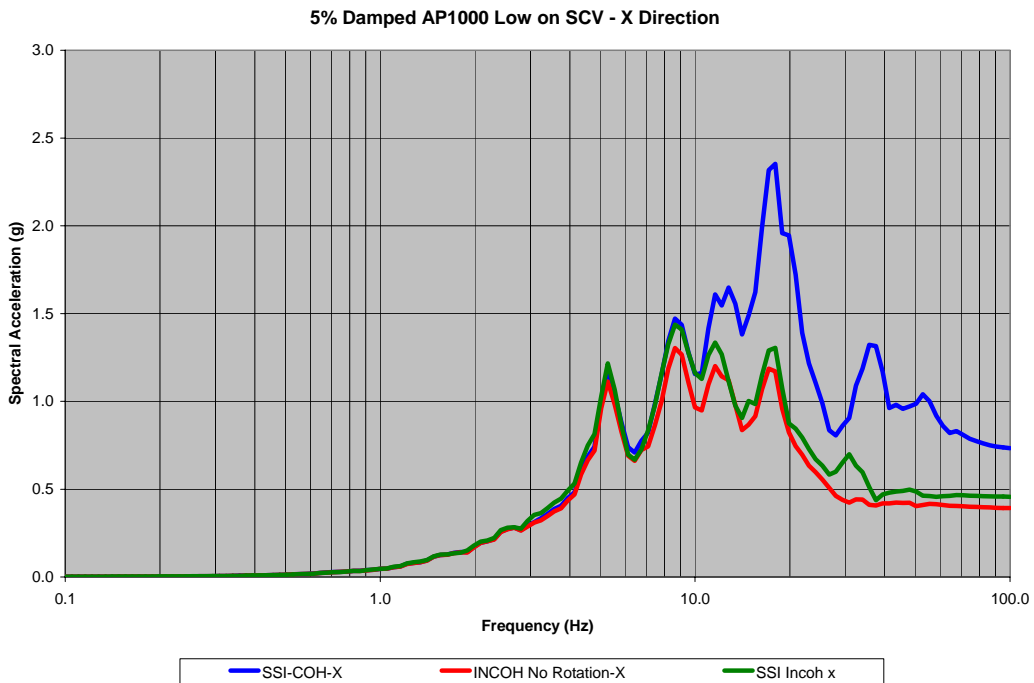


**Figure 0-23**  
**Low on SCV Response Spectra – X Direction – SSI Coherent, SSI Incoherent, SSI Incoherent with no Rotations (Node 406)**

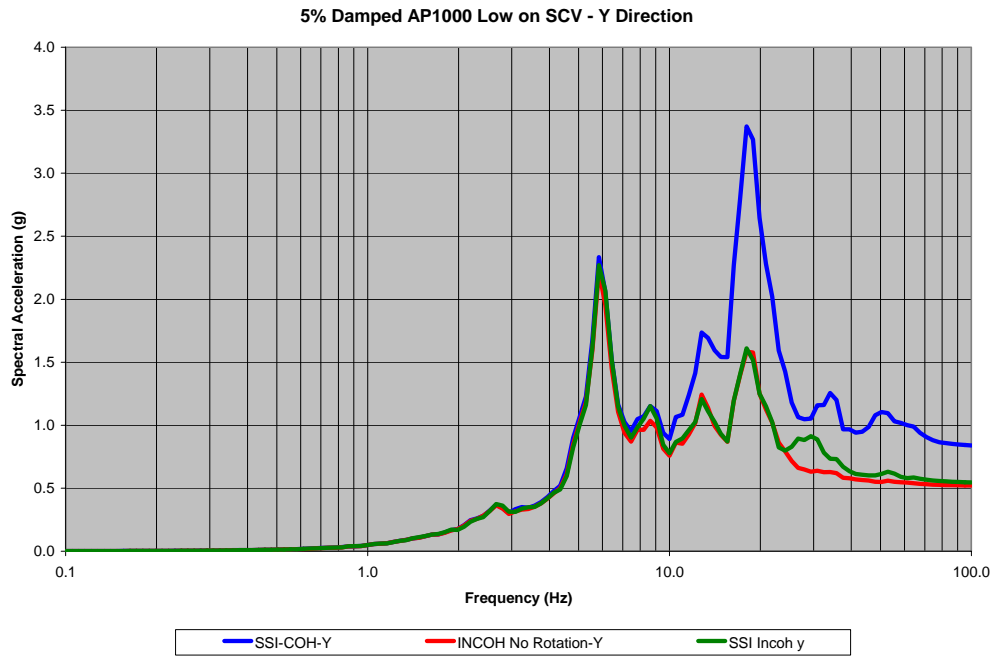


**Figure 0-24**  
**Low on SCV Response Spectra – Y Direction – SSI Coherent, SSI Incoherent, SSI Incoherent with no Rotations (Node 406)**

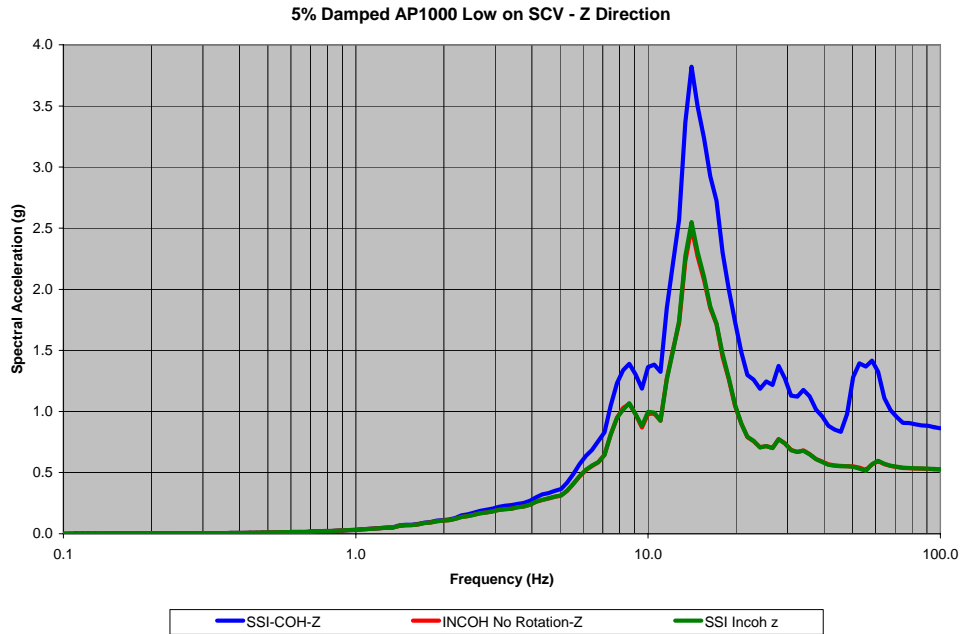


**Figure 0-25**  
**Low on SCV Response Spectra – Z Direction – SSI Coherent, SSI Incoherent, SSI Incoherent with no Rotations (Node 406)**

*Note: The green SSI Incoh curve underlies the red INCOH No Rotation curve on this figure.*

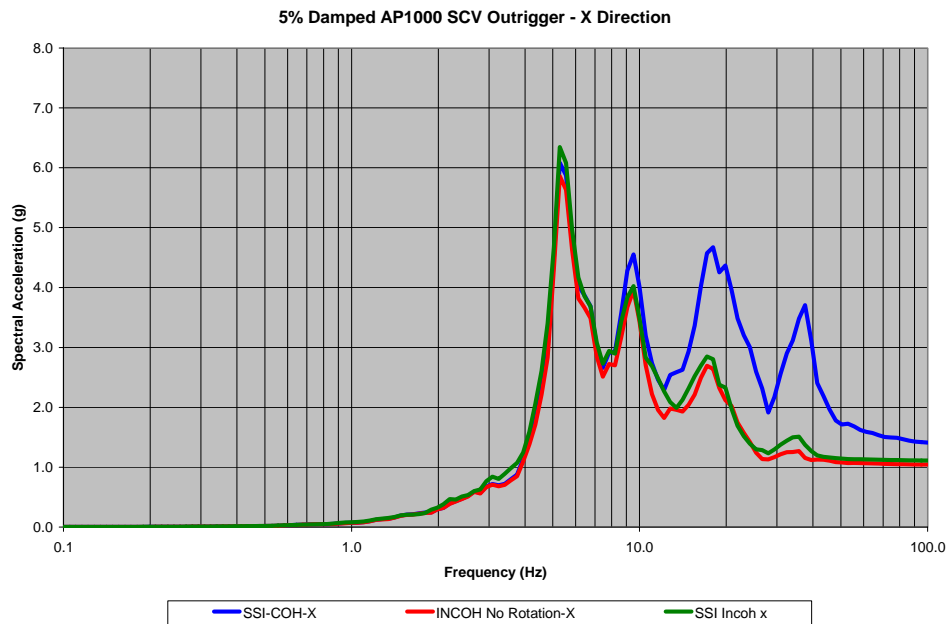


**Figure 0-26**  
**SCV Outrigger Response Spectra – X Direction – SSI Coherent, SSI Incoherent, SSI Incoherent with no Rotations (Node 417out)**

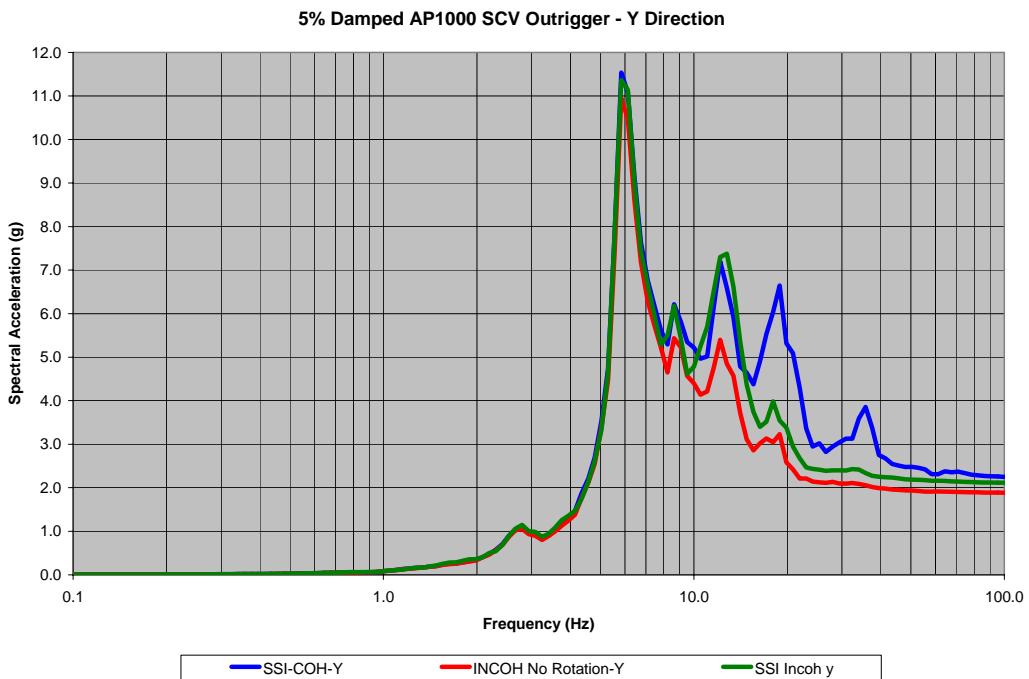


**Figure 0-27**  
**SCV Outrigger Response Spectra – Y Direction – SSI Coherent, SSI Incoherent, SSI Incoherent with no Rotations (Node 417out)**

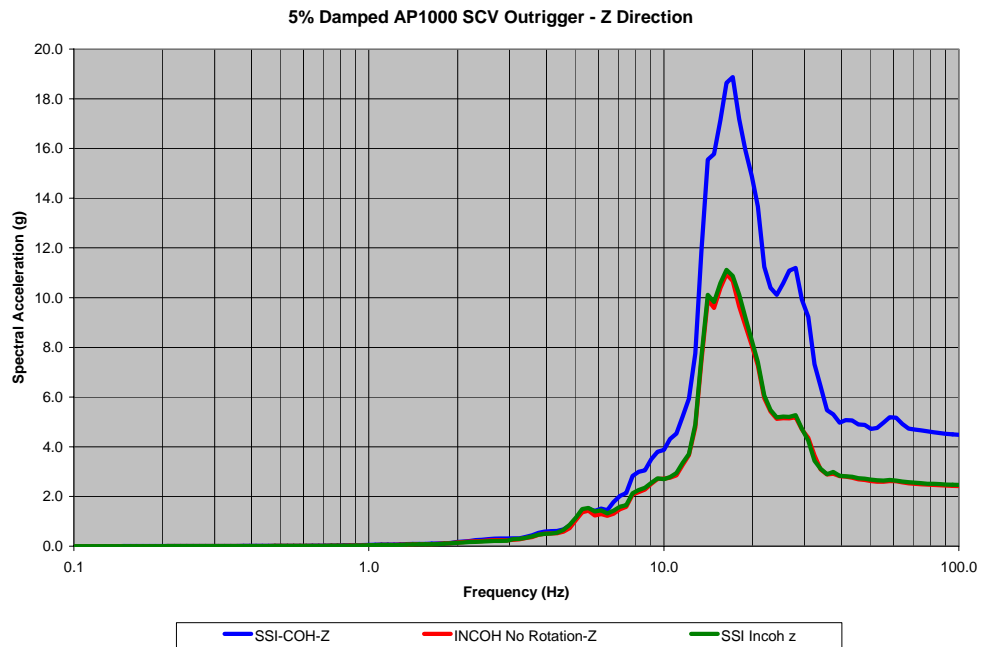


**Figure 0-28**  
**SCV Outrigger Response Spectra – Z Direction – SSI Coherent, SSI Incoherent, SSI Incoherent with no Rotations (Node 417out)**

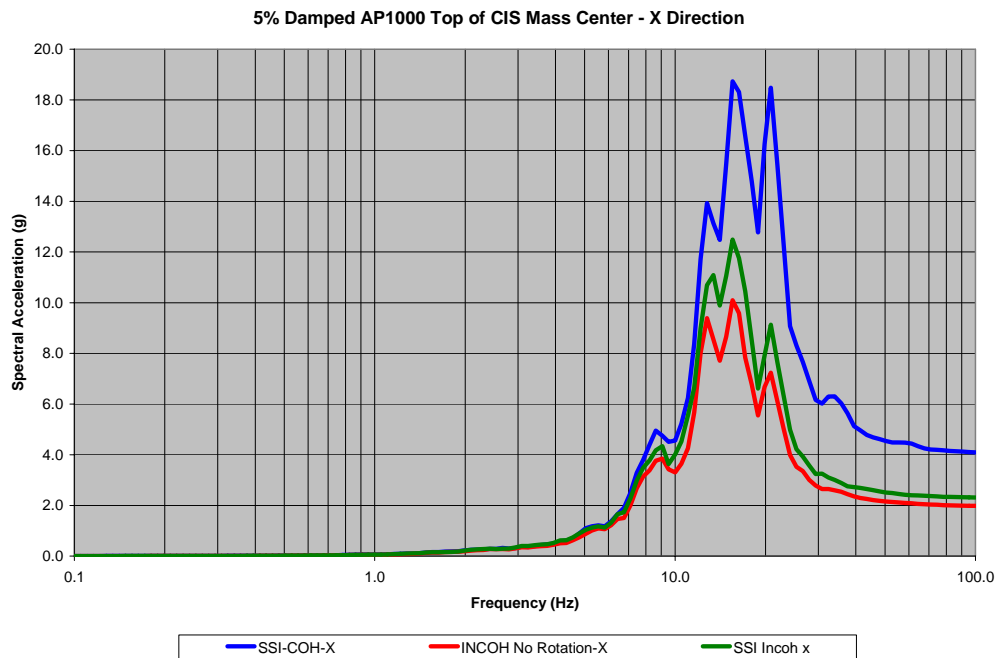


**Figure 0-29**  
**Top of CIS Response Spectra – X Direction – SSI Coherent, SSI Incoherent, SSI Incoherent with no Rotations (Node 538mc)**

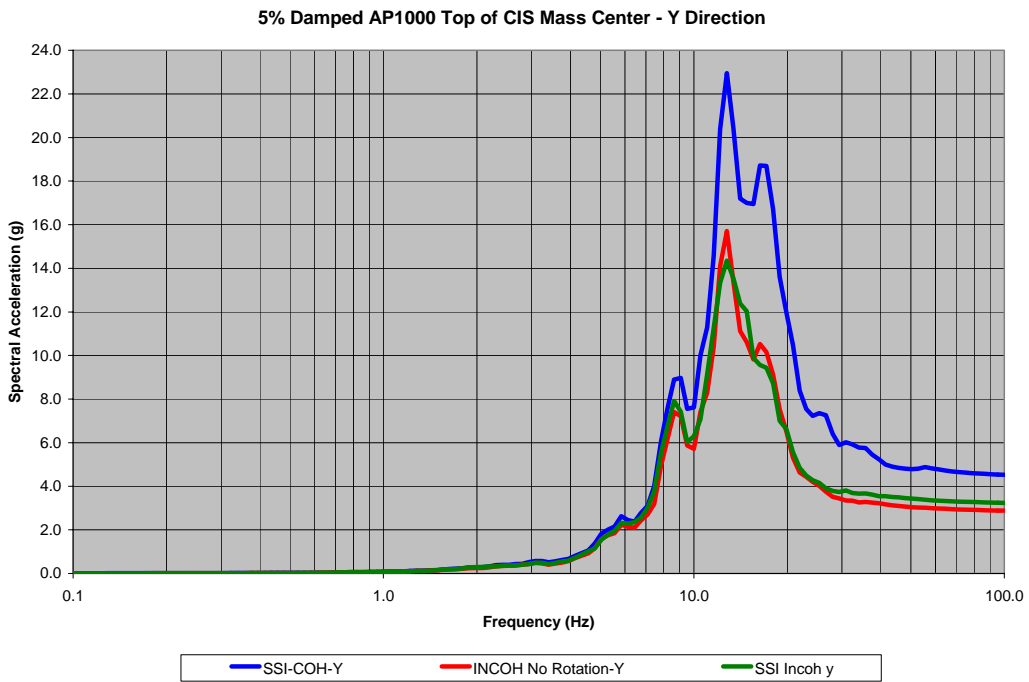


**Figure 0-30**  
**Top of CIS Response Spectra – Y Direction –SSI Coherent, SSI Incoherent, SSI Incoherent with no Rotations (Node 538mc)**

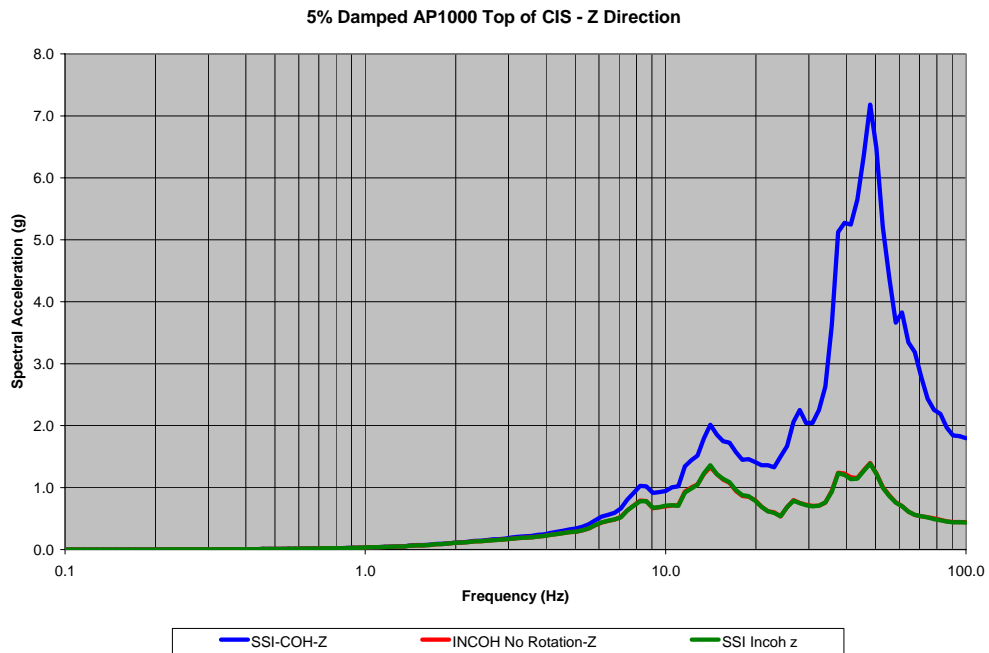


**Figure 0-31**  
**Top of CIS Response Spectra – Z Direction –SSI Coherent, SSI Incoherent, SSI Incoherent with no Rotations (Node 538)**

*Note: The green SSI Incoh curve underlies the red INCOH No Rotation curve on this figure.*

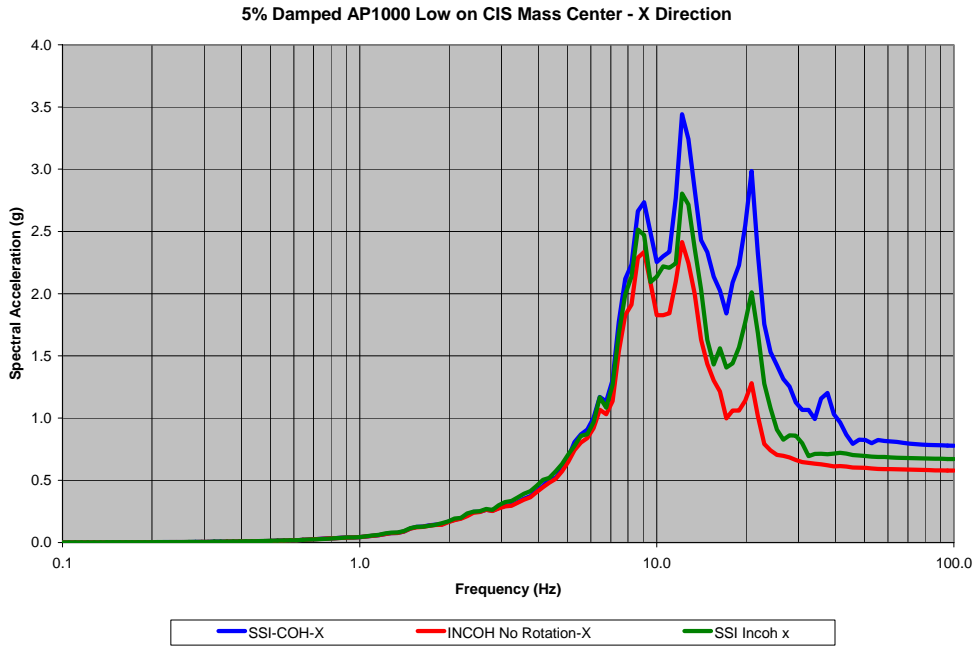


**Figure 0-32**  
**Low on CIS Response Spectra – X Direction –SSI Coherent, SSI Incoherent, SSI Incoherent with no Rotations (Node 535mc)**

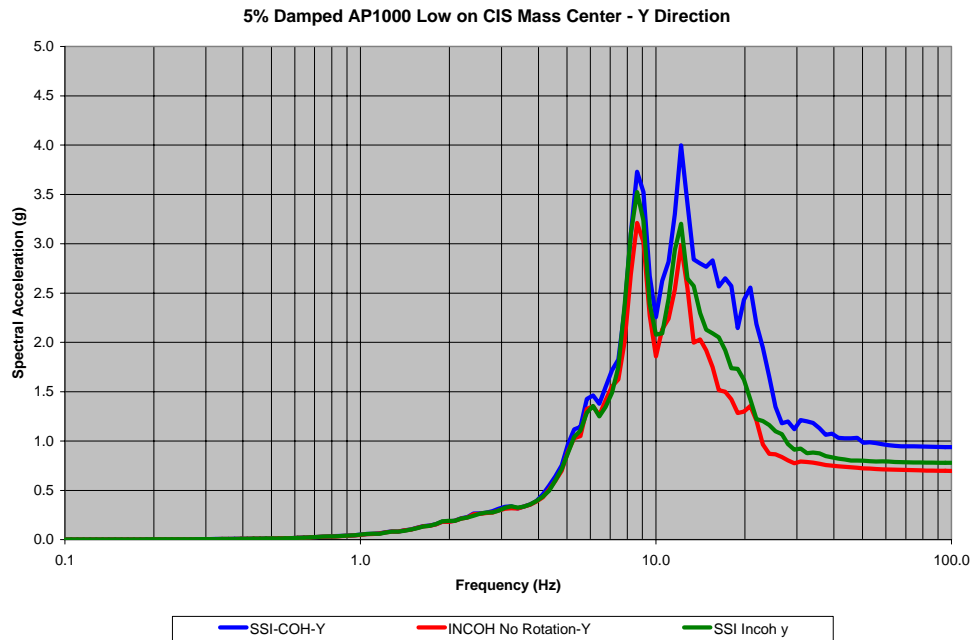


**Figure 0-33**  
**Low on CIS Response Spectra – Y Direction –SSI Coherent, SSI Incoherent, SSI Incoherent with no Rotations (Node 535mc)**

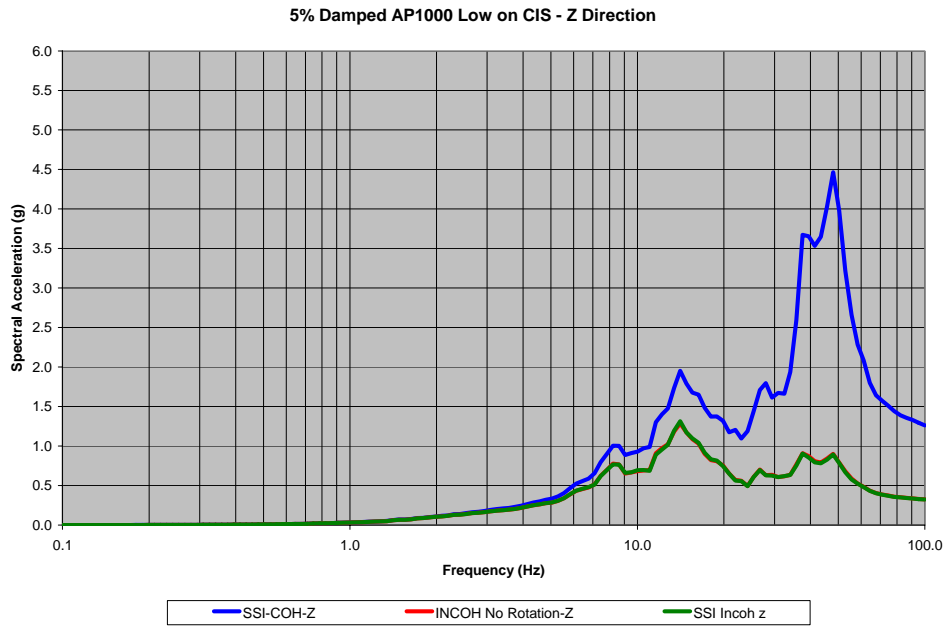


**Figure 0-34**  
**Low on CIS Response Spectra – Z Direction – SSI Coherent, SSI Incoherent, SSI Incoherent with no Rotations (Node 535)**

*Note: The green SSI Incoh curve underlies the red INCOH No Rotation curve on this figure.*

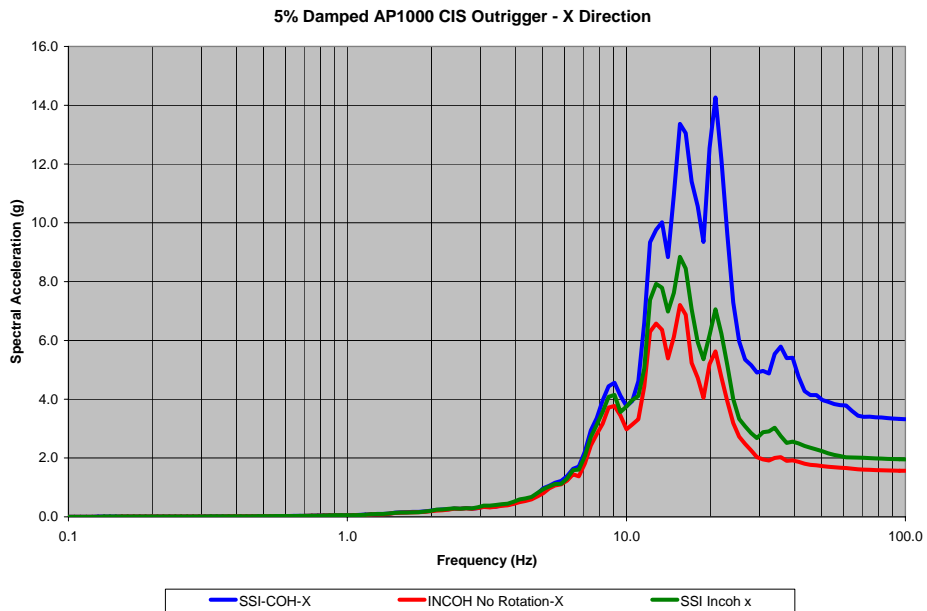


**Figure 0-35**  
**CIS Outrigger Response Spectra – X Direction – SSI Coherent, SSI Incoherent, SSI Incoherent with no Rotations (Node 538out)**

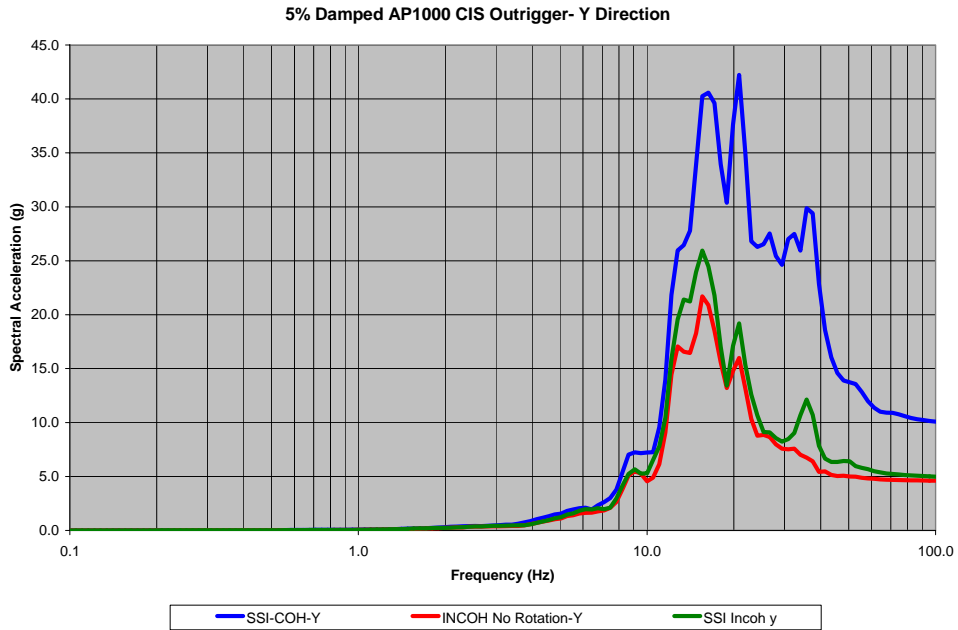


**Figure 0-36**  
**CIS Outrigger Response Spectra – Y Direction – SSI Coherent, SSI Incoherent, SSI Incoherent with no Rotations (Node 538out)**

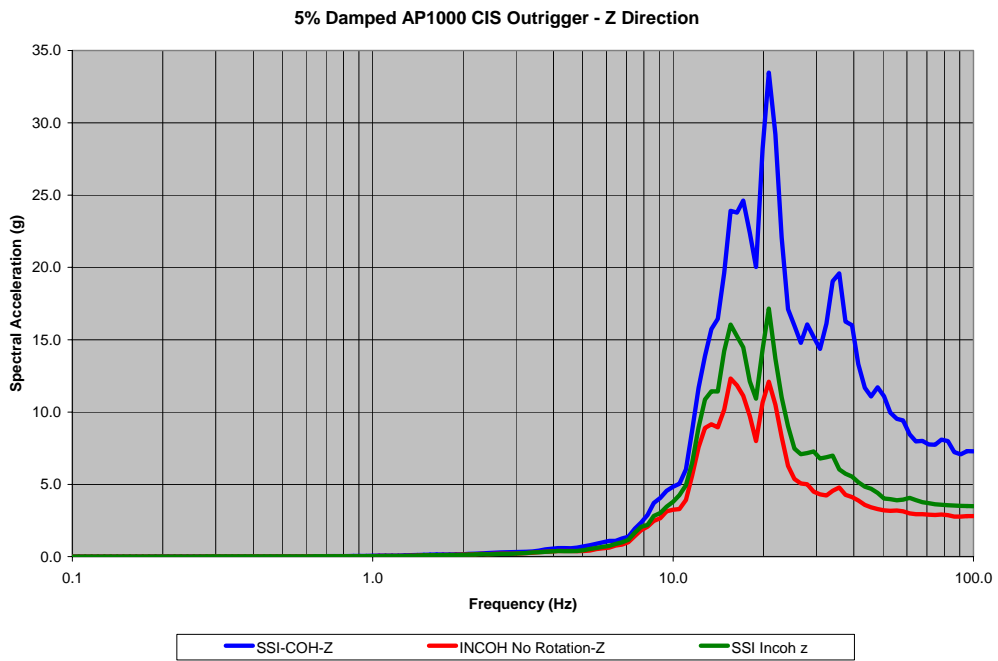


**Figure 0-37**  
**CIS Outrigger Response Spectra – Z Direction – SSI Coherent, SSI Incoherent, SSI Incoherent with no Rotations (Node 538out)**

## **SSI and Incoherence – Scaling Input Fourier Amplitude**

*(This section is a work in progress and will be included within the final report.)*